

THE MECHANISM OF ANTI TUMORIGENIC EFFECTS OF 15-LOX-1 IN  
COLON CANCER

A THESIS SUBMITTED TO  
THE GRADUATE SCHOOL OF NATURAL AND APPLIED SCIENCES  
OF  
MIDDLE EAST TECHNICAL UNIVERSITY

BY

İSMAİL ÇİMEN

IN PARTIAL FULFILLMENT OF THE REQUIREMENTS  
FOR  
THE DEGREE OF DOCTOR OF PHILOSOPHY  
IN  
BIOLOGY

DECEMBER 2012

Approval of the thesis:

**THE MECHANISM OF ANTI TUMORIGENIC EFFECTS OF 15-LOX-1 IN  
COLON CANCER**

submitted by **İSMAİL ÇİMEN** in partial fulfillment of the requirements for the degree of **Doctor of Philosophy in Biyology Department, Middle East Technical University** by,

Prof. Dr. Canan Özgen \_\_\_\_\_  
Dean, Graduate School of Natural and Applied Sciences

Prof. Dr. Gülay Özçengiz \_\_\_\_\_  
Head of Department, **Biology**

Assoc. Prof. Dr. Sreeparna Banerjee \_\_\_\_\_  
Supervisor, **Biology Dept.**, METU

**Examining Committee Members:**

Prof. Dr. Emel Arınc \_\_\_\_\_  
Biology Dept., METU

Assoc. Prof. Dr. Sreeparna Banerjee \_\_\_\_\_  
Biology Dept., METU

Assoc. Prof. Berna Savaş \_\_\_\_\_  
Pathology Dept., Ankara University

Assoc. Prof. Dr. Mesut Muyan \_\_\_\_\_  
Biology Dept., METU

Assoc. Prof. Dr A. Elif Erson-Bensan \_\_\_\_\_  
Biology Dept., METU

**Date:** \_\_\_\_\_

**I hereby declare that all information in this document has been obtained and presented in accordance with academic rules and ethical conduct. I also declare that, as required by these rules and conduct, I have fully cited and referenced all material and results that are not original to this work.**

Name, Last name: İSMAIL ÇİMEN

Signature:

## **ABSTRACT**

### **THE MECHANISM OF ANTI TUMORIGENIC EFFECTS OF 15-LOX-1 IN COLON CANCER**

Çimen, İsmail

Ph.D., Department of Biology

Supervisor: Assoc. Prof. Dr. Sreeparna Banerjee

December 2012, 127 pages

Colorectal cancer is the 4<sup>th</sup> most widespread cause of cancer mortality. One of the pathways that are involved in the development of colorectal cancer is the arachidonic acid metabolizing lipoxygenase (LOX) pathway. Inflammatory molecules formed from this pathway exert profound effects that may exacerbate the development and progression of colon and other cancers. 15 lipoxygenase-1 (15-LOX-1) is a member of LOX protein family that metabolizes primarily linoleic acid to 13-(S)-HODE. Several lines of evidence support an antiangiogenic role for 15-LOX-1, especially through 13-(S)-HODE. The expression of 15-LOX-1 is lost in colon cancer cells.

Our aim in this thesis was to study whether 15-LOX-1 expression has an anticarcinogenic role, particularly on the metastatic and angiogenic potential of colon cancer cells. For this purpose, 15-LOX-1 was introduced into HCT-116 colon cancer cell lines. Having confirmed 15-LOX-1 expression and activity it was observed that expression of 15-LOX-1 significantly decreased cell proliferation, cell motility, anchorage-independent growth, migration and invasion across Matrigel, the

expression of the metastasis-related MTA-1 protein, neoangiogenesis and induced apoptosis. Mechanistically, most of these effects were arbitrated by the 15-LOX-1 mediated inhibition of the inflammatory transcription factor NF- $\kappa$ B via the orphan nuclear receptor PPAR $\gamma$ . In conclusion, we propose that 15-LOX-1 has anti-tumorigenic properties and can be exploited for therapeutic benefits.

Keywords: Colon cancer, 15-Lipoxygenase-1, apoptosis, NF- $\kappa$ B, PPAR $\gamma$ , metastasis, angiogenesis.

## ÖZ

# KOLON KANSERİ HÜCRELERİNDE ANTİ-TÜMÖR ETKİSİ OLAN 15-LİPOKSİJENAZ-1 ENZİMİNİN REGÜLASYON MEKANİZMALARI

Çimen, İsmail

Doktora, Biyoloji Bölümü

Tez Yöneticisi: Doç. Dr. Sreeparna Banerjee

Aralık 2012, 127 sayfa

Kolon kanseri dünyada ölüme neden en yaygın dördüncü kanserdir. Kolon kanserinde rol oynayan ve araştırılan yolaklardan bir tanesi de araşidonik asitin metabolize edildiği LOX (Lipoksijenaz) yolağıdır. Bu yolaktan ortaya çıkan inflamatuar moleküller, kolon ve diğer kanser türlerinin ilerlemesini ve gelişimini kötü yönde etkileyen etmenleri ortaya çıkarır. LOX protein ailesinden olan 15-lipoksijenaz-1 (15-LOX-1) enzimi lineloik asiti 13-(S)-HODE'ye metabolize etmektedir. Bir çok bulgu 15-LOX-1 anti-karsinojenik rolünü özellikle 13-S-HODE yoluyla yaptığını desteklemektedir. Bu genin ifadesi kolon kanser hücrelerinde kaybedilir.

Bu tezde amacımız 15-LOX-1 ekspresyonun, özellikle kolon kanseri hücrelerinin metastatik ve anjiogenik potansiyelli bir antikarsinojenik rolü olup olmadığını araştırmaktır. Bu amaçla, HCT-116 kolon kanseri hücre hattında 15-LOX-1 geninin ifadesi saglandı. 15-LOX-1'un ifadesi ve aktivitesi doğrulandıktan sonra, 15-LOX-1'in ifadesinin hücre çoğalmasını hücre hareketini, yüzeye bağlanma gereksinimi duymadan büyümeye özelliğini, hücre göçünü ve Matrijele karşı  
vi

invasyonunu, metastazla ilgili olan MTA-1 proteini ifadesini, damar oluşumunu anlamlı olarak azalttığı ve apoptozun arttığı gözlemlendi. Mekanizma ile ilgili olarak, bu etkilerin çoğu 15-LOX-1 aracılıklı nükleer reseptör PPAR $\gamma$  yoluyla inflamatuar transkripsiyon faktörü NF- $\kappa$ B engellenmesi hakemlik eder. Sonuç olarak, 15-LOX-1'in anti-tumorigenik özelliğe sahip olduğunu ve terapötik amaçlı kullanılabileceğini ileri sürmekteyiz.

Anahtar Kelimeler: Kolon kanseri, 15-Lipoksijenaz-1, apoptoz, NF- $\kappa$ B, metastaz, anjiyogenez.

To My Family

## **ACKNOWLEDGMENTS**

I wish to express my deepest gratitude to my supervisor Assoc. Prof. Dr. Sreeparna Banerjee for their guidance, advice, criticism, encouragements and insight throughout the research.

I would like to thank Assoc. Prof. Dr. A. Elif Erson-Bensan from Department of Biological Sciences, METU for her invaluable help and support during my study.

My very special thanks should be devoted to Assoc. Prof. Dr. Berna Savaş from Department of Pathology, Ankara University for her suggestions and comments.

My special thanks should go to my laboratory friends, for their help my study.

I would like to thank Assoc. Prof. Dr. Mayda Gürsel for flow cytometry data analysis from Department of Biological Sciences, METU and Assist. Prof. Dr. Can Özen from METU Central Laboratory for the use of the Confocal microscopy.

I would also like to thank Assoc. Prof. Dr. İhsan Gürsel and Phd Candidate Tamer Kahraman, Department of Molecular Biology and Genetics, Bilkent University for the use of the flow cytometer.

Finally, I want to express my sincere thanks to my family, my parents Hasan Hüseyin-Latife Çimen and my sisters and brother for their encouragement, support and tolerance during the study.

This study was supported by TÜBİTAK Grants No: 106S193, 110S165 and 111S308 and by the Turkish Academy of Sciences (TÜBA).

## TABLE OF CONTENTS

ABSTRACT .....	IV
ÖZ .....	VI
ACKNOWLEDGMENTS .....	IX
TABLE OF CONTENTS .....	X
LIST OF TABLES .....	XIV
LIST OF FIGURES .....	XV
LIST OF ABBREVIATIONS .....	XIX
CHAPTERS .....	1
1. INTRODUCTION .....	1
1.1 Cancer .....	1
1.2 The hallmarks of cancer .....	2
1.2.1 Sustaining Proliferative Signaling.....	3
1.2.2 Evading Growth Suppressors .....	3
1.2.3 Resisting Cell Death.....	4
1.2.4 Enabling Replicative Immortality .....	5
1.2.5 Inducing Angiogenesis.....	5
1.2.6 Activating Invasion and Metastasis .....	6
1.4 Inflammation and Colorectal cancer .....	8
1.5 Arachidonic Acid Pathway .....	12
1.6 Lipoxygenase pathway and colon cancer.....	13
1.7 15-Lipoxygenase-1 (15-LOX-1) .....	13
1.8 15-LOX-1, 13-(S)-HODE, in colon tumorigenesis.....	15
1.9 15-LOX-1 and Apoptosis .....	16
1.10 15-LOX-1 and CRC Metastasis .....	18

1.11 15-LOX-1 and CRC Angiogenesis .....	20
1.12 Mechanism of 15-LOX-1 tumor suppressive effect in CRC .....	22
<b>2. MATERIALS AND METHODS .....</b>	<b>25</b>
<b>2.1 Cell Culture and transfection .....</b>	<b>25</b>
<b>2.1.1 Plasmids .....</b>	<b>25</b>
<b>2.1.2 Plasmid isolation and measurement.....</b>	<b>26</b>
<b>2.1.3. Transfections .....</b>	<b>26</b>
<b>2.2. Cell Treatments .....</b>	<b>27</b>
<b>2.3. RNA isolation and RT-PCR.....</b>	<b>28</b>
<b>2.3.1 RNA isolation and measurement .....</b>	<b>28</b>
<b>2.3.2 DNase-1 treatment .....</b>	<b>28</b>
<b>2.3.3 15-LOX-1 RT-PCR.....</b>	<b>29</b>
<b>2.4 Protein Isolation .....</b>	<b>31</b>
<b>2.5 Nuclear and cytoplasmic Protein Isolation .....</b>	<b>31</b>
<b>2.6 Western blot analysis .....</b>	<b>32</b>
<b>2.7 15-LOX-1 activity measurement.....</b>	<b>33</b>
<b>2.8 Cellular proliferation .....</b>	<b>33</b>
<b>2.9 Apoptosis assays.....</b>	<b>34</b>
<b>2.9.1 Acridine orange staining .....</b>	<b>34</b>
<b>2.9.2 Caspase-3 activity assay.....</b>	<b>35</b>
<b>2.9.3 Annexin V Staining.....</b>	<b>36</b>
<b>2.10 Colony formation in soft agar .....</b>	<b>36</b>
<b>2.11 In vitro scratch wound healing assay .....</b>	<b>37</b>
<b>2.12 Cell adhesion assay .....</b>	<b>37</b>
<b>2.13 Boyden chamber cell migration assay.....</b>	<b>38</b>
<b>2.14 Boyden chamber cell invasion assays .....</b>	<b>39</b>
<b>2.15 Luciferase Reporter Assays.....</b>	<b>40</b>
<b>2.16 Immunofluorescence Studies .....</b>	<b>40</b>
<b>2.17 DNA-Binding Elisa Assay .....</b>	<b>41</b>
<b>2.18 VEGF Elisa Assay .....</b>	<b>41</b>

2.19 HUVEC Cell proliferation Assay.....	42
2.20 HUVEC Wound Healing Assay.....	42
2.21 In vitro Angiogenesis Assay .....	43
2.22 Statistical analyses .....	43
 3. RESULTS .....	44
Section I: Biological effects of 15-LOX-1 in colorectal cancer .....	44
3.1.1 Expression of 15-LOX-1 in HCT-116 cells .....	44
3.1.2 15-LOX-1 expression and 13-(S)-HODE reduces proliferation in vitro .....	47
3.1.3 15-LOX-1 expression induces apoptosis in vitro.....	48
3.1.4 Expression of 15-LOX-1 reduces anchorage-independent growth in HCT-116 cells .....	53
3.1.5 Expression of 15-LOX-1 reduces motility in HCT-116 cells .....	54
3.1.6 Expression of 15-LOX-1 reduces adhesion to fibronectin in HCT-116 cells ...	56
3.1.7 15-LOX-1 expression reduces migration in HCT-116 cells .....	57
3.1.8 15-LOX-1 expression reduces invasion of HCT-116 cells.....	59
3.1.9 15-LOX-1 reduces neoangiogenesis in HCT-116 cells. ....	61
3.1.9.1 Reduction in VEGF-A <sub>165</sub> secretion .....	61
3.1.9.2 15-LOX-1 expression in HCT-116 cell line reduces HUVEC proliferation and mobility and tube formation .....	62
Section II: The mechanism of antitumorigenic effect of 15-LOX-1 in CRC .....	68
3.2.1 15-LOX-1 Expression Reduces Nuclear Translocation of NF-κB .....	68
3.2.2 15-LOX-1 expression reduces the DNA-binding activity of NF-κB .....	70
3.2.3 15-LOX-1 expression reduces the transcriptional activity of NF-κB .....	71
3.2.4 13(S)-HODE increases PPAR $\gamma$ transcriptional activity .....	73
3.2.5 PPAR $\gamma$ inhibition activates NF-κB nuclear translocation in 15-LOX-1 expressing cells .....	75
3.2.6 PPAR $\gamma$ inhibition enhances the transcriptional activity of NF-κB in 15-LOX-1 expressing cells .....	85
3.2.7 Inhibition of PPAR $\gamma$ increases cellular proliferation .....	87

<b>4. DISCUSSION .....</b>	<b>89</b>
<b>4.1 Functional effects of 15-LOX-1 expression in CRC HCT-116 Cells.....</b>	<b>92</b>
<b>4.1.1 Effect on proliferation and apoptosis .....</b>	<b>92</b>
<b>4.1.2 Effect on cellular motility and metastasis .....</b>	<b>93</b>
<b>4.1.3 Effect on neoangiogenesis.....</b>	<b>95</b>
<b>4.2 The mechanism of antitumorigenic effect of 15-LOX-1 in CRC via inhibition of NF-<math>\kappa</math>B .....</b>	<b>96</b>
<b>5. CONCLUSIONS.....</b>	<b>102</b>
<b>REFERENCES.....</b>	<b>105</b>
<b>APPENDICES .....</b>	<b>117</b>
<b>APPENDIX A .....</b>	<b>117</b>
<b>VECTOR MAPS.....</b>	<b>117</b>
<b>A.1 pcDNA3.1/Zeo (+) Control Vector .....</b>	<b>117</b>
<b>A.2 pSV-<math>\beta</math>-Galactosidase Control Vector (Promega, USA).....</b>	<b>118</b>
<b>APPENDIX B .....</b>	<b>119</b>
<b>SCREENING OF 15-LOX-1 EXPRESSING MONOCLOONE CELLS WITH RT-PCR ANALYSIS .....</b>	<b>119</b>
<b>B1: Screening of 15-LOX-1 expressing 1E7 monoclonal cells with RT-PCR analysis after stable transfection of HCT-116 cell lines. ....</b>	<b>119</b>
<b>B2: Screening of 15-LOX-1 expressing 1F4 monoclonal cells with RT-PCR analysis after stable transfection of HCT-116 cell lines. ....</b>	<b>120</b>
<b>APPENDIX C .....</b>	<b>121</b>
<b>STANDART CURVES.....</b>	<b>121</b>
<b>C.1 Protein concentration standard curve .....</b>	<b>121</b>
<b>C.2 13-HODE enzyme activity standard curve.....</b>	<b>122</b>
<b>C.3 Activated NFkB standard curve.....</b>	<b>123</b>
<b>C.4: VEGF-A protein concentration standard curve.....</b>	<b>124</b>
<b>CURRICULUM VITAE .....</b>	<b>125</b>

## **LIST OF TABLES**

### **TABLES**

Table 1. Transfection mixture for 5× 10 <sup>5</sup> cells in 6-well plates .....	27
Table 2: 15-LOX-1 PCR reaction mixture.....	29
Table 3: 15-LOX-1 PCR thermal cycling conditions .....	29
Table 4: GAPDH PCR reaction mixture.....	30
Table 5: GAPDH PCR thermal cycling conditions .....	30

## LIST OF FIGURES

### FIGURES

Figure 1. 1: The hallmarks of cancer .....	2
Figure 1. 2 Colorectal carcinogenesis: adenoma—carcinoma sequence .....	7
Figure 1. 3: Inflammation affects the three stages of CRC which are tumor initiation, promotion and progression .....	9
Figure 1. 4 NF- $\kappa$ B signaling pathways. The classical NF- $\kappa$ B pathway activation occurs in response to TNF- $\alpha$ , IL-1 $\beta$ , TLRs, or viruses. ....	10
Figure 1. 5 Mechanism the immune cells and epithelial cells may interact during inflammation and result in the malignant transformation of epithelial cells .....	11
Figure 1. 6 15-LOX-1 enzymes catalyzes conversion of linoleic acid to 13-S-hydroxyoctadecadienoic acid (13-S-HODE) .....	14
Figure 1. 7 Signal transduction of apoptosis.....	17
Figure 1. 8 Metastatic cascade. ....	19
Figure 1. 9 Secreted VEGF-A binds to VEGFR1 and VEGFR2 receptors Red circles are VEGF-A .....	21
Figure 3.1: 15-LOX-1 mRNA expression in HCT-116 CRC cell lines.....	44
Figure 3. 2: 15-LOX-1 protein expression in HCT-116 CRC cell lines.....	45
Figure 3. 3: The enzymatic activity of 15-LOX-1 in HCT-116.....	46
Figure 3. 4: 15-Lipoxygenase-1 (15-LOX-1) reduces the proliferation of HCT-116 CRC cells. ....	47
Figure 3. 5: The lower proliferation of 15-LOX-1 expressing cells can be reversed with the use of a specific inhibitor PD146176. ....	48
Figure 3. 6: Acridine orange staining of 15-LOX-1 expressing HCT116 cells and control cells. ....	49
Figure 3. 7: 15-LOX-1 expression induces apoptosis in colon cancer cells according to acridine orange staining. ....	49
Figure 3. 8: 15-LOX-1 expression induces apoptosis in colon cancer cells by increasing caspase-3 activity.....	50
Figure 3. 9: Distribution of early, late and total apoptotic cells percentages in 15-	

LOX-1 expressing and control HCT116 cells by Annexin V staining. ....	51
Figure 3. 10: 15-LOX-1 expression induces apoptosis in colon cancer cells according to Annexin V staining assay.....	51
Figure 3. 11: 15-LOX-1 expression induces apoptosis in colon cancer cells by decreasing XIAP anti apoptotic protein levels.....	52
Figure 3. 12: 15-LOX-1 expression induces apoptosis in colon cancer cells by decreasing Bcl-xL anti apoptotic protein expression.....	52
Figure 3. 13: Representative photographs show 15-LOX-1 expressing HCT116 cells and control cells colonies by Soft agar assay.....	53
Figure 3. 14: 15-LOX-1 expression decreases anchorage-independent growth on soft agar.....	54
Figure 3. 15: Representative photographs show 15-LOX-1 expressing HCT116 and control cells motility by wound healing assay. ....	55
Figure 3. 16: 15-LOX-1 expression causes a reduction in cell motility. ....	56
Figure 3. 17: 15-LOX-1 expression reduces the ability of HCT-116 cells to adhere to fibronectin. ....	57
Figure 3. 18: Representative photographs show 15-LOX-1 expressing HCT116 and control cells migration by Transwell migration assay. ....	58
Figure 3. 19: 15-LOX-1 expression reduces migration in HCT-116 cells when compared to empty vector (EV) controls. ....	58
Figure 3. 20: Representative photographs show 15-LOX-1 expressing HCT116 and control cells invasion by Matrigel Transwell invasion assay.....	59
Figure 3. 21: 15-LOX-1 expression reduces invasion in HCT-116 colorectal carcinoma cells when compared to empty vector (EV) controls. ....	60
Figure 3. 22: 15-LOX-1 expression decreased colon metastasis associated protein-1 (MTA-1) expression in HCT-116 cells. ....	61
Figure 3. 23: 15-LOX-1 expression reduced secreted VEGF-A165 levels in HCT-116 cells. ....	62
Figure 3. 24: Conditioned medium collected from 15-LOX-1 expressing HCT 116 cells after 72h reduced HUVEC proliferation compared control cells. ....	63
Figure 3. 25: Conditioned medium collected from 15-LOX-1 expressing HCT 116 cells after 72h reduced HUVEC migration compared conditioned medium collected	

from control cells.....	64
Figure 3. 26: Conditioned medium collected from 15-LOX-1 expressing HCT 116 cells after 72h reduced HUVEC motility compared control cells.....	65
Figure 3. 27: Representative photographs show HUVEC Tube Formation Assay (10x objective) in 15-LOX-1 expressing HCT116 and control cells.....	66
Figure 3. 28: Conditioned medium collected from 15-LOX-1 expressing HCT 116 cells after 72h reduced HUVEC tube formation compared conditioned medium collected from control cells.....	67
Figure 3. 29: 15-LOX-1 expression reduces NF- $\kappa$ B p65 nuclear translocation. ....	69
Figure 3. 30: 15-LOX-1 expression affects p-I $\kappa$ B- $\alpha$ and I $\kappa$ B- $\alpha$ amount in cytoplasm in HCT116 cells. ....	70
Figure 3. 31: 15-LOX-1 expression reduces NF- $\kappa$ B DNA binding. ....	71
Figure 3. 32: Luciferase assays indicate reduced NF- $\kappa$ B transcriptional activity in 15-LOX-1 expressing cells.....	72
Figure 3. 33: The 15-LOX-1 expressing cells showed higher PPAR $\gamma$ transcriptional activity compared to the control cells. ....	74
Figure 3. 34: Exogenous 13-(S)-HODE (15-LOX-1 metabolite) showed higher PPAR $\gamma$ transcriptional activity. ....	75
Figure 3. 35: Representative photographs show 15-LOX-1 expressing and control HCT116 cells immunofluorescence assay result for p65.....	76
Figure 3. 36: Inhibition of NF- $\kappa$ B in 15-LOX-1 expressing cells (1E7) could be reversed by treatment with the PPAR $\gamma$ -specific antagonist GW9662 (GW). ....	77
Figure 3. 37: Representative photographs show 15-LOX-1 expressing (1F4) and control HCT116 cells immunofluorescence assay result for p65. ....	78
Figure 3. 38: Inhibition of NF- $\kappa$ B in 15-LOX-1 expressing cells (1F4) could be reversed by treatment with the PPAR $\gamma$ -specific antagonist GW9662 (GW). ....	78
Figure 3. 39: Representative photographs show 15-LOX-1 expressing and control HCT116 cells immunofluorescence assay result for p50.....	79
Figure 3. 40: Inhibition of NF- $\kappa$ B in 15-LOX-1 expressing cells (1E7) could be reversed by treatment with the PPAR $\gamma$ -specific antagonist GW9662 (GW). ....	80
Figure 3. 41: Representative photographs show 15-LOX-1 expressing (1F4) and control HCT116 cells immunofluorescence assay result for p50. ....	81

Figure 3. 42: Inhibition of NF-κB in 15-LOX-1 expressing cells (1F4) could be reversed by treatment with the PPAR $\gamma$ -specific antagonist GW9662 (GW) .....	81
Figure 3. 43: Representative photographs show parental HCT-116 cells immunofluorescence studies for p50. ....	82
Figure 3. 44: Nuclear translocation of NF-κB p50 reduced after 13(S)-HODE treatment in parental HCT-116 cells. ....	83
Figure 3. 45: Representative photographs show parental HCT-116 cells immunofluorescence studies for p65. ....	84
Figure 3. 46: Nuclear translocation of NF-κB p65 reduced after 13(S)-HODE treatment in parental HCT-116 cells. ....	84
Figure 3. 47: Luciferase assays indicating increased transcriptional activity of NF-κB when the 15-LOX-1 expressing HCT-116 cells (1F4) were treated with the PPAR $\gamma$ -specific antagonist GW9662 (GW). ....	85
Figure 3. 48: Luciferase assays indicating increased transcriptional activity of NF-κB when wild-type HCT-116 cells incubated with 100 $\mu$ M 13(S)-HODE were treated with the PPAR $\gamma$ -specific antagonist GW9662 (GW).....	86
Figure 3. 49: The proliferation of 15-LOX-1 expressing cells increases when PPAR $\gamma$ is inhibited.....	88
Figure 5. 1: pcDNA3.1/Zeo (+) 5015 nucleotides Plasmid Map .....	117
Figure 5. 2: pSV- $\beta$ -Galactosidase Plasmid Map .....	118
Figure 5. 3: Screening of 15-LOX-1 expressing 1E7 monoclonal cells with RT-PCR analysis after stable transfection of HCT-116 cell lines. ....	119
Figure 5. 4: Screening of 15-LOX-1 expressing 1F4 monoclonal cells with RT-PCR analysis after stable transfection of HCT-116 cell lines. ....	120
Figure 5. 5: Protein concentration standard curve .....	121
Figure 5. 6: 13-HODE enzyme activity standard curve .....	122
Figure 5. 7: Activated NFKB standard curve.....	123
Figure 5. 8: VEGF-A protein concentration standard curve .....	124

## **LIST OF ABBREVIATIONS**

- TNF- $\alpha$ : Tumor necrosis factor alpha  
H<sub>2</sub>O<sub>2</sub> : Hidrojen peroksit  
DNA: Deoxyribonucleic acid  
BRCA1: Breast cancer type 1 susceptibility gene  
BLM: Bloom syndrome gene  
ATM : Ataxia telangiectasia mutated gene  
Rb: Retinoblastoma  
TP53: Tumor protein 53  
Bax: Bcl-2–associated X protein  
Bim: bcl-2 interacting mediator protein  
Puma: p53 upregulated modulator of apoptosis  
VEGF-A: Vascular endothelial growth factor-A  
TSP-1: Thrombospondin-1  
ECM: Extracellular matrix  
CRC: Colorectal cancer  
ACF: Aberrant crypt foci  
FAP: Familial adenomatous polyposis  
APC: adenomatous polyposis coli  
HNPCC: Hereditary nonpolyposis colorectal cancer  
MLH1: MutL homolog 1  
MSH2: mutS homolog 2  
MSH6: mutS homolog 6  
NF- $\kappa$ B: transcription factor nuclear factor kappa B  
I- $\kappa$ B: Inhibitor of kappa B  
IL-1 $\beta$ : Interleukin-1 beta  
IKK: Inhibitor of kappa kinase  
IL-6: Interleukin-6  
STAT3: Signal transducer and activator of transcription 3  
COXs: Cyclooxygenases  
LOXs: Lipoxygenases

COX-2: Cyclooxygenase-2  
AA: Arachidonic acid  
PGG2: hydroperoxy endoperoxide prostaglandin G2  
PGH2: prostaglandin H2  
TXs: Thromboxanes  
5-LOX: 5-Lipoxygenase  
8-LOX: 8-Lipoxygenase  
12-LOX: 12-Lipoxygenase  
15-LOX: 15-Lipoxygenase  
HPETEs: Hydroperoxy-eicosatetraenoic acids  
5-HETE: 5-Hydroxyeicosatetraenoic acid  
8-HETE: 8-Hydroxyeicosatetraenoic acid  
12-HETE: 12-Hydroxyeicosatetraenoic acid  
15-HETE: 15-Hydroxyeicosatetraenoic acid  
15-LOX-1: 15-Lipoxygenase-1  
13-(S)-HODE: 13-S-hydroxyoctadecadienoic acid  
*ALOX15*: Arachidonate 15-lipoxygenase gene  
IGFR-1: insulin like growth factor- receptor 1  
PPAR- $\gamma$ : Peroxisome proliferator-activated receptor gamma  
MAPK: Mitogen-activated protein (MAP) kinase  
MEK/ERK: Extracellular signal-regulated kinase  
p21: p21 protein  
C-erbB-2: avian erythroblastosis oncogene B 2  
HDACIs: Histone deacetylase inhibitors  
GATA-6: GATA binding protein 6  
TRAIL: TNF-related apoptosis inducing ligand  
FASL: Fas ligand  
TNFR: Tumor necrosis factor receptor  
FADD: Fas-associated death domain  
TRADD: TNF-receptor associated death domain  
Bcl-xL: B cell lymphoma like X  
Bcl-w: Bcl-2-like protein 2

Mcl-1: Myeloid cell leukemia sequence 1  
A1: BCL2-related protein A1  
cIAP1: cellular inhibitor of apoptosis-1  
cIAP2: cellular inhibitor of apoptosis-2  
XIAP: X-linked inhibitor of apoptosis protein  
Smac/DIABLO: a second mitochondria-derived activator of caspases/direct IAP-binding protein with low PI  
MMPs: Matrix metalloproteinases  
MTA1: Metastasis-associated protein 1  
VEGF-A: Vascular endothelial growth factor A  
VEGF-B: Vascular endothelial growth factor B  
VEGF-C: Vascular endothelial growth factor C  
VEGF-D: Vascular endothelial growth factor D  
VEGF-E: Vascular endothelial growth factor E  
PIGF 1-2: Placenta growth factor 1 and 2  
VEGF-A<sub>165</sub>: Vascular endothelial growth factor A isoform  
VEGFR-1: Vascular endothelial growth factor receptor 1  
VEGFR-2: Vascular endothelial growth factor receptor 2  
VEGFR-3: Vascular endothelial growth factor receptor 3  
PC-3 : human prostate cancer cell lines  
PPAR $\alpha$ : Peroxisome proliferator-activated receptor alpha  
PPAR $\delta$ : Peroxisome proliferator-activated receptor delta  
RXR: retinoid X receptor  
PPRE: peroxisome proliferator response elements  
iNOS: Inducible Nitric oxide synthase  
FBS: fetal bovine serum  
DMSO: Dimethylsulfoxide  
LB: Luria-Bertani medium  
OD: Optical density  
PD146176: 6,11-dihydro-[1]benzothiopyrano[4,3-b]indole ( inhibitor of reticulocyte 15-lipoxygenase-1)  
GW9662: 2-chloro-5-nitrobenzanilide (PPAR $\gamma$  antagonist)

U0126: 1,4-diamino-2,3-dicyano-1,4-bis[2-aminophenylthio] butadiene ( inhibitor of ERK 1 and ERK 2

RNA: Ribonucleic acid

DNase-1: Deoxyribonuclease I

MgCl<sub>2</sub>: Magnesium chloride

EDTA: Ethylenediaminetetraacetic acid

DNTPs: deoxynucleotide triphosphates

PCR: polymerase chain reaction

GAPDH: Glyceraldehyde 3-phosphate dehydrogenase

UV: Ultraviolet

MPER: Mammalian Protein Extraction Reagent

PBS: Phosphate buffered saline

NP40: Nonyl phenoxypolyethoxylethanol

HEPES: 4-(2-hydroxyethyl)-1-piperazineethanesulfonic acid

KCl: Potassium chloride

DTT: Dithiothreitol

NaCl: Sodium chloride

PVDF: Polyvinylidene Fluoride

TBS: Tris Buffered Saline

β-meOH: β-mercaptoproethanol

SDS: sodium dodecyl sulfate

Tris-HCl: 2-Amino-2-(hydroxymethyl)-1,3-propanediol hydrochloride

PBS-T: Phosphate Buffered Saline Tween-20

MTT: 3-(4, 5-dimethylthiazol-2-yl)-2, 5-diphenyltetrazolium bromide

SN-50: NF-κB cell permeable inhibitory peptide

AO: Acridine orange

HCl: Hydrochloric acid

RNase A: Ribonuclease A

dH<sub>2</sub>O: Distilled Water

ρNA: ρ-Nitroanilide

CLB: Cell Lysis Buffer

PI: Propidium iodide

FACS: Fluorescence-activated cell sorter analysis  
CO<sub>2</sub>: Carbon dioxide  
BSA: Bovine Serum Albumin  
EBM: Endothelial Basal Medium  
EV: Empty vector  
HUVEC: Human umbilical vein endothelial cells  
DNMT-1: DNA methyltransferase 1  
NuRD: Nucleosome remodeling and histone deacetylase  
IL-4: Interleukin-4  
IL-13: Interleukin-13  
ICAM-1: intercellular adhesion molecule-1  
VCAM-1: vascular cell adhesion molecule-1  
MMP-9: Matrix metalloproteinase 9  
IL-8: Interleukin-8  
1E7: 15-LOX-1 expressing HCT-116 cells monoclonal antibody  
1F4: 15-LOX-1 expressing HCT-116 cells monoclonal antibody

# **CHAPTER 1**

## **INTRODUCTION**

### **1.1 Cancer**

Cancer caused about 7.6 million deaths in 2008 worldwide with about 12.7 new million cancer cases were reported that year according to global cancer statistics in 2011 (Jemal et al, 2011). Cancer is developed by multi-step process which is called tumorigenesis or carcinogenesis and this process is induced basically by carcinogens (Dorai & Aggarwal, 2004). Different environmental carcinogens (cigarette smoke, industrial emissions, gasoline vapors etc.), inflammatory agents (tumor necrosis factor (TNF), H<sub>2</sub>O<sub>2</sub> etc.), tumor promoters (phorbol esters) are able to activate tumorigenesis (Aggarwal et al, 2006; Vickers, 2000). Tumorigenesis is known to be a result of alterations of three types of genes: oncogenes, tumor-suppressor genes and stability genes. The ways that oncogenes are mutated makes the genes constitutively active. Oncogene activations can result from gene amplifications, from chromosomal translocations, or from subtle intragenic mutations affecting important residues that regulate the activity of the gene product. On the other hand, genetic alterations result with the opposite way on tumor-suppressor genes: mutations decrease the activity of these genes' protein. Such inactivations originate from mutations that result in a truncated protein, from missense mutations at residues that are crucial for its activity, from deletions or insertions of various sizes, or from epigenetic silencing. Mutation of stability genes which are the nucleotide-excision repair, mismatch repair, and base-excision repair genes and responsible for repairing mistakes made during normal DNA replication or induced by exposure to mutagens, promotes carcinogenesis in a completely distinctive way. There are some other stability genes such as BRCA1, BLM and ATM that are responsible for controlling processes (mitotic recombination and

chromosomal segregation etc.) which contain large portions of chromosomes. When these three types genes are mutated in single somatic cells or in the germline, this results in sporadic tumors or hereditary predispositions to cancer, respectively. In the germline, subtle mutations are seen widespread, while tumor cells can contain all types of mutations. The clonal expansion that begins the neoplastic process is a result of the first somatic mutation in an oncogene or tumor-suppressor gene. Further rounds of clonal expansion comes from subsequent somatic mutations (Vogelstein & Kinzler, 2004).

## 1.2 The hallmarks of cancer

There are six biological capabilities, which called the hallmarks of cancer, gained during the multistep development of human tumors. They involve sustaining proliferative signaling, evading growth suppressors, resisting cell death, enabling replicative immortality, inducing angiogenesis and activating invasion and metastasis (Fig 1.1) (Hanahan & Weinberg, 2011).

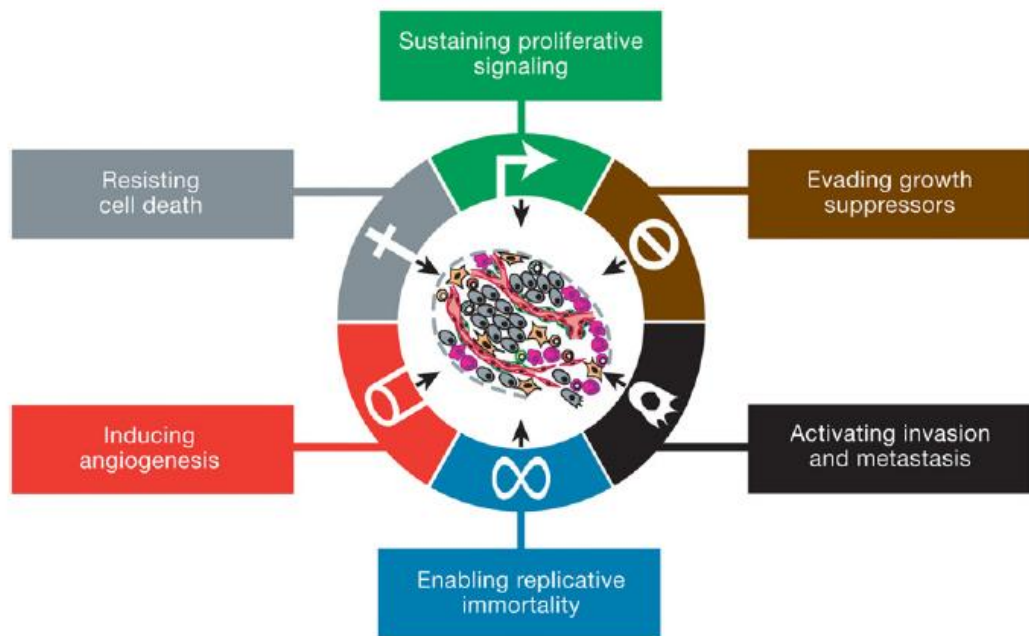


**Figure 1. 1: The hallmarks of cancer (Hanahan & Weinberg, 2011).**

### **1.2.1 Sustaining Proliferative Signaling**

Normal cells need mitogenic growth signals in order to pass into an active proliferative state. These signals are transmitted into the cell by transmembrane receptors that bind discrete classes of signaling molecules: extracellular matrix components, diffusible growth factors, and cell-to-cell adhesion/ interaction molecules. On the other hand, tumor cells produce many of their own growth signals, thereby decreasing their dependence on stimulation from their normal tissue microenvironment (Hanahan & Weinberg, 2000). They may generate growth factor ligands themselves, to which they respond in an autocrine manner through the expression of cognate receptors. Additionally, cancer cells may send signals to normal cells within the supporting tumor-associated stroma which induce the latter to provide the former with various growth factors. Raising the levels of receptor proteins displayed on the cancer cell surface and making such cells hyperresponsive to otherwise-limiting amounts of growth factor ligand may also deregulate receptor signaling. Similarly, structural changes in the receptor molecules may allow the receptor to activate downstream pathways even in the absence of a ligand. The constitutive activation of components of signaling pathways which operate downstream of these receptors may cause cancer cells to become independent from growth factors (Hanahan & Weinberg, 2011).

### **1.2.2 Evading Growth Suppressors**

Operation of multiple anti-proliferative signals in a normal tissue ensures cellular quiescence and tissue homeostasis. These signals which are generally received by the receptor of cell surface contain both soluble growth inhibitors and inhibitors embedded in the extracellular matrix and on nearby cells' surfaces. There are two distinct mechanisms which can block cellular proliferation. First of them involves forcing the cells out of cell cycle into the inactive G0 state where they can stay so until the permission of extracellular signals in the future. Second mechanism

includes induction of cells for proliferative potential loss by the induction that gets them into postmitotic states (Hanahan & Weinberg, 2000).

Emerging cancer cells must escape these anti-proliferative signals in order to proliferate. Many of the signaling pathways that enables normal cells to respond to growth inhibiting signals is related with progression through the cell cycle, specifically the components governing the transit of the cell through the G1 phase of its growth cycle (Hanahan & Weinberg, 2000). The two tumor suppressor genes which encode the Rb and TP53 proteins operate at a key branch point that helps the cell to decide whether to proliferate or, alternatively, enter into senescence or be induced to die by apoptosis (Hanahan & Weinberg, 2011).

### **1.2.3 Resisting Cell Death**

Several sensors that sense cellular abnormalities are known to play key roles in tumor development. DNA damage sensor functioning via the TP53 tumor suppressor is the most prominent one. TP53 is known to induce apoptosis by upregulating the expression of the Noxa and Puma proteins and it also responds to DNA breaks and other chromosomal abnormalities. Tumor cells may have different ways to escape from apoptosis. Most widespread is the loss of TP53 tumor suppressor function, which eliminates this critical damage sensor (Hanahan & Weinberg, 2011).

Alternatively, tumors may increasing the expression of antiapoptotic regulators, such as Bcl-2 family and IAP family or of survival signals (Hanahan & Weinberg, 2011; Miura et al, 2011). Tumor cells may also down regulate proapoptotic factors such as Bax, Bim and Puma, or by destabilizing the extrinsic ligand-induced death pathway (Hanahan & Weinberg, 2011).

#### **1.2.4 Enabling Replicative Immortality**

Proliferation of the most normal cells is limited to a low number of successive growth-and-division cycles due to senescence and crisis which are two distinct proliferation barriers. Senescent cells are usually in irreversible non-proliferative state but they remain viable.

However, crisis includes death of the cells. Accordingly, when cells are grown in culture, there are numerous circumstances leded by repeating cell division cycles. Firstly, they induce the senescence phase and then the cells that are able to overcome this barrier get into a crisis phase in which most of the cells in the population die. Occasionally, cells arise from a crisis phase population and show unlimited replicative capability. This transition is known as immortalization, a trait that most stable cell lines have due to their ability to proliferate in culture without showing either senescence or crisis phase property. Telomeres that provide protection for the ends of chromosomes are actually implicated in the potential for unlimited proliferation. Telomerase is almost absent in nonimmortalized cells but expressed at functionally significant levels in the vast majority (90%) of spontaneously immortalized cells, including human cancer cells. The presence of telomerase activity is correlated with a resistance to induction of both senescence and crisis/apoptosis. On the other hand, suppression of telomerase activity causes telomere shortening and induction of either of these proliferative barriers (Hanahan & Weinberg, 2011).

#### **1.2.5 Inducing Angiogenesis**

Angiogenesis is essential for tumor growth and progression because absence of it limits tumor growth to a few millimeters in diameter by virtue of inadequate nutrients and oxygen diffusion (Chia et al, 2010). An angiogenic switch is almost always activated and stays on during tumor progression and this causes normally

quiescent blood vessels to consistently produce new vessels that help maintain spreading neoplastic growths. Known angiogenic regulators are signaling proteins that bind to stimulatory or inhibitory cell surface receptors demonstrated by vascular endothelial cells. Vascular endothelial growth factor-A (VEGF-A) is a typical inducer of angiogenesis and thrombospondin-1 (TSP-1) is a typical angiogenesis inhibitor (Hanahan & Weinberg, 2011).

### **1.2.6 Activating Invasion and Metastasis**

Tumors' potential to metastasize is a crucial factor of mortality and morbidity of cancer (Il Lee et al, 2011). Malignant carcinomas are characterized by local invasion and distant metastasis (Hanahan & Weinberg, 2011). Invasion ability of tumors beyond hemostatic boundaries and their ability to form metastatic colonies need the complex interaction of different cell surface-related components regulating the proteolytic deterioration of the ECM and the change of cell adhesion features. Integrins, a receptor family, which mediate the cell-ECM interactions mentioned above intervene the adhesion of cells to both ECM proteins to promote cell survival, proliferation and migration (Pidgeon et al, 2007). The most widely observed alteration in cell-to-environment interactions in carcinoma cells involves the loss of the junctional protein E-cadherin. Downregulation and mutations of E-cadherin in human carcinomas provided strong support for its role as a key suppressor of invasion and migration. Additionally, some highly aggressive carcinomas have altered expression of genes encoding other cell-to-cell and cell-to-ECM adhesion molecules. Conversely, adhesion molecules normally related with the cell migrations are often upregulated (Hanahan & Weinberg, 2011).

### 1.3 Colorectal cancer (CRC)

Colorectal cancer develops in the colon or the rectum which are parts of the gastrointestinal system. Over 1 million new cases of colorectal cancer (CRC) are diagnosed worldwide every year. CRC is the 4th most widespread cause of cancer mortality and the 3rd most widespread malignancy worldwide (Terzic et al, 2010). Colon tumors appear when there is a disruption of the homeostatic mechanisms regulating cell proliferation, differentiation, and cell death. Adenomatous polyps develop as an early appearance of an imbalance in tissue homeostasis. These widespread neoplastic lesions appear initially as aberrant crypt foci (ACF), later go through the sequel of adenoma, carcinoma *in situ*, and finally, invasive adenocarcinoma (Fig. 1.2) (Cathcart et al, 2011).

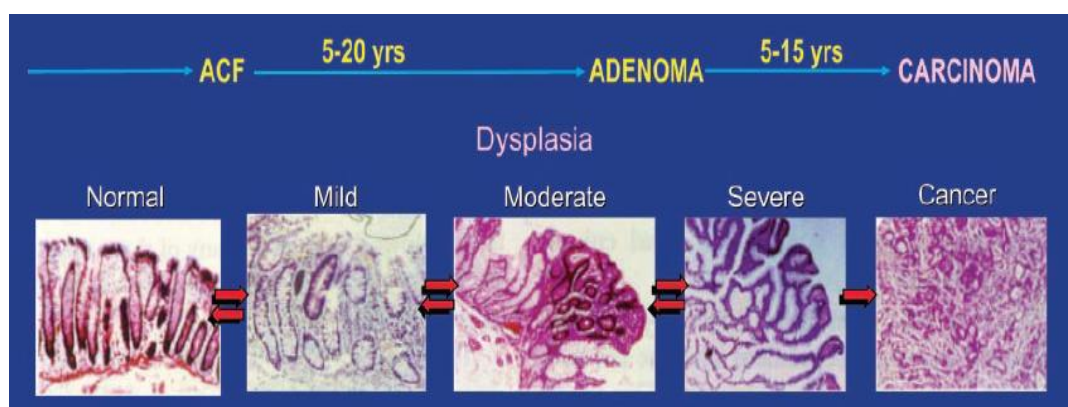


**Figure 1. 2 Colorectal carcinogenesis: adenoma—carcinoma sequence**  
(Kelloff et al, 2004).

A large body of evidence indicates that genetic mutations, epigenetic changes, chronic inflammation, diet, lifestyle and aging are risk factors for CRC (Wang & DuBois, 2010). There are minimum three main forms of CRC which are hereditary, sporadic, and colitis-associated makes it called as a heterogeneous disease. Familial adenomatous polyposis (FAP) occurs due to a germ-line mutation in one allele of the tumor suppressor gene adenomatous polyposis coli (APC) and patients with FAP have nearly a 100% risk of developing CRC by the age of 40, if

left untreated. Sporadic CRC corresponds to over 90% of all cases and approximately 85% of the cases show a loss of APC function. While sporadic colon tumors are generally related with dietary and environmental factors, a small proportion of cases can comprise due to autosomal dominant single gene defects. Hereditary nonpolyposis colorectal cancer (HNPCC) is due to inherited mutations in the DNA mismatch repair genes MLH1, MSH2, and MSH6 and it is responsible for approximately 2 to 7 percent of all diagnosed cases of CRC (Terzic et al, 2010).

#### **1.4 Inflammation and Colorectal cancer**

Inflammation is the body's response to acute tissue damage. It is characterized by leukocyte infiltration to the affected area as a result of exposure to allergens and toxic chemicals, microbial infections, autoimmune disease and obesity (Hartnett & Egan, 2012). In inflammation, the first response is the extravasation of leukocytes including, eosinophils, neutrophils and monocytes to the sites of damage. ECM which is formed by neutrophils serves as a scaffolding unit for proliferation and migration of endothelial cells and fibroblasts (Coussens & Werb, 2002).

CRC is considered as an inflammatory cancer (Karin, 2006b). Inflammation affects the three stages of CRC, which are, tumor initiation, tumor promotion and tumor progression (Fig 1.3). The inflammatory environment, which consists of cytokines, chemokines and reactive oxygen and nitrogen species, results in DNA mutations, epigenetic changes and genomic instability that can contribute to tumor initiation. Chronic inflammation promotes tumor promotion, which involves the proliferation of genetically altered cells, by inhibiting apoptosis and accelerating angiogenesis. Inflammation also affects metastasis, which involves an increase in tumor size, additional genetic changes and the spreading of the tumor from its primary site to multiple sites. In this case, the close interaction of cancer cells, immune cells and stromal elements and the factors produced by each of these cell types can act to promote metastasis (Hartnett & Egan, 2012).

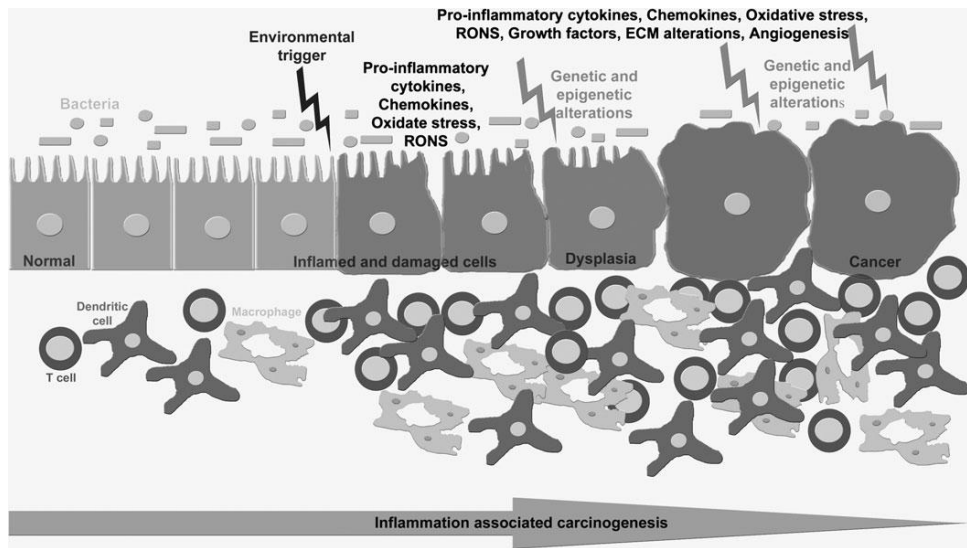


**Figure 1. 3: Inflammation affects the three stages of CRC which are tumor initiation, promotion and progression (Hartnett & Egan, 2012).**

Cytokines can be considered to have pro-inflammatory or anti-inflammatory effects. The balance between the levels of these cytokines plays a crucial role in inflammation-associated carcinogenesis. The pro-inflammatory cytokine tumor necrosis factor- $\alpha$  (TNF- $\alpha$ ) is a well-known player in chronic inflammation and it is also crucial in cancer where it acts as a tumor initiator by inducing the production of molecules that lead to DNA damage and mutations, and as a tumor promoter by altering cell proliferation and cell death (Hartnett & Egan, 2012).

Inflammatory mediators activate the oncogenic transcription factor nuclear factor kappa B (NF- $\kappa$ B), which plays a critical role in linking inflammation and carcinogenesis. NF- $\kappa$ B is frequently dysregulated in many cancers including colorectal cancer, leading to increased cellular transformation, proliferation and loss of apoptosis. NF- $\kappa$ B family has five proteins in mammalian cells: RelA (also known as p65), c-Rel, RelB, p105/p50 (NF- $\kappa$ B1), and p100/p52 (NF- $\kappa$ B2) (Dai et al, 2011). In unstimulated cells, the NF- $\kappa$ B subunits bind to inhibitor of kappa B (I- $\kappa$ B) and are sequestered away from the - $\kappa$ B elements of target promoter regions (Karin, 2006a). Following a pro-inflammatory stimulus such as bacterial products via Toll-like

receptors or cytokines (IL-1 $\beta$  and TNF- $\alpha$ ) and viruses, I- $\kappa$ B is degraded in the proteosome following phosphorylation by inhibitor of kappa kinase (IKK). NF- $\kappa$ B dimers (most commonly p65 and p50) then translocate to the nucleus and activate the transcription of several hundred target genes which have roles in processes as diverse as immune response, cellular differentiation, proliferation, and survival (Fig 1.4) (Hayden & Ghosh, 2008; Karin, 2006b; Wang et al, 2009).

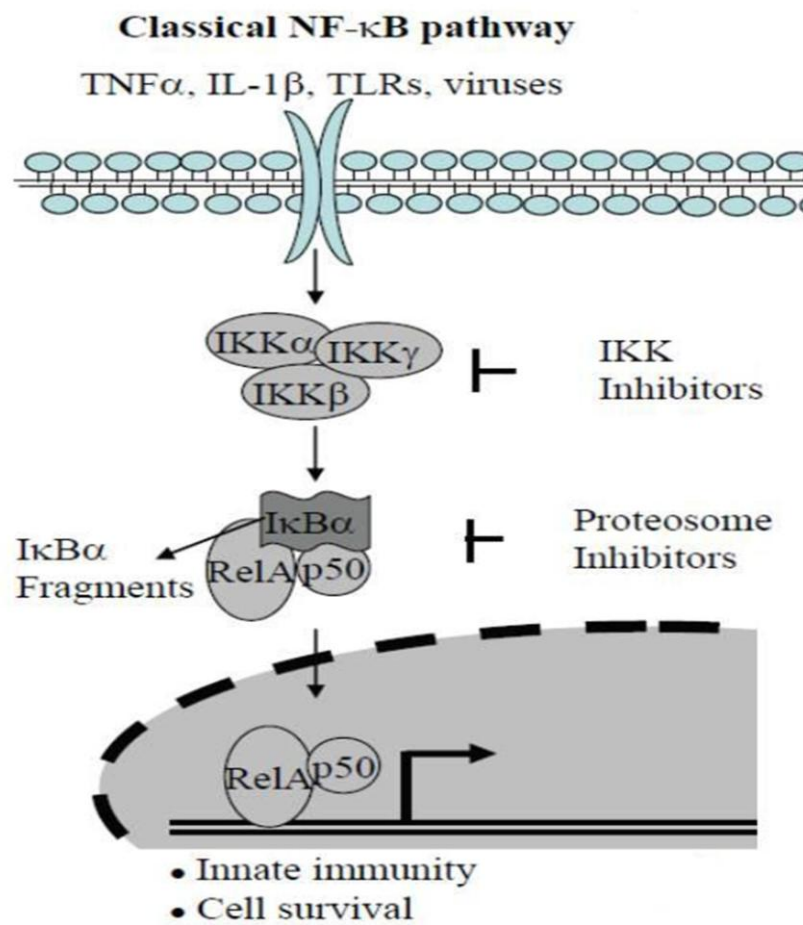


**Figure 1. 4 NF- $\kappa$ B signaling pathways. The classical NF- $\kappa$ B pathway activation occurs in response to TNF- $\alpha$ , IL-1 $\beta$ , TLRs, or viruses.**

Intermediated kinases convey signals to the I $\kappa$ B complex formed by I $\kappa$ B $\alpha$  and proteasome degradation. P105/RelA is processed to p50/RelA, which translate to the nucleus and bind promoters of genes regulating innate immunity and cell survival (Wang et al, 2009).

Numerous studies have showed that NF-κB can block apoptosis by regulating the anti-apoptotic proteins such as inhibitor of apoptotic proteins (IAPs). Another mechanism whereby NF-κB may suppress apoptosis is via its inhibition ability prolonged c-Jun N-terminal kinases (JNK) activation and accumulation of reactive oxygen species (Wang et al, 2009).

Activated of NF-κB provides an environment that can promote tumorigenesis if an immune response is sustained (Grivennikov & Karin, 2010). During inflammation, NF-κB is activated in the immune cells and this ends up with raised TNF- $\alpha$  and IL-6. These cytokines, can, in turn up regulate NF-κB and STAT3 in the epithelial cells, ending up with inhibition of apoptosis and increased proliferation of the epithelial cells. In addition, the increased IL-6 can also activate methyl transferases in the epithelial cells, which can change gene expression of tumor suppressor genes. Overall, this provides an environment conducive to malignant transformation (Fig. 1.5) (Hartnett & Egan, 2012).

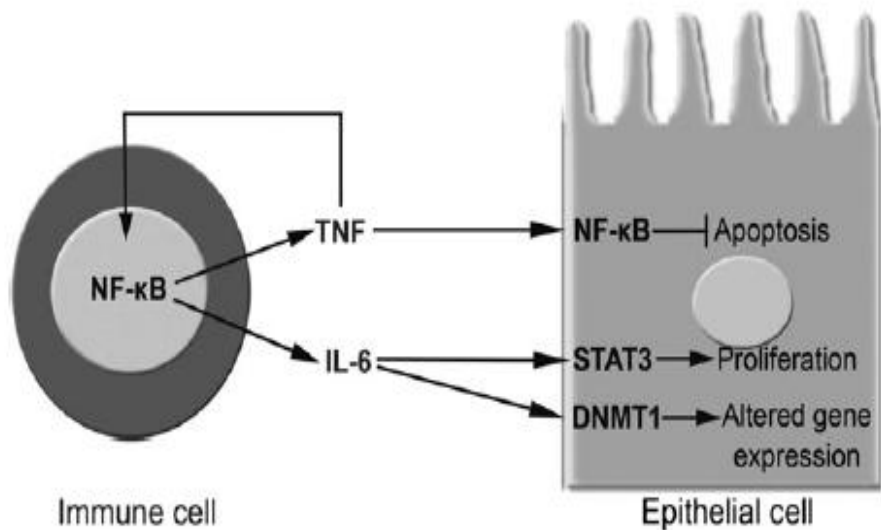


**Figure 1. 5 Mechanism the immune cells and epithelial cells may interact during inflammation and result in the malignant transformation of epithelial cells (Hartnett & Egan, 2012).**

Alternatively, eicosanoids such as prostaglandins, leukotrienes, thromboxanes and hydroxyl eicosatetraenoic acids play a crucial role in associating inflammation with CRC. Overexpression of COX-2 and LOX enzymes, which metabolize arachidonic acid to produce bioactive lipids, which act as endogenous mediators of inflammation as well as carcinogenesis (Mal et al, 2011).

### **1.5 Arachidonic Acid Pathway**

The arachidonic acid (AA) pathway is responsible for the production of various bioactive metabolites (Cathcart et al, 2011). Eicosanoids are derivatives of twenty carbon fatty acids that constitute a crucial class of bioactive lipid mediators. Type IV cytosolic phospholipase A2 initiates arachidonic acid release from the cell membrane and then arachidonic acid is subsequently turned into eicosanoids such as prostaglandins, leukotrienes and lipoxins (Krishnamoorthy & Honn, 2011).

Cyclooxygenases (COXs) and lipoxygenases (LOXs) are two major pathways for eicosanoid production. The COX pathway, which has two isoforms known as COX-1 and COX-2, forms the prostaglandins PGG2 and PGH2. Then these prostaglandins are further turn into prostacyclin and thromboxanes (TXs). LOXs form a family of non-heme iron dioxygenases that add molecular oxygen into specific regions of free and/or esterified polyunsaturated fatty acids. LOX enzymes are termed as 5-LOX, 8-LOX, 12-LOX and 15-LOX according to the position of the carbon on the fatty acid where the oxygen is inserted. The LOX enzymes catalyze arachidonic acid (AA) to the biologically active metabolites hydroperoxy-eicosatetraenoic acids (HPETEs). After that, reduction of HPETEs ends up with the production of corresponding HETEs. 5-, 8-, 12- and 15-HETE are the main AA metabolites produced by mammalian LOXs. Addionally, LOX enzymes metabolize linoleic acid oxygenation reaction which produces 9- and 13-HODE. The expression of these enzymes varies throughout the progression of various cancers, and thereby they have been shown to regulate various aspects of tumor development (Pidgeon et al, 2007).

## **1.6 Lipoxygenase pathway and colon cancer**

There are various isoforms of LOXs that have been found in humans which complicates our understanding on the role of them in colorectal cancer development and progression (Cathcart et al, 2011). Wasilewicz et al. (2010) stated a strong correlation between 5-LOX expression and polyp size increase, higher tumor grade and histological determination of localization supporting the expression of 5-LOX in the early stages of colorectal cancer (Wasilewicz et al, 2010). In another study, Melstrom et al (2008) observed increased expression of 5-LOX in villous adenoma and colon adenocarcinoma as compared to normal colorectal mucosa (Melstrom et al, 2008). Additionally, Cathcart et al (2011) found a small increase in expression of 12-LOX in many colorectal cancers. According to these findings, 5-LOX expression is an event observed in early periods of colon cancer, with increased expression in adenoma frequent. However, 12-LOX expression seems to be an event occurring later, probably mediating invasion and metastasis (Cathcart et al, 2011). Recently, Shureiqi et al. (2010), investigated 5-LOX, 12-LOX, 15-LOX-1 and 15-LOX-2 levels in a prospective study of 125 patients and they figured out no differences in 12- or 15-HETE or leukotriene B4 levels between normal, polyp and cancer mucosa. However, the expression of 13(S)-HODE which is a 15-LOX-1 metabolite disappeared through this progressive sequence (Shureiqi et al, 2010).

## **1.7 15-Lipoxygenase-1 (15-LOX-1)**

15-LOX-1 is an inducible and highly regulated enzyme in normal human cells that plays a key role in the conversion of linoleic acid to 13-S-hydroxyoctadecadienoic acid (13-S-HODE) (Fig 1.6) (Zuo & Shureiqi, 2012).

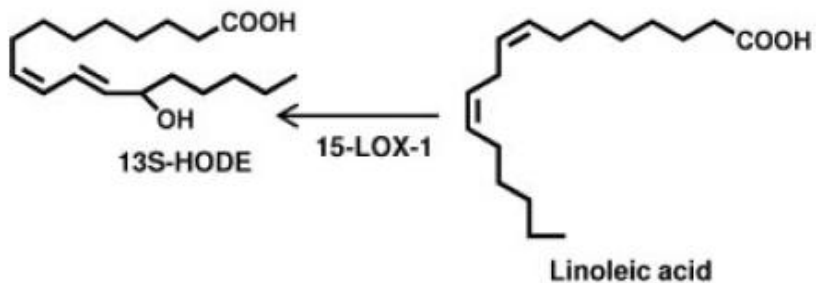


**Figure 1. 6 15-LOX-1 enzymes catalyzes conversion of linoleic acid to 13-S-hydroxyoctadecadienoic acid (13-S-HODE) (Mal et al, 2011).**

Fluorescent in situ hybridization (FISH) indicated the localization of the human *ALOX15* gene on chromosome 17p13.3 (Kelavkar et al, 1998). Human 15-LOX-1 is a 75 kDa protein and consists of a single polypeptide chain. The crystal structure of rabbit of 12/15 lipoxygenase, which shares 81% amino acid identity to human 15-LOX-1 has been solved (Gillmor et al, 1997; Kuhn & Thiele, 1999). It consists of two domains: the large C-terminal domain is believed to be the catalytic domain and essential for enzymatic activity; the catalytic non-heme iron is buried deeply inside and shuttles between the active ferric and inactive ferrous forms during the catalytic cycles; the small N-terminal domain is involved in membrane binding (Walther et al, 2002).

In humans, expression of 15-LOX-1 is observed predominantly in eosinophils, airway epithelial cells, macrophages, dendritic cells and mast cells (Gulliksson et al, 2007; Kuhn et al, 2002). 15-LOX-1 expression was reported in normal colorectal and pancreatic tissue while abolished in the corresponding tumor tissue (Hennig et al, 2007; Shureiqi et al, 2007). Several studies have shown that 15-LOX-1 is present at higher levels in prostate cancer tissue when compared with the normal surrounding tissue (Kelavkar et al, 2002). 15-LOX-1 is also downregulated in lung cancer and breast cancer (Zuo & Shureiqi, 2012).

## **1.8 15-LOX-1, 13-(S)-HODE, in colon tumorigenesis**

15-LOX-1 enzyme plays a role in inflammation, cell differentiation and maturation, asthma, atherogenesis and carcinogenesis (Krishnamoorthy & Honn, 2011). Although 15-LOX-1 expression loss is common in human cancer cells (Zuo & Shureiqi, 2012), earlier studies reported a protumorigenic role for 15-LOX-1 based on the following observations: 1) 15-LOX-1 could be induced by an oncogenic mutant form of p53 in prostate cancer cells (Kelavkar & Badr, 1999). 2) The enzyme could exert pro-tumorigenic effect by upregulating the MAP kinase pathway and disrupting the balance of Bcl family members across mitochondrial membrane through its main metabolite 13(S)-HODE in prostate cancer (Kelavkar et al, 2002). 3) 15-LOX-1 also contributes to prostate cancer bone metastasis by increasing insulin like growth factor- receptor (IGFR-1) expression (Kelavkar & Cohen, 2004). 4) Hsi et al. (2001) demonstrated that 13-S-HODE down-regulated PPAR- $\gamma$  expression by increasing its phosphorylation via an MAPK-signaling-dependent pathway in HCT-116 colon cancer cell line, 5) Yoshinaga et al. (2004) showed that forced expression of 15-LOX-1 in colon cancer cell lines and resultant increase in the 13-S-HODE metabolite activated the MEK/ERK signal transduction pathway and inhibited expression of the p21 tumour suppressor (Yoshinaga et al, 2004) 6) Transfection of C-erbB-2, which is a proto-oncogene similar to epidermal growth factor, increases 13-S-HODE production in normal fibroblast cells (Glasgow & Everhart, 1997). 7) The activity of 13-HODE dehydrogenase, that catalyzes 13-S-HODE to 13-oxooctadecadienoic acid, reduces as colonic epithelial cells undergo malignant transformation (Bronstein & Bull, 1993).

However, following studies support that 15-LOX-1 has an anti-tumorigenic role in colorectal and other cancer cells. 1) Nixon et al. (2004) showed that 15-LOX-1 expression was downregulated in colorectal cancer epithelia compared with normal colonic epithelia (Nixon et al, 2004). 2) Higher ratios of 15-LOX-1 expression in tumor tissue to 15-LOX-1 expression in normal tissue were related with better prognosis in patients with stage IV colorectal cancer (Heslin et al, 2005).

3) 15-LOX-1 re-expression via nonsteroidal anti-inflammatory drugs, histone deacetylase inhibitors (HDACIs) or transfection with plasmid or adenoviral vectors inhibits tumorigenesis in cancer cells (Zuo et al, 2008b). 4) The induction of terminal differentiation in transformed Caco-2 colonic cells was related with 15-LOX-1 expression and 13-HODE production in these cells (Kamitani et al, 1998). 5) Promoter analysis of *ALOX15* indicated that expression of the gene is suppressed in tumors by several mechanisms acting in concert, such as promoter methylation, binding of the nucleosome remodeling and histone deacetylase repression complex, and through the overexpression of the transcription factor GATA-6 (Liu et al, 2004; Shureiqi et al; Zuo et al, 2009). 6) Selective molecular targeting of 15-LOX-1 expression was shown to be sufficient to inhibit tumorigenesis in mice (Wu et al, 2008). 7) Recently, Zuo et al. have reported that targeted transgenic 15-LOX-1 expression in the intestine suppresses azoxymethane-induced colonic tumorigenesis (Zuo et al, 2012). 8) 13-HODE inhibits proliferation and induces apoptosis in cancer cells via peroxisome proliferator-activated receptor-gamma activation (Zuo & Shureiqi, 2012). 9) Other studies also indicated that 13-HODE inhibit tumorigenesis: 13-HODE attenuates ornithine decarboxylase activity in rat colons, reverses skin hyperproliferation in guinea pigs, and induces apoptosis in leukemia cells in vitro (Zuo & Shureiqi, 2012).

### **1.9 15-LOX-1 and Apoptosis**

Programmed cell death, known as apoptosis, is considered as a natural barrier to development of cancer (Hanahan & Weinberg, 2011). Definition of apoptosis is made with its morphological characteristic, involving cell shrinkage, membrane blebbing, chromatin condensation and nuclear fragmentation at the beginning (Lowe & Lin, 2000). There are two main apoptosis pathways, namely, extrinsic pathway (the death receptor-mediated apoptotic pathway) and intrinsic pathway (the mitochondrial-mediated apoptotic pathway). The extrinsic pathway is begun when TNF-related apoptosis inducing ligand (TRAIL), tumor necrosis factor- $\alpha$  (TNF- $\alpha$ ), or Fas ligand attaches to their receptors (Fig. 1.7) (Miura et al, 2011).

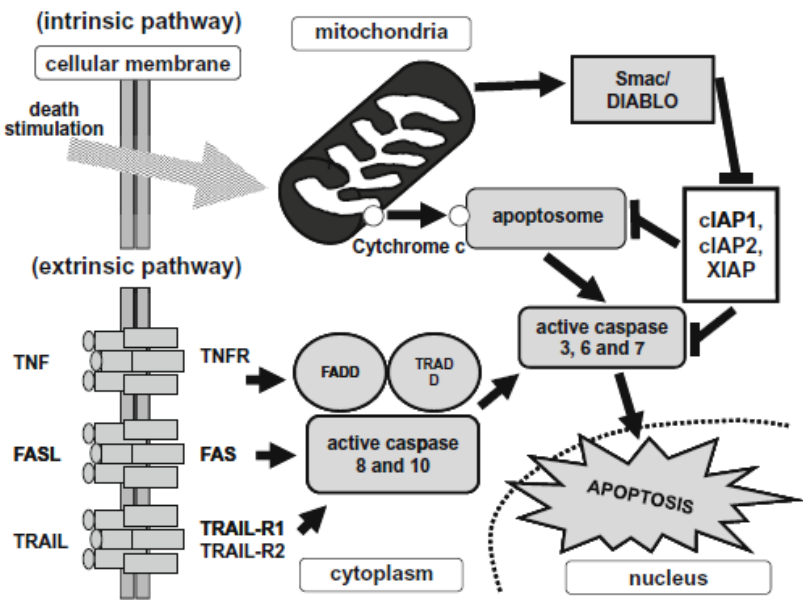


**Figure 1. 7 Signal transduction of apoptosis.**

TNF, tumor necrosis factor; TNFR, tumor necrosis factor receptor; TRAIL, TNF-related apoptosis-inducing ligand; FASL, FAS ligand; FADD, Fas-associated death domain; TRADD, TNF-receptor associated death domain (Miura et al, 2011).

However, the release of free cytosolic cytochrome c from mitochondria begins the intrinsic pathway. The caspase-activating complex assembly which is called the apoptosome is promoted by cytochrome c. The activity of apoptosome and caspase 9 are functionally identical. Both of them induce apoptosis by activating executor caspases 3, 6, and 7 (Miura et al, 2011).

Counterbalancing pro- and anti-apoptotic proteins control an apoptotic trigger that transmits signals between the regulators and effectors (Adams & Cory, 2007). Bcl-2 (closest relatives Bcl-xL, Bcl-w, Mcl-1, and A1) and IAP family (cIAP1, cIAP2, and XIAP) are inhibitors of apoptosis (Hanahan & Weinberg, 2011; Miura et al, 2011). Most of the members of Bcl-2 family suppress Bax and Bak (present on the outer membrane mitochondrial) proapoptotic triggering proteins by binding to them. The integrity of the outer mitochondrial membrane is deteriorated if Bax and Bak proteins get rid of inhibition by their antiapoptotic relatives (Hanahan &

Weinberg, 2011). Alternatively, cIAP1, cIAP2, and XIAP block activation of pro-caspase 9 which is induced by cytochrome c and by this way they can suppress the cleavage of pro-caspases 3, 6, and 7 in the intrinsic pathway. Therefore, the downregulation of cIAP1, cIAP2, and XIAP increases the apoptosis and susceptibility of colon cancer cells to anticancer drugs. However, these IAP proteins don't affect the extrinsic pathway. Recent evidence indicates that a second mitochondria-derived activator of caspases (Smac)/direct IAP-binding protein with low PI (DIABLO) (Smac/DIABLO) which is present in the mitochondrial inter membrane can inhibit the activity of cIAP1, cIAP2, and XIAP. In other words, Smac/DIABLO binds to IAP proteins in order to remove their inhibitory activity and this activates caspase 9 (Miura et al, 2011).

Previous studies indicated that 15-LOX-1 re-expression via plasmid or adenoviral vector transfection induces apoptosis in human CRC cells (Zuo & Shureiqi, 2012). Following studies by other independent groups further reported that 15-LOX-1 might increase apoptosis by down-regulation of anti-apoptotic proteins, like XIAP and BcL-XL in CRC cells both in vitro and in vivo (Wu et al, 2008; Yuri et al, 2007). 15-LOX-1 expression also induces apoptosis in other cancer, such as oesophageal and gastric cancer cells (Bhattacharya et al, 2009).

### **1.10 15-LOX-1 and CRC Metastasis**

Metastasis is a complex group of the process which includes the detachment of neoplastic cells from the primary tumor, penetration into the blood and lymphatic system, arrest at distant sites by adhesion to endothelial cells (intravasation), extravasation, induction of angiogenesis, evasion from host antitumor responses, and growth at metastatic sites (Fig. 1.8) (Kawasaki et al, 2008).

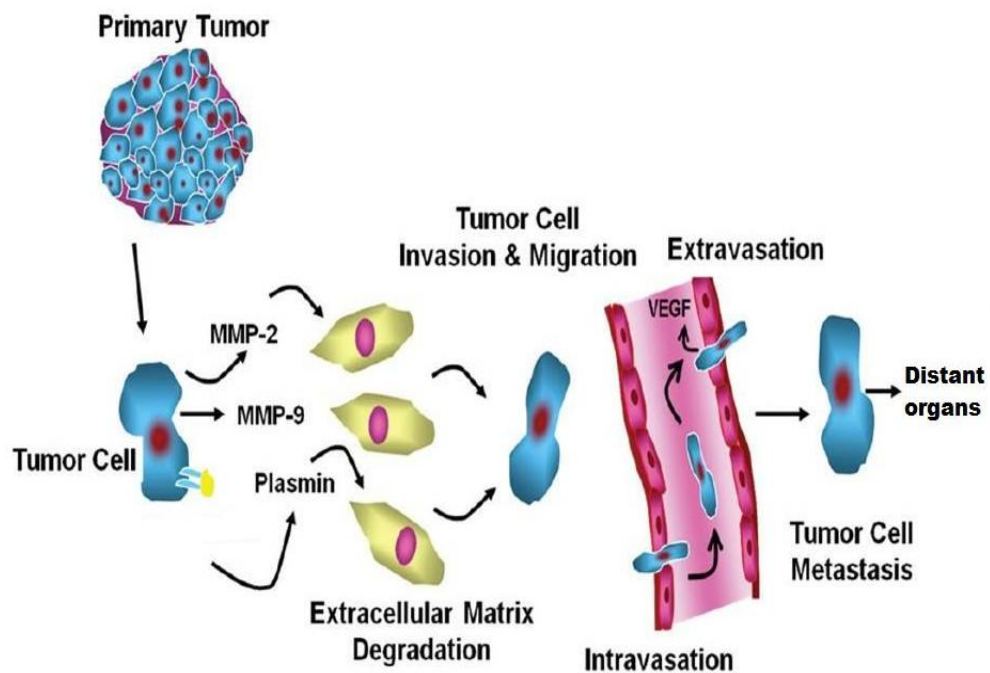


**Figure 1. 8 Metastatic cascade.**

The molecular basis of tumor metastasis depends on local invasion, intravasation, survival in the circulation, extravasation and colonization. Tumor cells secrete several factors including proteases like MMPs and plasmin which degrade extracellular matrix facilitating their migration and invasion. Tumors cells then intravasate through the endothelial lining of blood vessels into the circulation, and extravasate to distant organs like lymph nodes, bones and rectum (Dasgupta et al, 2012).

There are many metastasis-related genes which are controlling metastasis. One of these genes which is named as Metastasis-associated gene 1 (MTA1) is positively related with cancer metastasis (Qian et al, 2007). MTA1 protein is a component of the nucleosome remodeling and histone deacetylation complex, and is related with ATP-dependent chromatin remodeling and histone deacetylase activity (Kawasaki et al, 2008). The experimentally forced expression of MTA1 indicated that MTA1 increases migration and invasion of carcinoma cells initiating and promoting metastatic spread (Hofer et al, 2009). MTA1 mRNA levels are significantly higher and correlated with deeper invasion and lymph node metastasis in patients with colorectal and gastric carcinomas (Kai et al, 2011; Kawasaki et al, 2008).

According to many experimental models, metastasis capability of tumor cells is significantly affected by 15-LOX-1. The attachment ability of cancer cells to endothelial cells and their metastasis capability have been inversely related with 13-HODE levels in mice. Additionally, metastasis in murine endothelial cells is suppressed by transgenic 15-LOX-1 expression (Il Lee et al, 2011). Furthermore, 15-LOX-1 re-expression in CRC cell lines suppresses invasion in vitro model and peritoneal metastases invasiveness in vivo model (Sasaki et al, 2006). Therefore, lack of 15-LOX-1 expression in CRC cells seems to improve their metastatic capability. Recently, Zuo et al. (2009) reported that MTA1 which acts as part of the NuRD complex contributes to colonic tumorigenesis by inhibiting 15-LOX-1 transcription, suggesting the presence of an interaction between MTA1 and 15-LOX-1 (Zuo et al, 2009).

### **1.11 15-LOX-1 and CRC Angiogenesis**

Angiogenesis is known as a process of new blood vessel formation and this process has an important role in the tumor growth and metastasis (Chia et al, 2010). After binding of angiogenic factors to specific receptors in endothelial cell, endothelial cells proliferate, invade the basement membrane, migrate, differentiate, and finally form new capillary tubes (Reinmuth et al, 2003).

Vascular endothelial growth factor (VEGF) family is commonly examined and known to be the most specific regulator of angiogenesis (Zhang et al, 2010). There are six secreted glycoproteins in this family with names; VEGF-A, VEGF-B, VEGF-C, VEGF-D, VEGF-E, and placenta growth factor (PlGF) 1 and 2 (Prat et al, 2007). The human VEGF-A gene which is localized in chromosome 6p21.3 is organized in eight exons, separated by seven introns (Ferrara, 2004). Four different isoforms are generated as a result of alternative exon splicing in humans. These isoforms consist of 121, 165, 189, and 206 amino acids, respectively and therefore called VEGF-A<sub>121</sub>, VEGF-A<sub>165</sub> and VEGF-A<sub>189</sub> and VEGF-A<sub>206</sub>. VEGF-A<sub>165</sub> is a heparin-binding homodimeric glycoprotein of 45 kDa and is the major VEGF isoform (Ferrara, 2004; Mackenzie & Ruhrberg, 2012).

There are three VEGF receptors: VEGFR-1, VEGFR-2, and VEFGR-3. They possess tyrosine kinase activity and are expressed almost exclusively on endothelial cells (Reinmuth et al, 2003). All secreted VEGF-A isoforms bind to VEGFR1 and VEGFR2 receptors (Fig 1.9) (Mackenzie & Ruhrberg, 2012). After VEGF is bound to these two receptors, they dimerize, and become autophosphorylated by each other's tyrosine kinase domain, which leads to an active receptor initiating a signaling cascade (Prat et al, 2007).

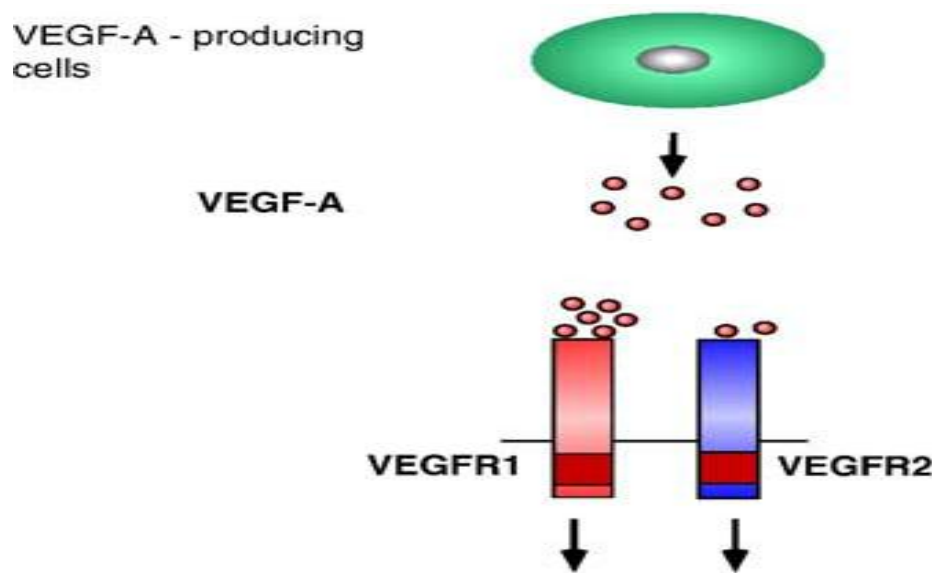


**Figure 1.9 Secreted VEGF-A binds to VEGFR1 and VEGFR2 receptors Red circles are VEGF-A (Shibuya & Claesson-Welsh, 2006).**

Many tumor cell lines secrete VEGF in vitro, which suggests the possibility that this diffusible molecule may be a primary mediator of tumor angiogenesis. In situ hybridization studies have showed that the VEGF mRNA is expressed in the vast majority of human tumors so far investigated, including lung carcinoma, breast carcinoma, gastrointestinal tract carcinoma, kidney carcinoma, and bladder carcinoma (Ferrara, 2004). Overexpression of VEGF has been correlated with tumor progression and poor prognosis in several tumor systems, involving CRC (Prat et al, 2007).

15-LOX-1 was shown to exert anti-angiogenic effects by inhibiting VEGF-A and placental growth factor in a rabbit skeletal muscle experimental model (Viita et al, 2008). However, the role of 15-LOX-1 in angiogenesis during tumorigenesis remains controversial. In one model, overexpression of 15-LOX-1 in PC-3 human prostate cancer cells increased VEGF in vitro and angiogenesis in subcutaneous xenografts (Kelavkar et al, 2001). In contrast, there are several evidence that supports an anti-angiogenic role for 15-LOX-1, particularly via 13-HODE. One study showed that 13-HODE suppresses tumor cell adhesion to subendothelial matrix, fibronectin and endothelial cells (Il Lee et al, 2011). Harats et al. (2005) demonstrated that 15-LOX-1 inhibits tumor growth and metastasis in transgenic mice models overexpressing 15-LOX-1 in endothelial cells (Harats et al, 2005). The cancer models used were mammary gland and Lewis lung carcinomas. The metastases of the transgenic mice had increased numbers of apoptotic cells and a complicated network of numerous small blood vessels, indicating that 15-LOX-1 may have an anti-angiogenic role in cancer (Bhattacharya et al, 2009). Viita et al. (2008) showed that 13-S-HODE acts as a ligand for PPAR $\gamma$  and binds to the promoter region of VEGFR2 and thus inhibits VEGF-induced VEGFR2 expression, inhibiting angiogenesis (Viita et al, 2008). However, evidence from similar studies related to colorectal cancer has been lacking (Bhattacharya et al, 2009).

### **1.12 Mechanism of 15-LOX-1 tumor suppressive effect in CRC**

The underlying mechanism through which 15-LOX-1 regulates apoptosis and cell proliferation has not been well studied yet. The possible mechanisms could be 1) introduction of 15-LOX-1 can lead to oxidative stress (Sordillo et al, 2005), 2) 15-LOX-1 induces growth arrest through protein kinase-dependent pathways and phosphorylation of p53 (Kim et al, 2005), 3) 15-LOX-1-derived oxidative metabolites of linoleic and arachidonic acid are natural ligands of peroxisome proliferator activated receptors (PPARs) which regulate cell proliferation and apoptosis (Shureiqi et al, 2003; Zuo et al, 2006), 4) 15-LOX-1-derived oxidative metabolites of linoleic acid inhibit PPAR $\gamma$  activity via MAP kinase phosphorylation (Shao et al, 1998).

PPARs are transcription factors belonging to the ligand-activated nuclear receptor superfamily. Three major types have been identified: PPAR $\alpha$ , PPAR $\delta$  and PPAR $\gamma$  (Lee et al, 2006). PPAR $\gamma$  is expressed in adipocytes and epithelial cells. Ligand activated PPAR $\gamma$  heterodimerizes with retinoid X receptor (RXR) and this complex then recruits coactivators and corepressors before binding to peroxisome proliferator response elements (PPRE) in the promoters of target genes regulating lipid and carbohydrate metabolism and inflammation (Rumi et al, 2004). A number of endogenous ligands/agonists for PPAR $\gamma$  such as fatty acid derivatives and synthetic ligands such as thiazolidinediones have been described (Itoh et al, 2008; Michalik et al, 2004). PPAR $\gamma$  activation is anti-inflammatory in nature and has been shown to inhibit cellular proliferation, induce differentiation and promote cell cycle arrest and apoptosis in colon cancer cell lines (Brockman et al, 1998; Michalik et al, 2004; Sarraf et al, 1998; Yang & Frucht, 2001).

Mechanistic studies on the anti-inflammatory actions of agonist activated PPAR $\gamma$  include inhibition of early events of NF- $\kappa$ B signaling, such as I $\kappa$ B $\alpha$  expression, phosphorylation and its subsequent degradation, as well as p65 nuclear translocation (Buroker et al, 2009; Kim et al, 2007; Wan et al, 2008). PPAR $\gamma$  has also been shown to transrepress NF- $\kappa$ B and thereby inhibit the expression of inflammatory target genes such as iNOS (Pascual et al, 2005). 13(S)-HODE and 15-HETE, the enzymatic products following oxygenation of linoleic acid and arachidonic acid respectively by 15-LOX-1, have been implicated as agonists for PPAR $\gamma$  in colon cancer cell lines (Bull et al, 2003; Nixon et al, 2003; Sasaki et al, 2006).

## **1.12 Aims of the Study**

Although most lipoxygenases metabolize arachidonic acid into inflammatory mediators that enhance tumor genesis, based on previous supporting evidence we have hypothesized that 15-LOX-1 has an anti-tumorigenic role in CRC. However, very little was known about the effect of the enzyme on colorectal cancer metastasis and angiogenesis. To that extent, we wanted to investigate the biological effect of 15-LOX-1 on the metastatic and angiogenic potential of CRC. 15-LOX-1 was stably expressed in HCT-116 CRC cell line, which does not express 15-LOX-1. The effects of stable 15-LOX-1 expression on cellular proliferation, apoptosis, metastatic potential (adhesion to the extracellular matrix, migration and invasion) and angiogenesis were then examined. Furthermore, to explain these effects mechanistically, the effect of 15-LOX-1 expression on the tumor promoting transcription factor NF-κB was examined in this thesis.

The study therefore was designed to answer two questions the answers to which were missing in the field:

1. The effect of re-expression of 15-LOX-1 on the functional characteristics of colorectal cancer cells, particularly in the context of metastasis and angiogenesis.
2. Whether 15-LOX-1 crosstalked with the inflammatory transcription factor NF-κB.

With these answers this thesis aimed to firmly establish the tumor suppressive functions of 15-LOX-1 in CRC and suggest the exploitation of this enzyme for therapeutic interventions.

## **CHAPTER 2**

### **MATERIALS AND METHODS**

#### **2.1 Cell Culture and transfection**

Human colorectal cancer cell line HCT-116 was purchased from ATCC. HCT-116 cells were cultured in RPMI 1640 medium supplemented with 1.5 mM L-Glutamine, 10% fetal bovine serum (FBS) and 1% Penicillin/Streptomycin. All cell culture reagents were purchased from Biochrom (Berlin, Germany). Human umbilical vein endothelial cells (HUVEC) were obtained from Lonza (Basel, Switzerland) and grown according to Lonza guidelines. The cells were grown in T25 tissue culture flasks containing 5 ml of the complete culture medium which is suitable for each cell types. Then, the cells are placed in a freezing medium which is prepared with addition of 5% Dimethylsulfoxide (DMSO) to RPMI-1640 complete culture medium (for HCT-116) or EBM basal complete medium (for HUVEC) and these cells are stored in liquid nitrogen tank.

##### **2.1.1 Plasmids**

The 15-LOX-1 cDNA cloned into a pcDNA3.1 vector with a zeocin mammalian marker was kindly provided by Dr Uddhav Kelavkar (Mercer University School of Medicine, Savannah Campus, GA) (Kelavkar et al, 1998). The Pathdetect NF-κB cis-Reporting system (Stratagene Agilent, CA) was used according to manufacturer's instructions. The PPRE-3xTK-Luc plasmid were kindly provided by Dr. Ronald Evans (Howard Hughes Medical Institute, CA) (Forman et al, 1995).

### **2.1.2 Plasmid isolation and measurement**

Escherichia coli Top10 strain carrying all used plasmids was grown in LB ampicillin broth at 37°C with shaking overnight. Plasmid isolation was performed with a Qiagen Plasmid isolation kit according to manufacturer's instructions. Plasmid DNA concentration and its purity was measured by using spectrophotometer. Plasmid DNA was diluted in 1:20 ratio with molecular biology grade water and the absorbances were read at 260 and 280 nm in a quartz cuvette. Then OD<sub>260</sub>/OD<sub>280</sub> ratio (this ratio indicates nucleic acid purity) was calculated to determine DNA purity. Pure DNA has an OD<sub>260</sub>/OD<sub>280</sub> ratio of ~1.8. To determine the concentration of plasmid DNA in the original sample, the following calculation was performed:

$$\text{DNA concentration } (\mu\text{g/ml}) = \text{OD}_{260} \times \text{dilution factor} \times 50 \mu\text{g/ml DNA}$$

### **2.1.3. Transfections**

HCT-116 cells were stably transfected with 5 µg pcDNA3.1-15-LOX-1 vector using FuGENE 6 or FuGENE HD (Roche, Mannheim, Germany). Control cells included the cells transfected with the empty pcDNA3.1 vector and parental untransfected cells.

HCT-116 cells ( $5 \times 10^5$ ) were seeded in 6-well plates the day before the experiment. Before the transfections, RPMI-1640 complete culture medium was changed with antibiotic free RPMI-1640 medium containing 1.5 mM L-glutamine, 1% FBS. FuGENE HD or FuGENE 6 was used as a transfection reagent in 3:1 ratio of FuGENE/ plasmid. The various transfection mixes were prepared in serum free OptiMEM medium (Table 1).

**Table 1. Transfection mixture for 5× 10<sup>5</sup> cells in 6-well plates**

Transfection mixture	pcDNA3.1-15-LOX-1	pcDNA3.1-(EV)	Mock	Cell only
DNA (5µg)	5µg	5µg	...	....
FuGENE 3:1(µl)	15	15	15	...
OptimemMEM (µl)	Complete to 100 µl	Complete to 100 µl	Complete to 100 µl	....

Two days after transfection, the transfection medium was changed with RPMI-1640 complete medium. The cells were incubated for 24 h and 250 µg/ml Zeocin (Invitrogen, Carlsbad, CA, USA) was added for selection. After 20 days, monoclones were picked using cloning cylinders (Chemicon, Temecula, CA, USA) and maintained in 125 µg/mL Zeocin. The concentration of Zeocin used was based on a kill curve assay. Several clones were screened and two monoclonal antibodies of 15-LOX-1-transfected HCT-116 (1E7 and 1F4) were expanded and used for the experiments.

## 2.2. Cell Treatments

HCT-116 cells were treated with 100 µM 13(S)-HODE (Cayman Chemical, MI) in ethanol and then processed for luciferase assay or immunofluorescence as described below. The final concentration of ethanol was kept below 0.5%. In order to inhibit PPAR $\gamma$ , the 15-LOX-1 expressing or control cells were incubated for 24 h with 1 µM of the PPAR $\gamma$  antagonist GW9662 (Sigma–Aldrich, Taufkirchen, Germany). To inhibit 15-LOX-1, the cells were treated with 1 µM PD146176 (Sigma– Aldrich), with 10 µM U0126 (Sigma–Aldrich) to inhibit ERK1/2 and with 32 µM SN-50 (Santa Cruz, CA) to inhibit NF-κB. GW9662, PD146176, and U0126 were dissolved in DMSO; SN-50 was dissolved in sterile deionized water. The final concentration of DMSO was kept below 0.1%.

## **2.3. RNA isolation and RT-PCR**

### **2.3.1 RNA isolation and measurement**

Total cellular RNA was isolated from 15-LOX-1 expressing HCT-116 cells and control cells by using the Qiagen RNeasy Minikit (Qiagen, Hilden, Germany) according to manufacturer's guidelines. Total RNA were stored at -20 °C until cDNA synthesis. RNA concentration was determined by using spectrophotometer. RNA was diluted in 1:20 ratio using molecular biology grade water and the absorbances were read at 260 and 280 nm in a quartz cuvette (Agilent). Then OD260/OD280 ratio (this ratio indicates nucleic acid purity) was calculated to determine RNA purity. Pure RNA has an OD260/OD280 ratio of ~2.0. To determine the concentration of RNA in the original sample, the following calculation was performed:

$$\text{RNA concentration } (\mu\text{g/ml}) = \text{OD260} \times \text{dilution factor} \times 40 \text{ } \mu\text{g/ml RNA}$$

### **2.3.2 DNase-1 treatment**

In order to get rid of any contaminating genomic DNA from the isolated RNA, DNase-1 treatment was performed using Fermentas DNase-1 treatment kit. Briefly, 1 µg RNA, 1 µl 10X Reaction Buffer with MgCl<sub>2</sub>, 1 µl DNase-1 was completed to 10 µl with DEPC-treated Water in a RNase-free tube and incubated at 37 °C for 30 minutes. Then, 1 µl 25 mM EDTA was added into the reaction mixture and incubated at 65 °C for 10 minutes in order to hydrolyze RNA during heating in the absence of chelating agent). The prepared RNA was used as a template for First strand cDNA synthesis.

### **2.3.3 15-LOX-1 RT-PCR**

First strand cDNA synthesis was performed with Fermentas cDNA synthesis kit from total RNA (1 µg) using oligo dT primers according to manufacturer's guidelines. cDNA was PCR amplified in a 30 µl reaction mixture (Table 2) containing cDNA as template with 15-LOX-1 gene-specific primers (5'-GAGTTGACTTGAGGTTCGC-3' and 5'-GCCCGTCTGTCTTATAGTGG-3') using PCR thermal cycling conditions as described in Table 3. pc.DNA.3.1-15-LOX-1 plasmid was used as a positive control in PCR reaction.

**Table 2: 15-LOX-1 PCR reaction mixture**

Chemical	Amount
Forward 15-LOX-1 primer (5 µM)	3 µl
Reverse 15-LOX-1 primer (5 µM)	3 µl
10X Taq polymerase buffer	3 µl
2 mM dNTPs	1,5 µl
25 mM MgCl <sub>2</sub>	4 µl
Taq polymerase (2,5 U/ µl)	0,2 µl
PCR grade water	up to 28 µl
cDNA	2 µl

**Table 3: 15-LOX-1 PCR thermal cycling conditions**

PCR Reaction Condition			
94 °C	3 minutes	initial denaturation	1 time
94 °C	40 seconds	Denaturation	23 cycles
62 °C	30 seconds	Annealing	
72 °C for	30 seconds	Extension	

As an internal control, cDNA was PCR amplified in a 30 µl reaction mixture (Table 4) containing cDNA as template with GAPDH (Glyceraldehyde 3-phosphate dehydrogenase) gene-specific primers (5'-GAGTTGACTTGAGGTTCGC-3' and 5'-GCCCGTCTGTCTTATAGTGG-3') using PCR thermal cycling conditions as described in Table 5. Negative control reaction mixture, without template cDNA was included for both PCR reactions.

**Table 4: GAPDH PCR reaction mixture**

Chemical	Amount
Forward GAPDH primer (5 µM)	3 µl
Reverse CAPDH primer (5 µM)	3 µl
10X Taq polymerase buffer	3 µl
2 mM dNTPs	1,5 µl
3 mM MgCl <sub>2</sub>	4 µl
Taq polymerase (2,5 U/ µl)	0,2 µl
PCR grade water	up to 28 µl
cDNA	2 µl

**Table 5: GAPDH PCR thermal cycling conditions**

PCR Reaction Condition			
94 °C	3 minutes	initial denaturation	1 time
94 °C	40 seconds	Denaturation	23 cycles
60 °C	30 seconds	Annealing	
72 °C for	30 seconds	Extension	

After the 15-LOX-1 and GAPDH PCR reaction, 8 µl of the final PCR products were electrophoresed on a 2% agarose gel at 100 V and photographed under UV light.

## **2.4 Protein Isolation**

Cell lysates were extracted using MPER assay buffer (Pierce, Rockford, IL, USA) containing protease inhibitors (Roche, Mannheim, Germany) according to the manufacturer's guidelines. Protein was diluted in 1:5 ratio using molecular biology grade water and then it was measured with the modified Bradford Assay using a Coomassie Plus protein assay reagent. Protein concentrations were calculated according to the standard curve given in appendix C1.

## **2.5 Nuclear and cytoplasmic Protein Isolation**

The cells were washed with ice-cold PBS three times and 0.5 ml cytoplasmic buffer (20 mM HEPES pH 7.9, 10 mM KCl, 0.1 mM EDTA, 1 mM DTT, and 1.5 mM MgCl<sub>2</sub> with 1x cocktail protein inhibitor and 1 x phosphatase inhibitor cocktail) was used to resuspend the cells which were then kept on ice for 30 min. NP40 (10%) was added to a final concentration of 0.15 % by gentle pipetting, and cells were incubated on ice for 5 min. The nuclei were pelleted at 12,000 x g for 2 minutes and the supernatant (cytoplasmic proteins) was transferred into a new tube. The nuclei were washed three times with 0.5 ml cytoplasmic buffer without NP40 and resuspended in 200 µl nuclear extraction buffer (20 mM HEPES pH 7.9, 10 mM KCl, 0.1 mM EDTA, 1 mM DTT, 1.5 mM MgCl<sub>2</sub>, 0.5 M NaCl, 25% glycerol with 1x cocktail protein inhibitor). The lysates were incubated on ice for 30 min and centrifuged at 12,000 x g for 10 min and the supernatant (nuclear proteins) was transferred into a new tube. Cytoplasmic and nuclear proteins were stored at -80°C. The protein content was measured using the modified Bradford Assay using a Coomassie Plus protein assay reagent (Pierce, Rockford, IL, USA).

## **2.6 Western blot analysis**

Proteins (50–80 µg) were separated in a 10% polyacrylamide gel using 100 volts for 105 minutes at room temperature and the proteins in the gel were transferred onto the PVDF membrane (Roche) using 100 volts for 105 minutes at 4°C. After the transfer, the membranes were blocked in skim milk (prepared with Phosphate Buffered Saline (PBS) containing 1% Tween-20) or Bovine serum albumin (BSA – prepared with Tris Buffered Saline (TBS) containing 1% Tween-20) at concentrations changing from 5% to 10%. The membranes were incubated overnight with the appropriate primary antibodies: 15-LOX-1 antibody (1:1000 dilution, Cayman Chemicals), XIAP (1/500), Bcl-xL (1/250), MTA1 (1/200), p65 (1:500 dilution), IκB-α (1:500 dilution) and p-IκB-α (1:250 dilution), (all from Santa Cruz) followed by incubation for 1 h with a horseradish peroxidase-conjugated goat anti-rabbit (1:2000; 1:3300), goat anti-mouse (1:2,000) and rabbit anti-sheep (1:2000 dilution) secondary antibody. The bands were visualized by using an enhanced chemiluminescence kit (ECL Plus; Pierce) according to the manufacturer's instructions. Briefly, 1.5 ml of solution A was mixed with 1.5 ml of solution B of the chemiluminescence kit and applied onto the surface of membrane, left for 1 minute after which the membrane was dried and wrapped in a stretch film. The image was taken by a Kodak X-ray processor. Equal protein loading was confirmed by probing the same membrane for GAPDH.

The membrane was stripped after 15-LOX-1 Western blot analysis by using a stripping buffer (100 mM β-meOH, 2% SDS, 62.5 mM Tris-HCl pH: 6.8) Membrane was stripped at 65°C for 15 minutes with shaking, and then it was blocked in 10% skim milk and probed with a GAPDH polyclonal antibody (1:2000 dilution), β-actin mouse monoclonal antibody (1/2000) and α-tubulin mouse monoclonal antibody (1/1000) followed by incubation for 1 h with a horseradish peroxidase-conjugated goat anti-rabbit (1:2000-1:3300) or goat anti-mouse (1:2000) secondary antibody. After final washing steps with PBS-T the bands were visualized by enhanced chemiluminescence kit as described above.

## **2.7 15-LOX-1 activity measurement.**

Concentration of 13(S)-HODE was determined using an enzyme immunoassay kit (Assay Designs, Ann Arbor, MI, USA) according to the manufacturer's instructions. This kit specifically determines 13(S)-HODE with less than 2% sensitivity for the racemic 13(R)-HODE.

Briefly, 15-LOX-1 expressing HCT-116 cells, 15-LOX-1 expressing HCT-116 cells treated with 1  $\mu$ M of the 15-LOX-1 specific inhibitor PD146176 (Cayman Chemical) for 48 h and control cells were grown in six-well plates. Then, they lysed, and acidified with 0.2 N HCl. Next, 13(S)-HODE was extracted with water-saturated ethyl acetate. 13(S)-HODE, being a lipid molecule, remained in the organic phase and was collected through 3 sequential centrifugation steps. The samples were dried under a general stream of nitrogen. Then they dissolved in ethanol and placed into the 96 well plates coated with an antibody to 13(S)-HODE. The level of 13(S)-HODE was measured colorimetric ally at 405 nm in a Bio-Rad microplate reader. The 13(S)-HODE concentrations were determined from a standard curve generated with standard 13-S-HODE given in appendix C2 and expressed as ng per mg of crude protein. Five independent experiments carried out.

## **2.8 Cellular proliferation**

Cell proliferation was determined using the Vybrant MTT assay kit (Invitrogen) according to the manufacturer's guidelines. Mitochondrial reductase in the mitochondria catalyzes the conversion of the water soluble MTT (3-(4,5-dimethylthiazol-2-yl)-2,5-diphenyltetrazolium bromide) to an insoluble formazan in viable cell. Then, the formazan is solubilized by adding SDS solution and the concentration is measured by optical density at 570 nm.

Briefly, 10,000 cells (15-LOX-1 expressing clones 1E7 and 1F8, empty vector transfected, and parental HCT-116 cells) were plated in a final volume of 100

$\mu$ L in complete RPMI-1640 medium in 96-well tissue culture dishes. After 24, 48, 72, and 96 h, 10  $\mu$ l the MTT labeling reagent was added, incubated for 4 h, and solubilized with a 1% solution of SDS-HCl for 18 h. The absorbance was determined in a Bio-Rad microplate reader at 570 nm. Three independent experiments carried out.

In some experiments, the 15-LOX-1 expressing cells were grown for 48 h, incubated with PD146176 for 48 h, and assayed for proliferation by MTT as above. Where indicated, after 24 h, the 15-LOX-1 expressing and control cells were treated with 1  $\mu$ M GW9662 for another 48 h. EV-transfected cells were treated with the NF- $\kappa$ B inhibitor 32  $\mu$ M SN-50 for 48 h.

## **2.9 Apoptosis assays.**

### **2.9.1 Acridine orange staining**

Apoptosis was determined by acridine orange staining assay using acridine orange dye (Sigma-Aldrich, Taufkirchen, Germany). This assay is based on the difference in the emission of fluorescence when acridine orange (AO) interacts with normal and apoptotic cells.

15-LOX-1 expressing HCT-116 and control cells were grown for 72 h in six-well plates. After 72 hour incubation, the supernatant media including dead cells as well as the attached cells be harvested and fixed in 1% paraformaldehyde/PBS. The fixed cells were centrifuged at 200 x g for 5 min and then resuspended in 5 ml PBS, which was followed by another centrifugation at 200 x g for 5 min. The cells were then re-suspended in 1 ml PBS and transferred to 9 ml 70% ethanol (v/v) and stored for at least 4 h at 4°C. Afterwards, the cell suspensions were centrifuged at 200 x g for 5 min, resuspended in 1 ml PBS and 0.2 ml of DNase free- RNase A solution was added and incubated at 37°C for 30 min. After incubation another centrifugation step at 200 x g for 5 min was performed and cells were resuspended in 0.2 ml PBS.

Following this, 0.5 ml of 0.1 M HCl was added into the cell suspensions at RT. After 30 to 45 seconds, 2 ml of acridine orange solution (6 mg/ml acridine orange mixed with 90ml 0.1M citric acid and 10ml 0.2 M Na<sub>2</sub>HPO<sub>4</sub> (pH 2.6)) was added to the cells. The cell suspension was pipetted onto a glass slide and visualized under a Leica fluorescence microscope (Leica, Wetzlar, Germany) with a blue-green filter at 490 nm. At least 500 cells were counted, and the number of apoptotic cells was determined. Three independent experiments carried out.

### **2.9.2 Caspase-3 activity assay**

Caspase-3 activity assay was carried out by using Biovision Caspase-3/CPP32 Colorimetric Assay Kit (BioVision, Mountain View, CA, USA) according to the manufacturer's protocol. This kit provides for assaying the activity of caspases which recognize the sequence of DEVD. This assay is based on spectrophotometric detection of the chromophore  $\rho$ -nitroanilide ( $\rho$ NA) preceding cleavage from the labeled substrate DEVD-  $\rho$ NA.

Equal numbers of 15-LOX-1 expressing and control HCT-116 cells were grown in six-well plates. Then, the cells lysed using 50  $\mu$ l chilled Cell Lysis Buffer and incubated on ice for 10 minutes. Next, cell suspensions were centrifuged at 10,000 x g for 1 min and the supernatant (cytosolic extract) was transferred to a fresh tube. The protein concentrations were measured with modified Bradford Assay using the Coomassie plus protein assay reagent standard curve given in appendix C1. In the assay, 100  $\mu$ g protein lysates from each sample were mixed with 50  $\mu$ l chilled Cell Lysis Buffer in fresh eppendorf tubes. 50  $\mu$ l of the 2X Reaction Buffer (containing 10 mM DDT) was added to each sample. Then 5  $\mu$ l 4 mM DEVD-  $\rho$ NA substrate (200  $\mu$ M final concentrations) was added to the tubes and mixture was incubated for 2 hours at 37°C. Finally the samples were diluted in Dilution Buffer (100  $\mu$ l sample in 900  $\mu$ l) and the absorbances were read by using a spectrophotometer at 405 nm. Three independent experiments carried out.

### **2.9.3 Annexin V Staining**

Annexin V staining was carried out according to the manufacturer's instructions (Annexin-VFLUOS Staining kit, Roche). Briefly, equal number of 15-LOX-1 expressing and control HCT-116 cells were grown in 6-well plates for 72 h., trypsinized, washed with PBS and centrifuged. The pellet was resuspended in 100 µl of Annexin-V-FLUOS labeling solution and PI solution, incubated for 10-15 minutes at RT and a minimum of 10,000 events were acquired, using a fluorescence-activated cell sorter analysis (FACS) using a FACS Calibur flow cytometer (Becton–Dickinson, NJ, USA) (Drs İhsan and Mayda Gürsel and Tamer Kahraman, Department of Molecular Biology and Genetics, Bilkent University are acknowledged for the use of the flow cytometer). The percentage of cells positive for Annexin V signal (early apoptotic phase, bottom right quadrant), PI signal alone (necrotic phase, upper left quadrant), both Annexin V and PI (late apoptotic phase, upper right quadrant) or neither Annexin V nor PI (viable cells, lower left quadrant) were deduced from the corresponding dot plots using the Cell Quest Pro software (Becton–Dickinson). Three independent experiments carried out.

### **2.10 Colony formation in soft agar**

To evaluate the ability of cells to grow in an anchorage-independent manner, 15-LOX-1 expressing and control HCT-116 cells were trypsinized and counted and 6000 cells were grown on noble agar (Difco; BD Biosciences, San Jose, CA, USA). A bottom agarose layer was prepared by layering 1.5 mL 1X RPMI-1640 medium containing 0.6% agar and allowing it to solidify for 1 h at room temperature in a six-well plate. 15-LOX-1 expressing or control HCT-116 cells were suspended in 400 µl RPMI-1640 containing 0.33% agarose. This solution (1 mL) was added onto the solidified bottom layer. After 2 weeks the plates were stained with crystal violet (0.005%) for 30 min, the image was captured under a Leica light microscope with 10X objective and a dissection microscope and the colonies were counted manually. Three independent experiments carried out.

## **2.11 In vitro scratch wound healing assay**

Cellular motility was measured by an in vitro scratch wound healing assay. 15-LOX-1 expressing and control HCT-116 cells were seeded in six-well plates and incubated until they were 90% confluent. The monolayer of cells was scratched with a sterile pipette tip. Debris was removed from the culture by washing twice with PBS, and the cells were then incubated in RPMI-1640 complete medium. Immediately after wounding, images were captured with an inverted microscope with 4X objective (Olympus, Hamburg, Germany), and wound sizes were verified with an ocular ruler to ensure that all wounds were the same width at the beginning of the experiment. Wound closure was monitored with microscopy after the wound was formed for 72 h. The distances between the wound edges were measured from images of the wound using the ImageJ 1.42 program.

## **2.12 Cell adhesion assay**

96-well plates were coated with 75 µl of fibronectin (Biological Industries, Kibbutz Bert Haemek, Israel) at a concentration of 50 µg/ml and left at 37°C in a CO<sub>2</sub> incubator for 45 min. Some wells were left uncoated as negative controls. Then, the 96 well plate was washed twice with washing buffer (0. 1% BSA in RPMI-1640 medium). The plate was blocked with 1% blocking buffer (1% BSA in RPMI-1640) by adding 100 µl of blocking buffer into the wells previously coated with fibronectin and incubated at 37°C in a CO<sub>2</sub> incubator for 1 h. After incubation, the plate was washed again with washing buffer and chilled on ice.

15-LOX-1 expressing and control HCT-116 cells were trypsinized, counted with a hemocytometer and 40,000 cells were added per well. Additionally, a second 96 well plate coated with fibronectin was also seeded with 40,000 cells as a total cell control. Both plates were left at 37°C in a CO<sub>2</sub> incubator for 2 h. The wells in first plate were then washed twice with PBS to withdraw non-adherent cells gently, while

the second plate retained all the cells to represent the total number of cells plated. Finally, 10 µl of MTT was added into the wells and incubated for 4 h, followed by solubilization of the formazan crystals with the addition of 100 µl of 1 mM SDS into each well. The absorbance value for each well was recorded in Bio-Rad 680 microplate reader at 570 nm. Adhesion values for each sample was calculated by dividing the obtained absorbance value in fibronectin coated wells by uncoated, total cell wells corresponding to each particular sample. The data was represented as percentage adherent cells with respect to the total number of cells plated. Two independent experiments carried out in five replicates.

### **2.13 Boyden chamber cell migration assay**

The migratory potential of HCT-116 15-LOX-1 expressing cells was determined by a Trans well cell migration assay. Trans well (Sigma Aldrich Chemie GmbH, Munich, Germany) consists of a two chamber 24 well plate which is composed of upper and lower chambers. Cells in 1% serum are placed in the upper chamber whereas the lower chamber contains medium with 10 % serum. The cells that can migrate move across a membrane with 8 µM pores towards the lower chamber.

15-LOX-1 expressing and control HCT-116 cells were trypsinized, collected in falcon tube and washed three times in RPMI-1640 media containing 1% FBS. Next, the cells were counted in a hemocytometer. 100 µl of the cell suspension containing 25,000 cells in RPMI-1640 media containing 1% FBS was applied onto the 8 µm Transwell filters (upper chamber). 600 µl RPMI-1640 complete medium (with 10% serum) containing 5µg/ml fibronectin (a chemoattractant) was added to the bottom of the well in order to stimulate migration of the cells through the 8 µm pored membranes. The cells were left at 37°C in a CO<sub>2</sub> incubator for 72 hours. After the incubation, Transwell membrane filters was swabbed off three times by the use of sterile cotton swabs. The Transwells were then fixed in 100% methanol for 10 minutes, and then stained with Giemsa solution for 2 minutes at RT. Then,

membrane filters were cut out and mounted onto a glass slide with a drop of oil. The total number of cells that had migrated in each Trans well filter was then counted at 20x magnification under a Leica light microscope. Three independent experiments carried out.

## **2.14 Boyden chamber cell invasion assays**

Matrigel (BD Biosciences) thawed in ice overnight at 4°C and was diluted in 1:5 ratios (matrigel/ RPMI-1640 media) and applied into upper chamber of the 24-well transwell plate and kept at 37°C incubator for 4 hours. Matrigel solidifies very quickly, thus matrigel preparation steps were performed on ice with all materials used were cold.

15-LOX-1 expressing and control HCT-116 cells were trypsinized, collected in falcon tube and washed three times in RPMI-1640 media containing 1% FBS. Next, cells were counted in a hemocytometer. 100 µl of the cell suspension containing 50,000 cells in RPMI-1640 media containing 1% FBS was applied onto the Matrigel. 600 µl RPMI-1640 complete media containing 5µg/ml fibronectin (chemoattractant) is added to the bottom of the well in order to stimulate invasion through Matrigel coated membranes. The Boyden chamber was incubated at 37°C in a CO<sub>2</sub> incubator for 72 h. After the incubation, the Transwells were removed from the 24-well plates and cells and Matrigel were scrapped off from the upper portion of the Transwell membrane filters by the use of sterile cotton swabs. The swabbing repeated at least three times. Then, the Transwells were fixed in 100 % methanol for 10 min, and then stained with Giemsa solution for 2 min at RT. Transwell membranes were cut out and mounted on a glass slide with a drop of oil. The total number of cells that had migrated in each Transwell filter was then counted at 20 x magnification under a Leica light microscope. Three independent experiments carried out.

## **2.15 Luciferase Reporter Assays**

15-LOX-1 expressing and control HCT-116 cells ( $2.5 \times 10^5$  cells/ well) were plated in 12-well culture plates. The cells were transfected with the Pathdetect NF- $\kappa$ B cis-Reporting system (Stratagene Agilent) plasmids using FuGENE HD (Roche). After 24 h, where indicated, the cells were treated with 100  $\mu$ M 13(S)-HODE or 1  $\mu$ M PD146176 or 1  $\mu$ M of the PPAR $\gamma$  antagonist GW9662 (Sigma–Aldrich) for 24 h with or without pretreatment with TNF- $\alpha$  (10 ng/ml) for 6 h. To determine the PPAR $\gamma$  transcriptional activity, the PPRE-3xTK-LUC plasmid was transfected into 15-LOX-1 expressing and control HCT-116 cells ( $2.5 \times 10^5$  cells/well) for 24 h using FuGENE HD. Where indicated, the 15-LOX-1 expressing cells were treated with 1  $\mu$ M GW9662 or parental HCT-116 cells were treated with 100  $\mu$ M 13(S)-HODE for 24 h and collected and analyzed for luciferase activity. Luciferase activity was assessed with Luciferase Reporter Gene Assay (Roche) according to the manufacturer's instructions using a Modulus luminometer (Turner Biosystems, CA). The enzyme activity was normalized for the efficiency of transfection in all assays on the basis of b-galactosidase activity levels and reported as normalized relative light units (RLU). All reporter assays were performed in four replicates at least three independent experiments.

## **2.16 Immunofluorescence Studies**

15-LOX-1 expressing and empty vector (EV) transfected HCT-116 cells, or HCT-116 cells treated with 100  $\mu$ M 13(S)-HODE or the vehicle (ethanol) control were cultured on glass coverslips for 24 h to 60–70% confluence. The cells were subsequently prepared for immunofluorescence to detect the NF- $\kappa$ B subunits p50 and p65. The cells were gently washed with sterile PBS, fixed with 4% paraformaldehyde for 10 min, washed, and permeabilized with 0.1% Triton X-100 in PBS for 10 min. Following this, the cells were washed, blocked with 1% BSA for 30

min at room temperature and incubated at 4°C overnight with the p65 or p50 antibody (both at 1:100 dilution in 1% BSA). The cells were then washed with 0.1% Tween 20 in PBS, and incubated with Alexa Fluor488 (AF488)-labeled goat anti-rabbit secondary antibody (1:500 dilution), (Invitrogen, CA) for 1 h at 37°C. Nuclear staining was performed by incubating the cells in propidium iodide (PI; AppliChem) for 30 min at RT. The slides were then photographed Zeiss LSM 510 (Jena, Germany) Confocal Laser Scanning Microscope. Image analysis was performed on the single-channel images to quantify the nuclear AF488/PI pixel intensity ratio of each dataset using Image J ([www.rsb.info.nih.gov/ ij/](http://www.rsb.info.nih.gov/ij/)). The results are shown as the average of four independent experiments.

## **2.17 DNA-Binding Elisa Assay**

The NF-κB (human p50) Transcription Factor Assay Kit (Cayman Chemical) was used according to manufacturer's instructions. The kit consists of a double-stranded DNA sequence containing the NF-κB response element immobilized to the wells of a 96-well plate. Nuclear extracts of the HCT-116 1E7 clone and empty vector transfected control cells were applied to the wells and allowed to bind to the response element. NF-κB DNA binding was detected by the subsequent addition of a primary antibody against p50 and a horseradish peroxidase-conjugated secondary antibody. A colorimetric readout was obtained at 450 nm using a Bio-Rad plate reader.

## **2.18 VEGF Elisa Assay**

Human VEGF Immunoassay (Quantikine, R&D Systems) was used according to the manufacturer's instructions. Briefly, 15-LOX-1 expressing and empty vector (EV) transfected HCT-116 cells were trypsinized, counted, and seeded in 12 well plates (  $2.5 \times 10^5$  cells/well ). After 72 hour incubation, conditioned

medium was collected from the wells. Standards and samples were pipetted into the wells and any VEGF present was bound by the immobilized antibody. Color development following the incubation with a substrate was measured at 450 nm and 570 nm (for correction).

## **2.19 HUVEC Cell proliferation Assay**

15-LOX-1 expressing and empty vector (EV) transfected HCT-116 cells were trypsinized, counted and seeded in 6 well plates ( $1.5 \times 10^6$  cells/well). After 72 hour incubation, conditioned medium was collected from the wells. Next, the cell proliferation was measured using the Vybrant MTT assay kit (Invitrogen) according to the manufacturer's guidelines as described previously.

## **2.20 HUVEC Wound Healing Assay**

15-LOX-1 expressing and empty vector (EV) transfected HCT-116 cells were trypsinized, counted and seeded in 6 well plates ( $1.5 \times 10^6$  cells/well). After 72 hour incubation, the conditioned medium was collected from the wells. Next, in vitro scratch wound healing assay was performed. HUVEC cells were seeded in six-well plates and incubated until they were 90% confluent. The monolayer of cells was scratched with a sterile pipette tip. Debris was removed from the culture by washing twice with PBS, and the cells were then incubated in EBM complete medium. Immediately after wounding, images were captured with an inverted microscope with 4X objective (Olympus, Hamburg, Germany) and wound sizes were verified with an ocular ruler to ensure that all wounds were the same width at the beginning of the experiment. Next, 1:1 ratio mix medium (EBM complete medium and RPMI-1640 condition medium) added to six-well plates and wound closure was monitored with microscopy after the wound was formed for 9 h. The distances between the wound edges were measured from images of the wound using the Image J 1.42 program.

## **2.21 In vitro Angiogenesis Assay**

15-LOX-1 expressing and empty vector (EV) transfected HCT-116 cells were trypsinized, counted and seeded in 6 well plates ( $1.5 \times 10^6$  cells/well). After 72 hour incubation, conditioned medium was collected from the wells. Next, HUVECs were harvested, resuspended in endothelial cell medium (EBM, Lonza) combined with conditioned medium in a ratio of 1:1 (150  $\mu$ l containing  $3 \times 10^4$  cells) and seeded in Matrigel pre-coated 96 wells plates. The assay plate was incubated at 37°C for 16h and 4X images were taken for evaluation of tube formation (number of tubes, branch points, nodal structures, and total skeleton length). Analysis was carried out by S.Co Lifesciences (Munich, Germany).

## **2.22 Statistical analyses**

Data analysis and graphing was performed using the GraphPad Prism 5 software package. Statistical analysis between experimental results was based on Mann Whitney U-test. Significant difference was statistically considered at the level of  $P<0.05$ . Densitometric analyses of Western blots were carried out with the Image J image processing program.

## CHAPTER 3

## RESULTS

### Section I: Biological effects of 15-LOX-1 in colorectal cancer

#### 3.1.1 Expression of 15-LOX-1 in HCT-116 cells

To identify the biological effects of 15-LOX-1 on CRC, we stably re-expressed 15-LOX-1 in HCT-116 cells using a plasmid (pcDNA3.1-15-LOX-1) and isolated two monoclonals. As a control, HCT-116 cells were transfected with the empty plasmid (pcDNA3.1) as described in ‘Materials and Methods’. After the transfection, we first confirmed expression of 15-LOX-1 at the mRNA level using RT-PCR (Fig 3.1)

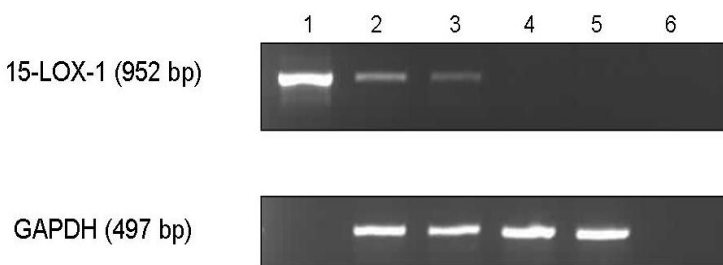


**Figure 3.1: 15-LOX-1 mRNA expression in HCT-116 CRC cell lines.**  
RT-PCR analysis of the 15-LOX-1 transcript. Lane 1, 15-LOX-1 vector (positive control); lane 2, 15-LOX-1 expressing clone 1E7; lane 3, 15-LOX-1 expressing clone 1F8; lane 4, empty vector (pcDNA3.1) transfected cells; lane 5, parental HCT-116 cells; lane 6, negative control.

The protein expression of 15-LOX-1 was confirmed by Western blot (Fig 3.2). Parental HCT-116 cells or HCT-116 cells transfected with the empty vector (EV) did not express any endogenous 15-LOX-1 mRNA and protein; however, transfection of the 15-LOX-1 vector resulted in robust expression.

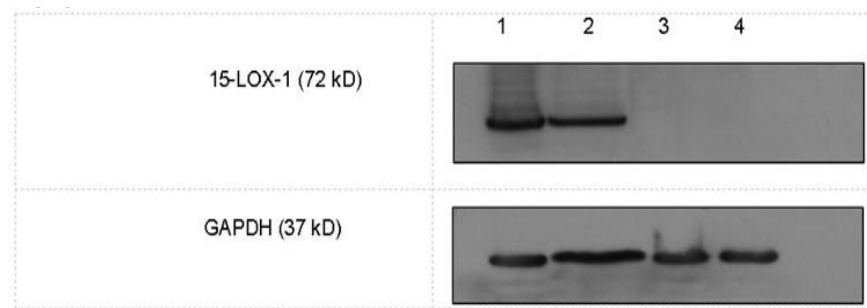


**Figure 3. 2: 15-LOX-1 protein expression in HCT-116 CRC cell lines.**  
Western blot analysis of 15-LOX-1 protein expression. Lane 1: 15-LOX-1 expressing clone 1E7; Lane 2: 15-LOX-1 expressing clone 1F8; Lane 3: empty vector transfected cells; Lane 4: Untransfected parental cells. Equal protein loading was confirmed by probing with a GAPDH antibody.

15-LOX-1 is an enzyme that catalyzes the oxygenation of linoleic acid to form 13-S-HODE. Therefore, the ectopically expressed 15-LOX-1 in the HCT-116 cells was next examined for the presence of an enzymatic activity. For this purpose, we performed a 13-S-HODE ELISA assay as described in ‘Materials and Methods’. The amount of 13(S)-HODE detected in 15-LOX-1 expressing HCT-116 cells was 166.4 ng/mg protein compared to 78.8 ng/mg protein in empty vector transfected cells (\*P < 0.05). When the cells were pre-incubated with 1 µM the 15-LOX-1 inhibitor PD146176, a specific inhibitor of 15-LOX-1 and lacks nonspecific antioxidant properties (Sendobry et al, 1997), the enzymatic formation of 13(S)-HODE was inhibited (Fig. 3.3). As can be seen in the figure 3.3, Empty vector transfected cells also have basal level of 13-S-HODE. This may be related with activity of 13-hydroxyoctadecadienoic acid (13-S-HODE) dehydrogenase which metabolizes 13-S-HODE to 13-oxooctadecadienoic acid (Bronstein & Bull, 1993).

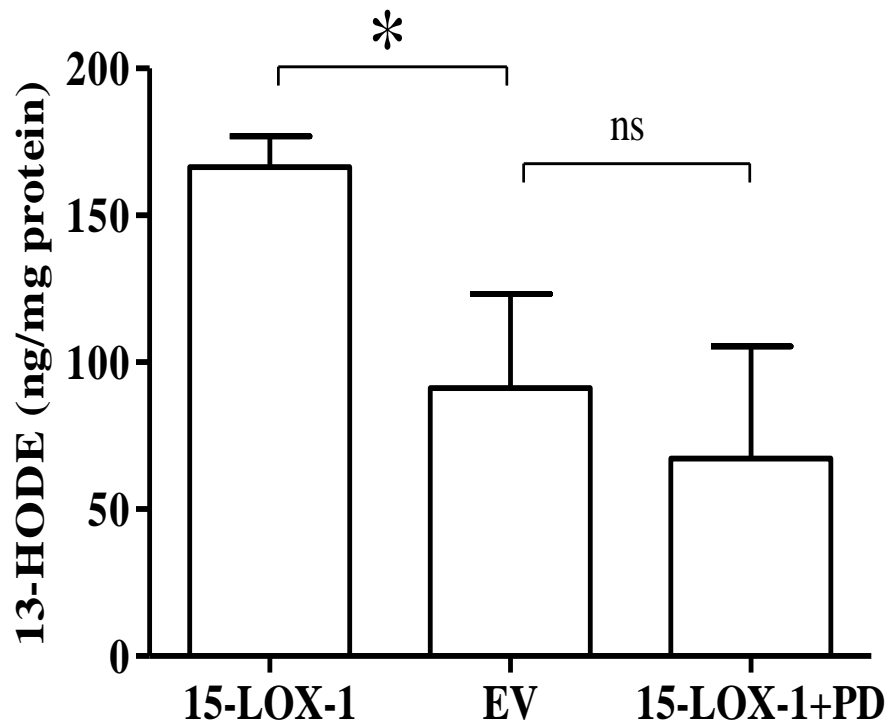


**Figure 3. 3: The enzymatic activity of 15-LOX-1 in HCT-116.**

The enzyme activity in HCT-116 cells was determined from their content of 13(S)-HODE by an ELISA assay. 15-LOX-1 expressing cells have significantly more 13(S)-HODE (\* $P < 0.05$ , Mann Whitney U-Test) compared to the empty vector (EV) expressing cells (HCT116\_EV) and 15-LOX-1 expressing cells that were incubated with 15-LOX-1 inhibitor PD146176 (1  $\mu$ M) for 24 h (15-LOX-1 + PD). Error bars represent the SD of five independent experiments. ns, not significant.

Taken together, these data indicate that a functionally active 15-LOX-1 protein could be expressed in the HCT-116 cells.

### 3.1.2 15-LOX-1 expression and 13-(S)-HODE reduces proliferation in vitro

To understand the role of 15-LOX-1 on CRC cell proliferation, a colorimetric MTT assay was performed. The results showed that 15-LOX-1 expression in HCT-116 cells induced a significant decrease in proliferation of the cells. For the clone 1E7, the reduction in proliferation compared to the empty vector transfected cells (EVE2) reached statistical significance between 48 and 96 h after plating ( $**P < 0.01$ ; Fig. 3.4). The reduction in proliferation for the clone 1F8 reached statistical significance at all-time points (24–96 h) after plating ( $*P < 0.05$ ,  $**P < 0.01$ ; Fig. 3.4).

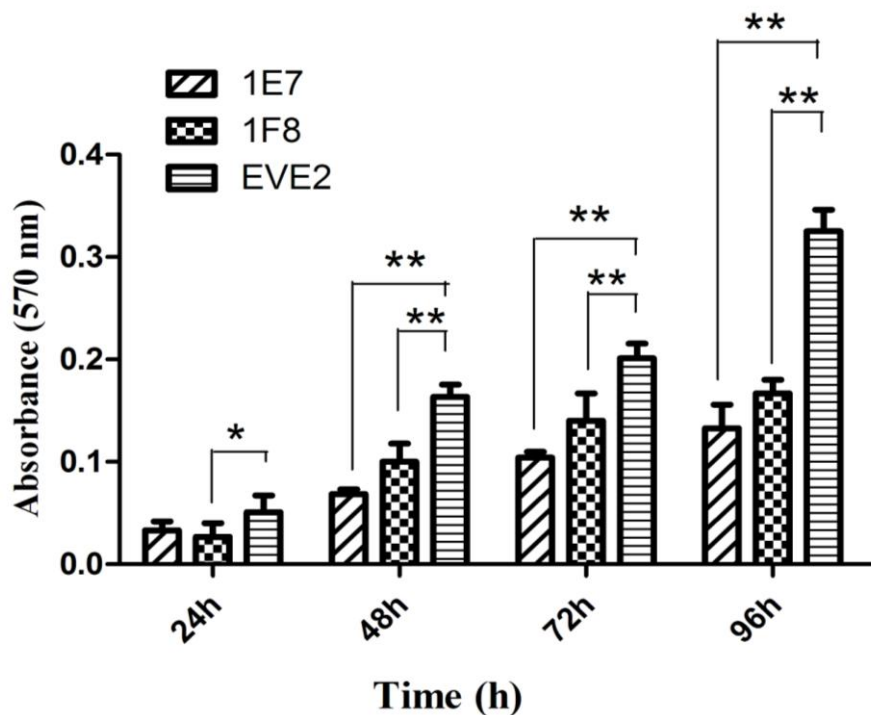


**Figure 3. 4: 15-Lipoxygenase-1 (15-LOX-1) reduces the proliferation of HCT-116 CRC cells.**

Two clones of HCT-116 cells stably expressing 15-LOX-1 (1E7 and 1F8) were plated in a 96-well plate and allow to grow for 96 h. The cellular proliferation was determined every 24 h by an MTT assay. The 15-LOX-1 expressing cells proliferated significantly more slowly ( $*P < 0.05$ ;  $**P < 0.01$ ) compared to empty vector (EV) transfected cells. Error bars represent the SD of three independent experiments.

To determine whether this decrease in proliferation was a consequence of 15-LOX-1 expression, the 1E7 cells were plated in 96-well plates, grown for 48 h then incubated for 48 h with the specific 15-LOX-1 inhibitor PD146176 (1  $\mu$ M). The presence of the 15-LOX-1 specific inhibitor could recover this reduced proliferation rate (Figure 3.5).

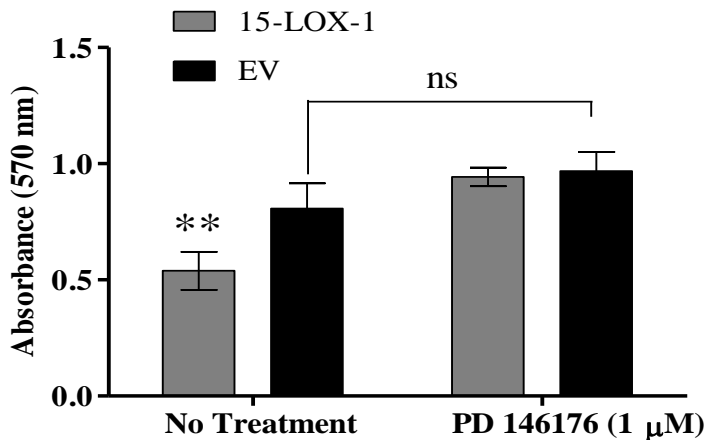


**Figure 3. 5: The lower proliferation of 15-LOX-1 expressing cells can be reversed with the use of a specific inhibitor PD146176.**

HCT-116 cells stably expressing 15-LOX-1 and empty vector expressing control cells were plated and allowed to grow for 48h. The cells were then either treated or not with 1 $\mu$ M PD146176 for 48h. The cellular proliferation was then determined by an MTT assay and read colorimetrically at 570nm. (\*\*P < 0.01). ns, not significant.

### 3.1.3 15-LOX-1 expression induces apoptosis in vitro

The ability of cancer cells to escape from apoptosis is a common requirement for tumorigenesis (Hanahan & Weinberg, 2000). Moreover, since a loss of proliferation is often accompanied by an induction of apoptosis, a qualitative analysis of apoptotic body formation and nuclear changes was carried out using the acridine orange assay as described in ‘Materials and Methods’. When the 15-LOX-1 expressing and control cells were fixed, stained with acridine orange, and viewed under a fluorescent microscope, the apoptotic cells, with their denatured DNA, displayed an intense red fluorescence whereas non-apoptotic cells appeared green (Fig 3.6). The results (Fig. 3.7) indicate that 15-LOX-1 expression significantly induced apoptosis in HCT-116 cell lines (\*P < 0.05) compared with control cells.

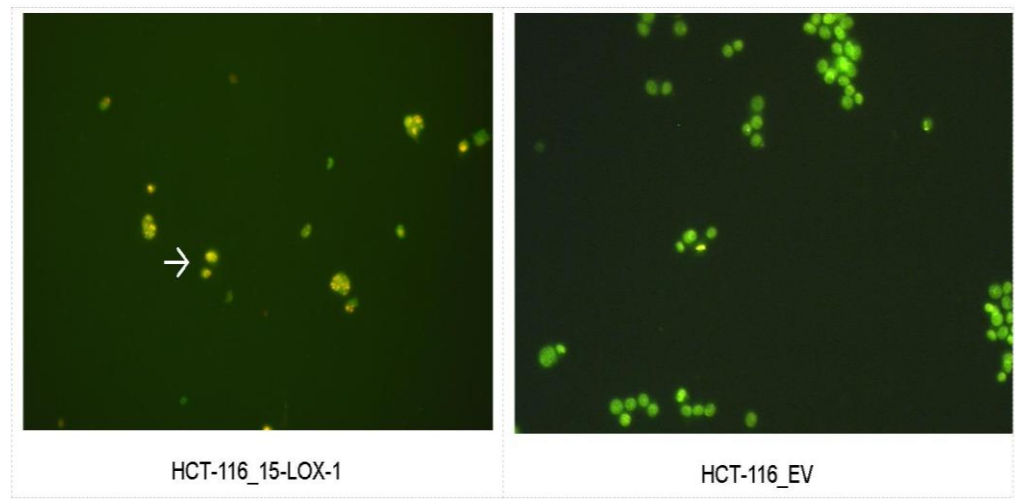


**Figure 3. 6: Acridine orange staining of 15-LOX-1 expressing HCT116 cells and control cells.**

HCT-116 cells stably expressing 15-LOX-1 (HCT116\_15-LOX-1) and control cells (HCT116\_EV) were fixed, stained with acridine orange dye and photographed under confocal microscope.

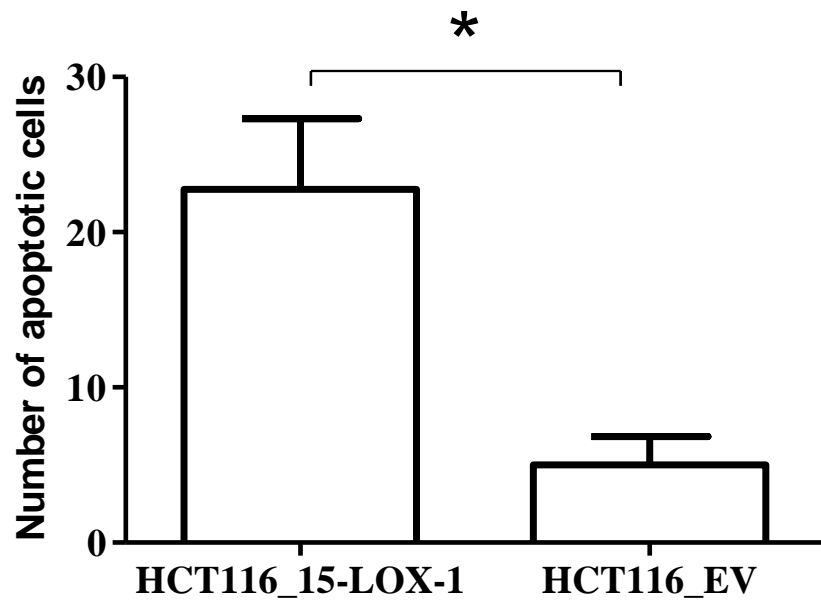


**Figure 3. 7: 15-LOX-1 expression induces apoptosis in colon cancer cells according to acridine orange staining.**

15-LOX-1 expressing HCT-116 cell lines had significantly ( $*P < 0.05$ ) greater numbers of apoptotic cells compared to control cells. Error bars represent SD of three independent experiments.

Since caspase-3 activation is one of the key events during apoptosis, the effect of 15-LOX-1 expression on caspase-3 activity was examined. 15-LOX-1 expression was observed to significantly increase caspase-3 activity in HCT-116 cells compared with control cells (\*P < 0.05; Fig. 3.8).

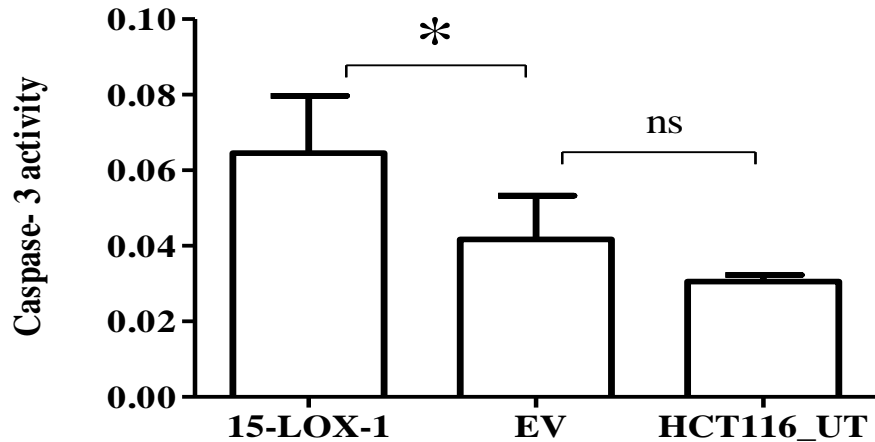


**Figure 3. 8: 15-LOX-1 expression induces apoptosis in colon cancer cells by increasing caspase-3 activity.**

Caspase-3 activity assay indicates significantly higher caspase-3 activity in HCT-116 expressing 15-LOX-1 (\*P < 0.05 for all comparisons) compared to control cells. Error bars represent SD of three independent experiments. ns, not significant.

Additionally, we carried out Annexin V staining to identify apoptosis in HCT-116 cells. For this purpose, 15-LOX-1 expressing and control cells were stained with annexin V and analyzed with a flow cytometer (Fig 3.9). The results (Fig. 3.10) indicate that 15-LOX-1 expression in the HCT-116 cell line significantly induced apoptosis compared to control cells (\*\*P < 0.01). However, control cells also have apoptotic cells

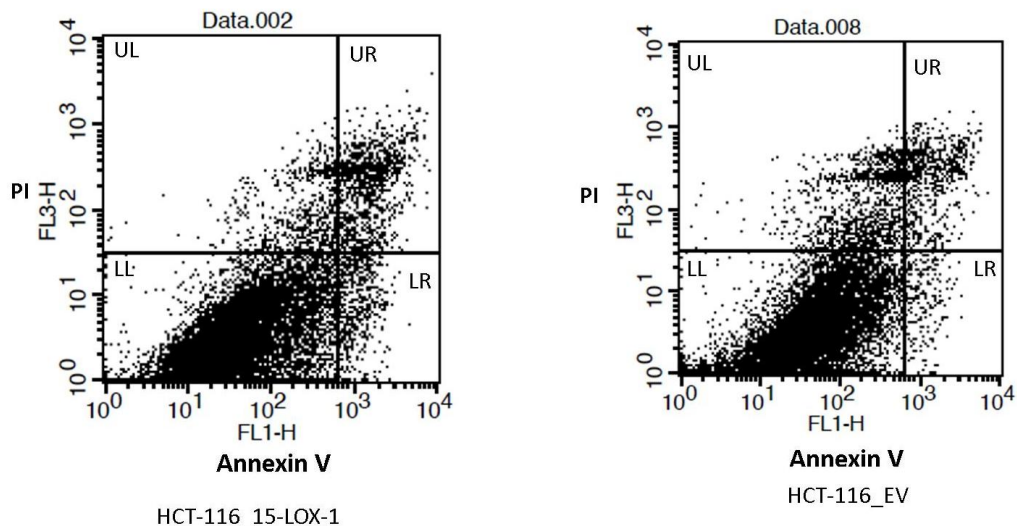


**Figure 3. 9: Distribution of early, late and total apoptotic cells percentages in 15-LOX-1 expressing and control HCT116 cells by Annexin V staining.**

UL: Necrotic cells; UR: Late apoptotic cells; LL: Viable cells; LR: Early Apoptotic cells. HCT-116 cells stably expressing 15-LOX-1 (HCT116\_15-LOX-1) and control cells (HCT116\_EV) were stained with Annexin V to identify apoptotic cells and analyzed with Flow cytometer.

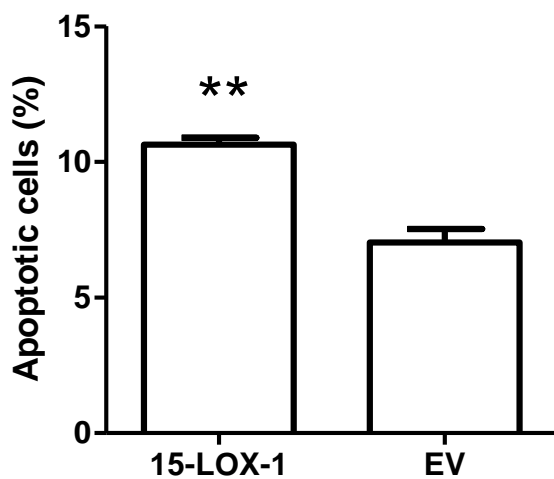


**Figure 3. 10: 15-LOX-1 expression induces apoptosis in colon cancer cells according to Annexin V staining assay.**

15-LOX-1 expressing HCT-116 cell lines had significantly (\*\* $P < 0.01$ ) greater numbers of apoptotic cells compared to control cells. Error bars represent SD of three independent experiments.

To determine whether 15-LOX-1 expression could alter the expression of anti-apoptotic proteins, a Western blot analysis was carried out for the anti-apoptotic proteins XIAP and Bcl-xL. A reduction in the protein levels of both XIAP (Fig. 3.11) and Bcl-xL (Fig. 3.12) was observed when compared to the control cells.

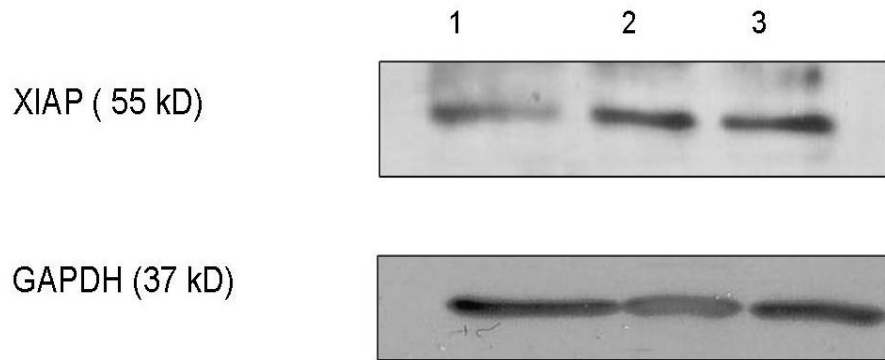


**Figure 3. 11: 15-LOX-1 expression induces apoptosis in colon cancer cells by decreasing XIAP anti apoptotic protein levels.**

Western blot analysis of X-linked inhibitor of apoptosis (XIAP) in 15-LOX-1 expressing cells (lane 1) showed reduced protein expression compared to EV transfected (lane 2) and parental HCT-116 (lane 3). Equal protein loading was confirmed by the levels of GAPDH.

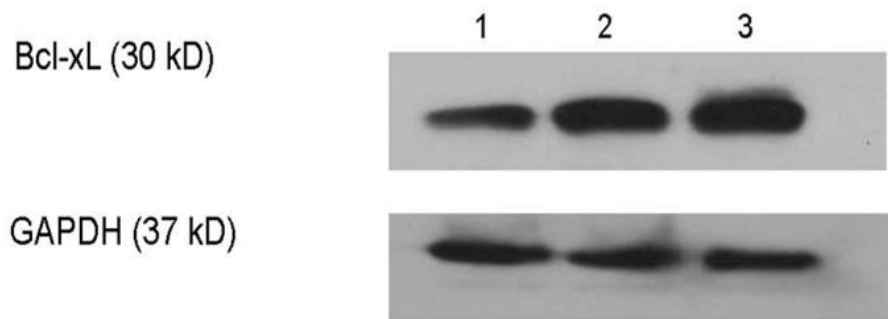


**Figure 3. 12: 15-LOX-1 expression induces apoptosis in colon cancer cells by decreasing Bcl-xL anti apoptotic protein expression.**

Western blot analysis of Bcl-xL in 15-LOX-1 expressing cells (lane 1) showed reduced protein expression compared to EV transfected (lane 2) and parental HCT-116 (lane 3). Equal protein loading was confirmed by the levels of GAPDH.

### 3.1.4 Expression of 15-LOX-1 reduces anchorage-independent growth in HCT-116 cells

Anchorage-independent growth is regarded as an in vitro characteristic of neoplastic cells (Kelavkar et al, 2001). To determine the effect of 15-LOX-1 expression on the ability of HCT-116 cells to grow in an anchorage-independent manner, a soft agar assay was carried out for colony formation analysis. 15-LOX-1 expression significantly (\*\*P < 0.01) decreased the number of colonies formed by HCT-116 cells compared to empty vector transfected or parental cells (Fig 3.13 and 3.14). We did not, however, observe any difference in the size of the colonies.

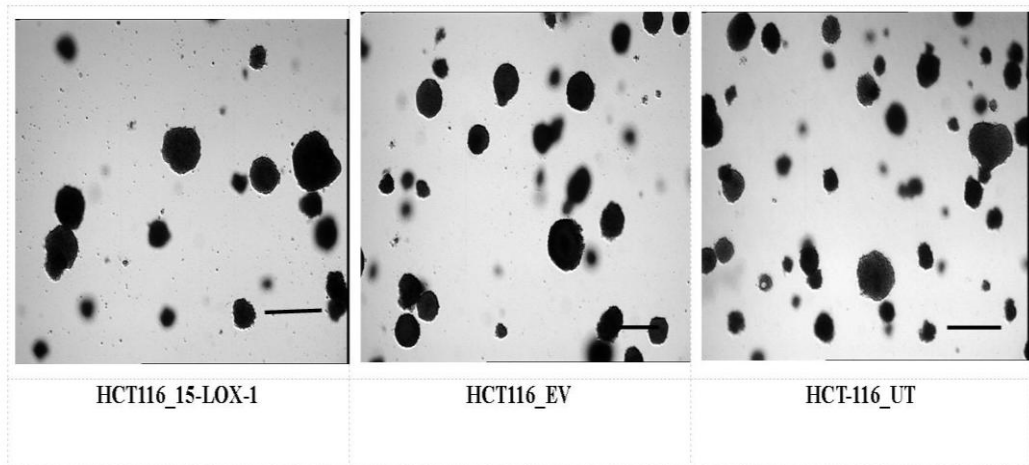


**Figure 3. 13: Representative photographs show 15-LOX-1 expressing HCT116 cells and control cells colonies by Soft agar assay.**

HCT-116 colorectal carcinoma cells stably transfected with 15-LOX-1 vector (HCT116\_15-LOX-1) or control cells (HCT116\_EV and HCT116\_UT) were grown on 0.6% noble agar for 2 weeks. Colonies were stained with 0.005% crystal violet and photographed under a light microscope. Scale bars, 100  $\mu$ m.

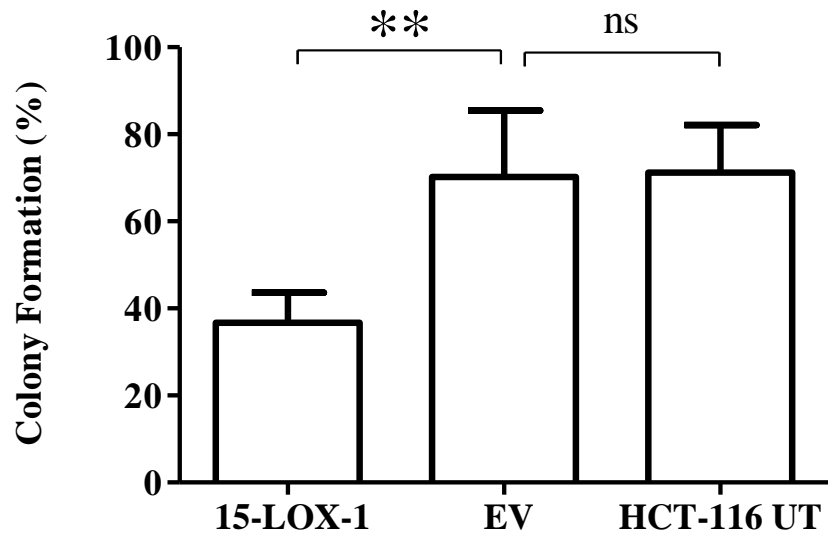


**Figure 3. 14: 15-LOX-1 expression decreases anchorage-independent growth on soft agar.**

The cells expressing 15-LOX-1 formed significantly fewer colonies (\*\*P < 0.01) compared to empty vector (EV) transfected and parental untransfected (UT) cells (colony formation represented as 100%). Error bars represent three independent experiments carried out in triplicate. ns, not significant.

### 3.1.5 Expression of 15-LOX-1 reduces motility in HCT-116 cells

To determine the role of 15-LOX-1 in the motility of HCT-116 cells, an in vitro scratch wound healing assay was carried out. As can be seen in Figure 3.15, cells expressing 15-LOX-1 (HCT116\_15-LOX-1) were not able to close the wound in the confluent culture, when compared with parental untransfected (HCT116\_UT) and empty vector (HCT116\_EV) controls, after 72 h. The results shown in Figure 3.16 indicate that after allowing the cells to grow for 72 h following application of the wound, the HCT116\_15-LOX-1 cells were significantly less motile and could not close the wound (\*\*P < 0.01) whereas the empty vector transfected and parental cells could completely heal the wound.

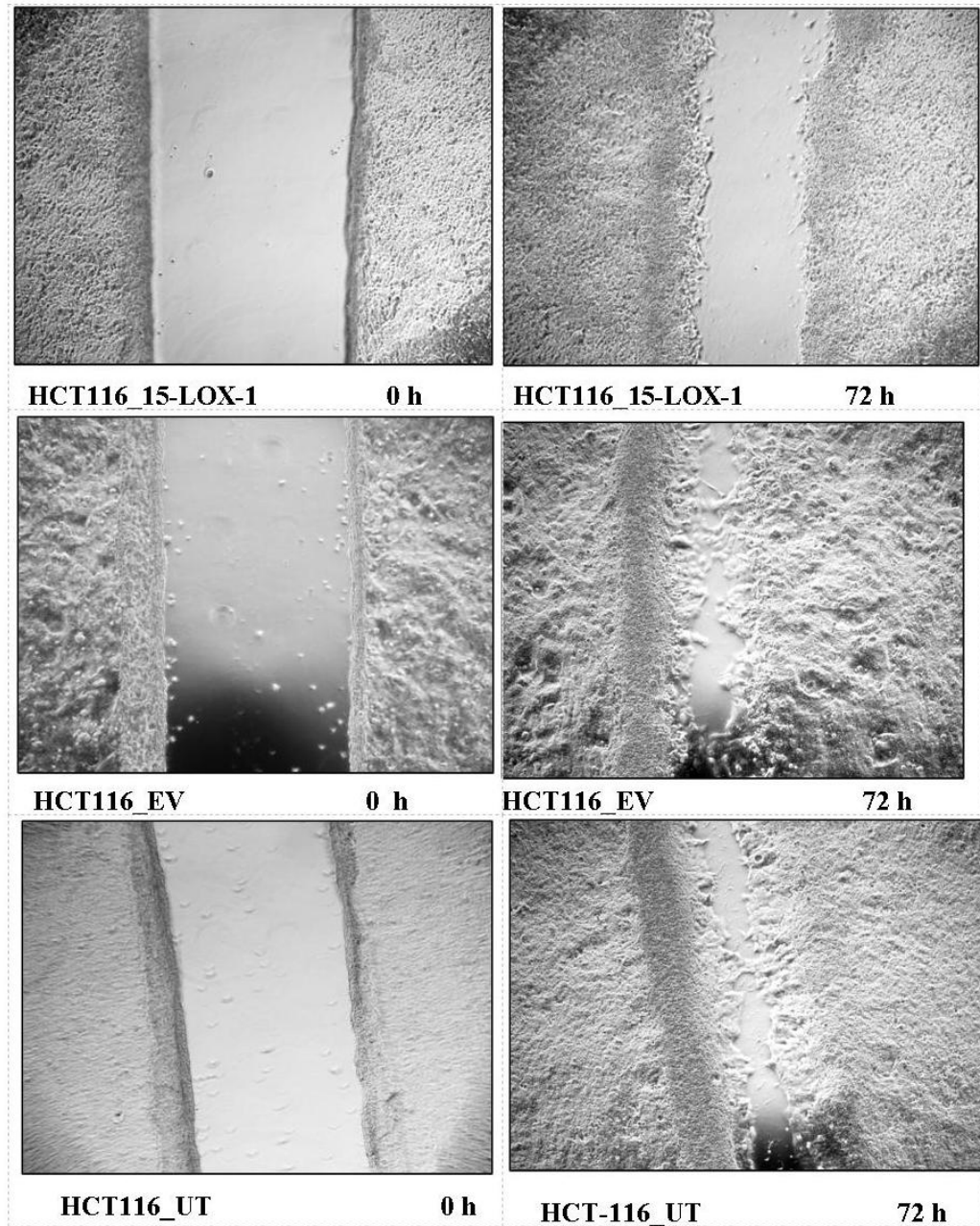


**Figure 3. 15: Representative photographs show 15-LOX-1 expressing HCT116 and control cells motility by wound healing assay.**

15-LOX-1 expressing HCT116 (HCT116\_15-LOX-1) and control cells (HCT116\_EV and HCT116\_UT) were seeded into 6 well plates and wounded with sterilized pipette tips for 0 h. After 72 h. incubation, wound closure photographed under light microscope.

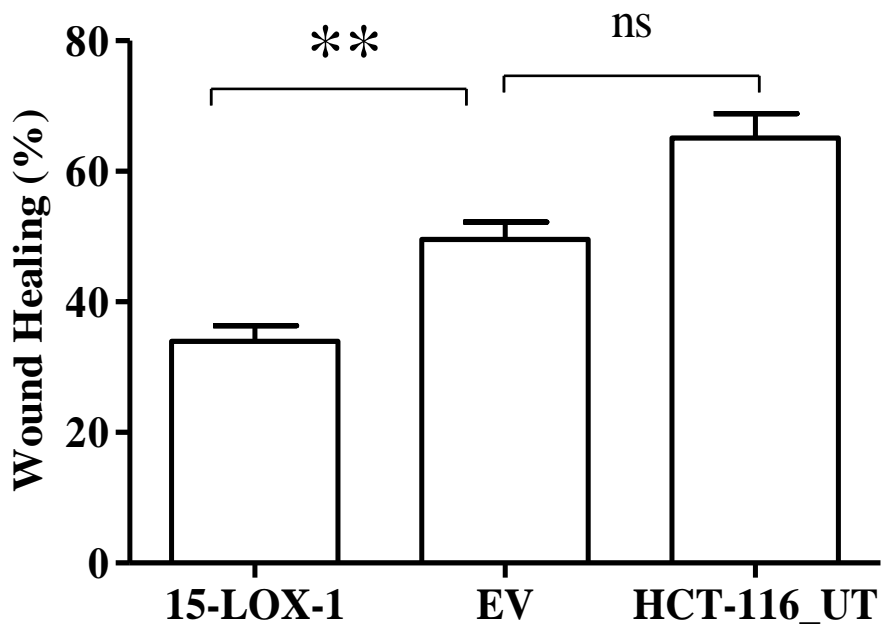


**Figure 3. 16: 15-LOX-1 expression causes a reduction in cell motility.**

The graphs show 15-LOX-1 expressing cells have significantly reduced motility (\*\*P < 0.01) with 32% wound closure compared to 56% for EV expressing and 69% for parental HCT-116 cells. The differences in wound closure between EV transfected and UT cells did not reach statistical significance. Error bars represent SD from three independent experiments each carried out three times. ns, not significant.

### 3.1.6 Expression of 15-LOX-1 reduces adhesion to fibronectin in HCT-116 cells

During tumor metastasis, cancer cell survival and adaptation to the new microenvironment is preceded by integrin-mediated cell adhesion to and migration on the ECM proteins such as fibronectin. The ability of 15-LOX-1 expressing HCT-116 cells and control cells to adhere to fibronectin was next established. The data (Fig 3.17) indicate that 15-LOX-1 expression significantly reduced the ability of HCT-116 cells to adhere to fibronectin (\*\*P < 0.001) when compared to control cells.

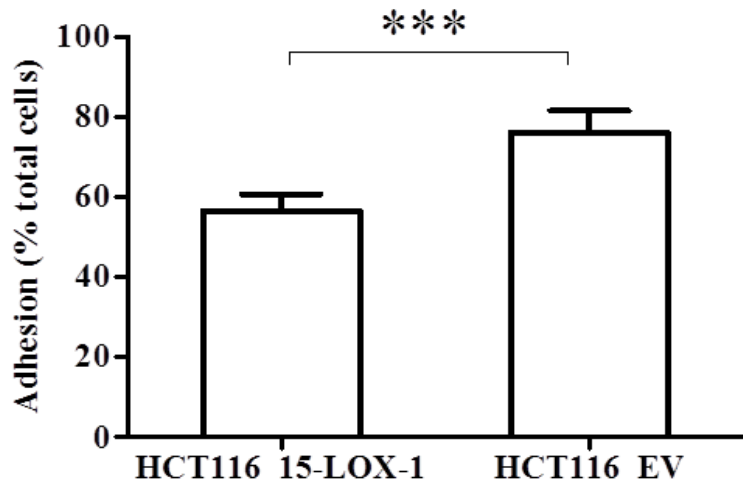


**Figure 3. 17: 15-LOX-1 expression reduces the ability of HCT-116 cells to adhere to fibronectin.**

HCT-116 cells stably transfected with 15-LOX-1 or with the empty vector (EV) were seeded in 96-well plates coated with 50 µg/mL fibronectin and blocked with BSA. The cells were allowed to attach for 2 h then the non-adherent cells were removed and the MTT assay was carried out to quantify the attached cells at 570 nm. The 15-LOX-1 expressing cells were found to adhere significantly less (\*\*P < 0.001) to the fibronectin compared to the control cells. Error bars represent SD from two independent experiments carried out in five replicates. ns, not significant.

### 3.1.7 15-LOX-1 expression reduces migration in HCT-116 cells

In order to show the effect of 15-LOX-1 expression on the migration of HCT-116 cells, the in vitro cell migration assay carried out based on the principle of the Boyden chamber assay. Cells in medium containing 1% serum were added to Transwell inserts containing membranes with 8 µm pores. The bottom chambers contained medium with 10% FBS and 5 µg/mL fibronectin. After 72 hour incubation, the membranes were fixed and stained and the number of cells that had migrated through the membrane was counted under a Leica light microscope (10 X objective) and a representative image was captured using the 20X objective (Fig 3.18). The data (Fig 3.19) indicate that HCT-116 cells expressing 15-LOX-1 showed a significant decrease in the number of cells that were able to migrate compared to the empty vector transfected cells (\*\*P < 0.01). Thus, the expression of 15-LOX-1 significantly inhibited the migration of HCT-116 cells.

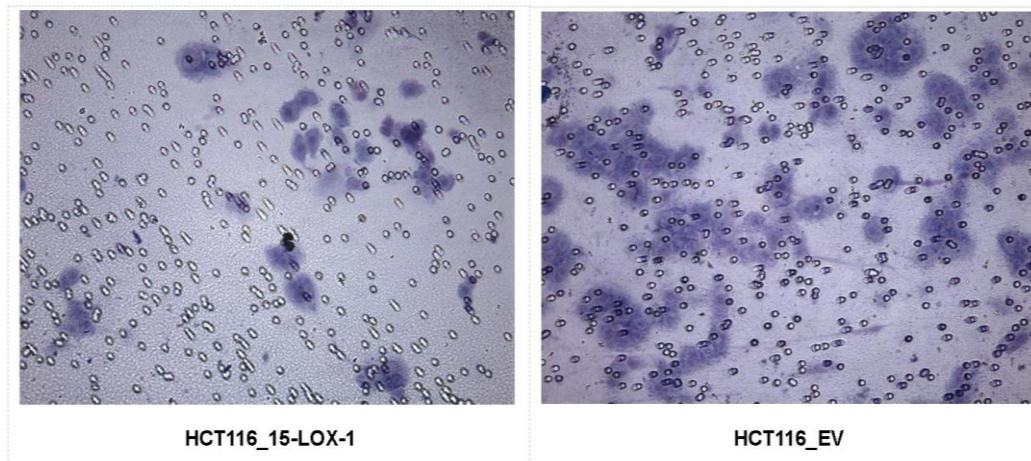


**Figure 3. 18: Representative photographs show 15-LOX-1 expressing HCT116 and control cells migration by Transwell migration assay.**

Both photographs of 15-LOX-1 expressing HCT116 cells (HCT116\_15-LOX-1) and control cells (HCT116\_EV) were captured in a Leica light microscope under 20X magnification.

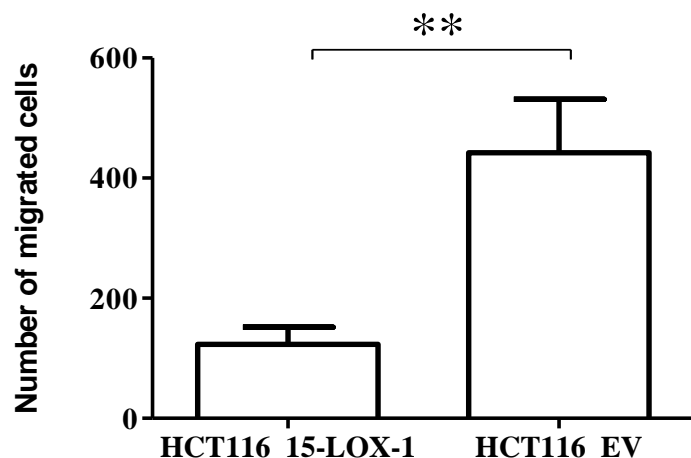


**Figure 3. 19: 15-LOX-1 expression reduces migration in HCT-116 cells when compared to empty vector (EV) controls.**

15-LOX-1 transfected HCT-116 cells migrated through the 8 µm pores of the Transwell in significantly less numbers (\*\*P < 0.01) compared to the control cells. The column graph represents the number of cells that migrate through the Transwell in the experimental and control cell lines. Error bars represent SD from three independent experiments carried out in four replicates. Scale bars, 40 µm.

### 3.1.8 15-LOX-1 expression reduces invasion of HCT-116 cells.

To determine the role of 15-LOX-1 in the invasion of HCT-116 cells, an invasion assay was carried out using Matrigel coated Transwell inserts. The Matrigel served as a reconstituted basement membrane in vitro. Cells in medium containing 1% serum were added to Transwell inserts. The bottom chambers contained medium with 10% FBS and 5 µg/mL fibronectin. After 72 hour incubation, the membranes were fixed and stained and the number of cells that had migrated or invaded through the membrane was counted under a Leica light microscope (10X objective) and a representative image was captured using the 20X objective (Fig 3.20). The results (Fig 3.21) indicate that HCT-116 cells expressing 15-LOX-1 showed a significant decrease in the number of cells that were able to invade across Matrigel-coated membranes compared to empty vector transfected cells (\*P < 0.05). Thus, the forced expression of 15-LOX-1 significantly inhibited the invasion of HCT-116 cells.

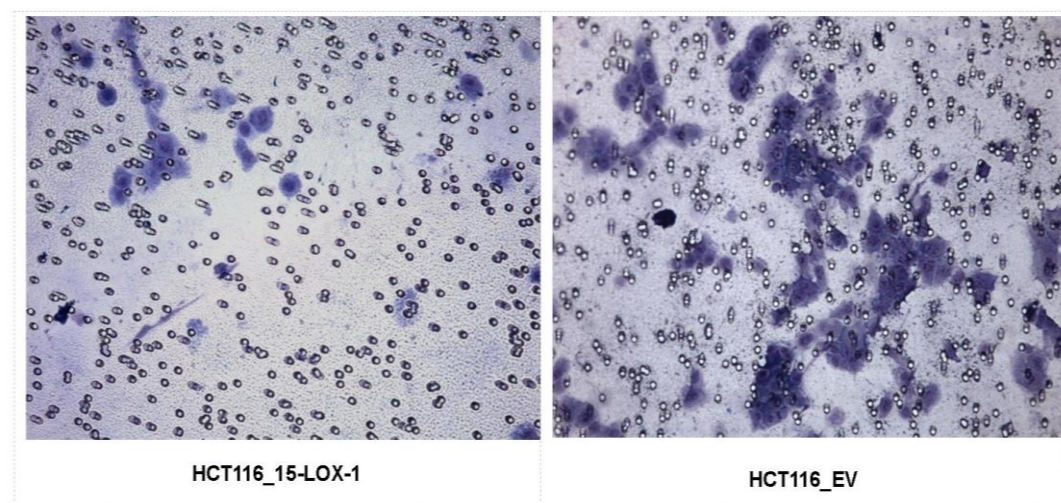


**Figure 3. 20: Representative photographs show 15-LOX-1 expressing HCT116 and control cells invasion by Matrigel Transwell invasion assay.**  
Both photographs of 15-LOX-1 expressing HCT116 cells (HCT116\_15-LOX-1) and control cells (HCT116\_EV) were captured in a Leica light microscope under 20X magnification.

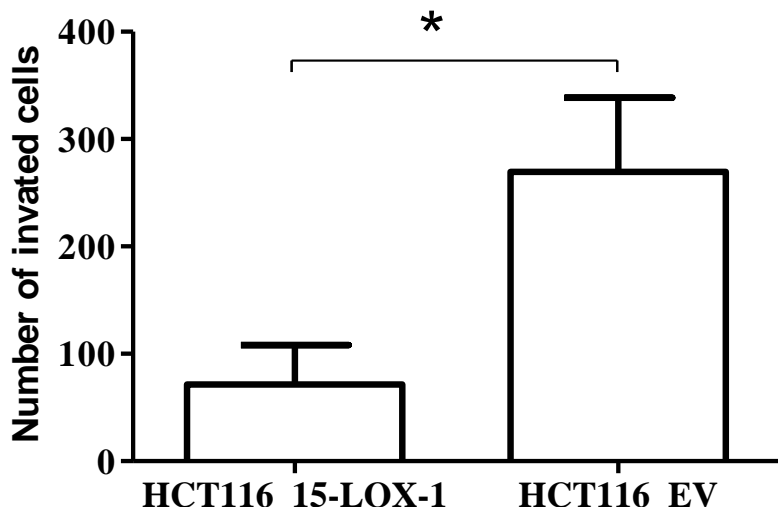


**Figure 3. 21: 15-LOX-1 expression reduces invasion in HCT-116 colorectal carcinoma cells when compared to empty vector (EV) controls.**

15-LOX-1 expression significantly reduces (\* $P < 0.05$ ) the ability of HCT-116 cells to invade through the basement membrane in vitro. The column graph represents the number of cells that could invade through the Transwell in the experimental and control cell lines. Error bars represent SD from three independent experiments carried out in four replicates. Scale bars, 40  $\mu\text{m}$ .

A protein that has been widely implicated cellular motility and invasiveness in recent years is Metastasis Associated Protein-1 (MTA1) (Marzook et al, 2012; Sankaran et al, 2012). This protein is also a part of the nuclear remodeling complex (NuRD) that was recently shown to silence 15-LOX-1 in colon cancer cells (Zuo et al, 2009). To understand whether ectopic expression of 15-LOX-1 reduced cell invasion via MTA1, a Western blot analysis was carried out to determine the expression of MTA1. The data (Fig. 3.22) indicate that HCT-116 cells expressing 15-LOX-1 had reduced protein levels of MTA-1 when compared to the empty vector transfected and parental cells. Additionally, preincubation with 1  $\mu\text{M}$  of the 15-LOX-1 specific inhibitor PD146176 restored the expression of MTA-1 to the same level as the control cell.

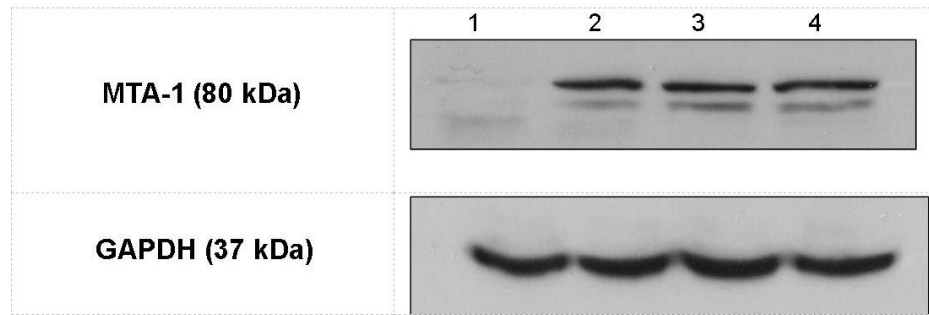


**Figure 3. 22: 15-LOX-1 expression decreased colon metastasis associated protein-1 (MTA-1) expression in HCT-116 cells.**

Total protein lysate isolated from stably expressing 15-LOX-1 and control HCT-116 cells were probed for MTA-1 expression using a mouse mAb. Lane 1, 15-LOX-1 expressing cells; lane 2, 15-LOX-1 expressing cells treated with 1 $\mu$ M PD146176; lane 3, empty vector expressing cells; lane 4, untransfected parental cells. Equal protein loading was confirmed with the use of GAPDH.

### 3.1.9 15-LOX-1 reduces neoangiogenesis in HCT-116 cells.

#### 3.1.9.1 Reduction in VEGF-A<sub>165</sub> secretion

Previous studies showed that 15-LOX-1 has been associated with angiogenesis (Shappell et al, 2003; Viita et al, 2009; Viita et al, 2008; Yan et al, 2012). However, whether 15-LOX-1 expression is also associated with a reduction in neoangiogenesis in CRC has not been established to date. Therefore, first VEGF-A<sub>165</sub> secretion was determined with an ELISA assay as described in ‘Materials and Methods’. The data (Fig 3.23) show that VEGF secretion in the 15-LOX-1 expressing HCT116 cells was significantly (\*P<0.05) reduced compared to the control cells.

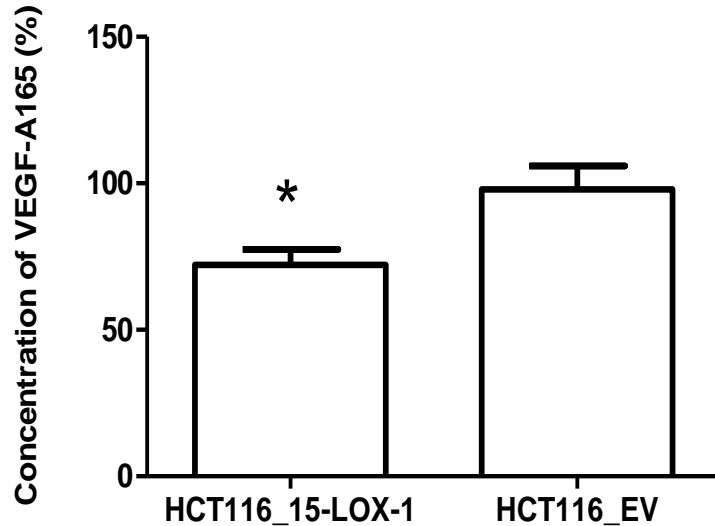


**Figure 3. 23: 15-LOX-1 expression reduced secreted VEGF-A<sub>165</sub> levels in HCT-116 cells.**

A Secreted VEGF levels (%). HCT116\_15-LOX-1: Conditioned medium from 15-LOX-1 expressing HCT116 cells, HCT116\_EV: Conditioned medium from empty vector transfected HCT-116 cells.

### 3.1.9.2 15-LOX-1 expression in HCT-116 cell line reduces HUVEC proliferation and mobility and tube formation

After the binding of angiogenic factors like VEGF-A<sub>165</sub> to specific receptors in the endothelial cells, the endothelial cells proliferate, migrate and form new capillary tubes (Reinmuth et al, 2003). Therefore, an MTT assay was performed to determine the proliferation of Human umbilical vein endothelial cells (HUVEC) grown in conditioned medium from cells expressing 15-LOX-1. The data (Fig 3.24) indicated that conditioned medium collected from 15-LOX-1 expressing HCT 116 cells after 72h caused significantly less HUVEC proliferation compared to control cells (\*\*P<0.01).

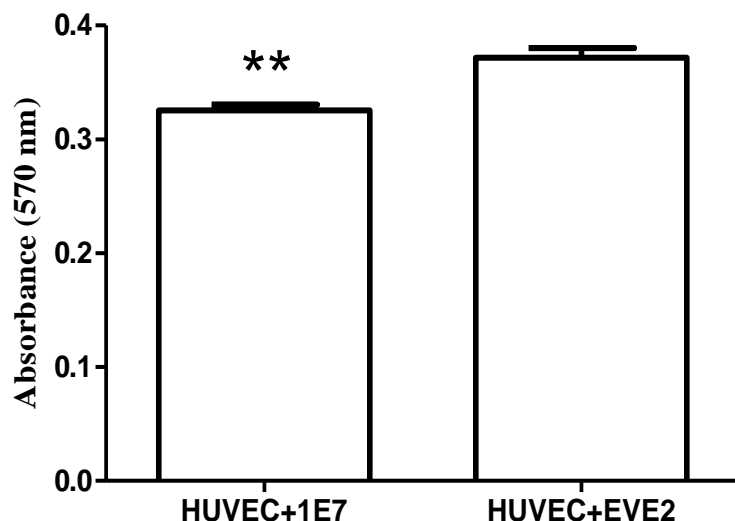


**Figure 3. 24: Conditioned medium collected from 15-LOX-1 expressing HCT 116 cells after 72h reduced HUVEC proliferation compared control cells.**  
 HUVEC+1E7: HUVEC grown in conditioned medium from 15-LOX-1 expressing HCT116 cells, HUVEC+EVE2: HUVEC grown in conditioned medium from empty vector transfected HCT-116 cells.

Next, an in vitro wound healing assay was performed to determine the motility of HUVEC grown in conditioned medium from cells expressing 15-LOX-1. As shown in Figure 3.25, conditioned medium obtained from 15-LOX-1 expressing HCT-116 cells resulted in a slower closure of the wound created in the HUVEC confluent culture compared to the control cells after 9 h. The data (Fig 3.26) indicated that conditioned medium collected from 15-LOX-1 expressing HCT 116 cells after 72h caused less HUVEC motility compared to control cells (\*P<0.05).

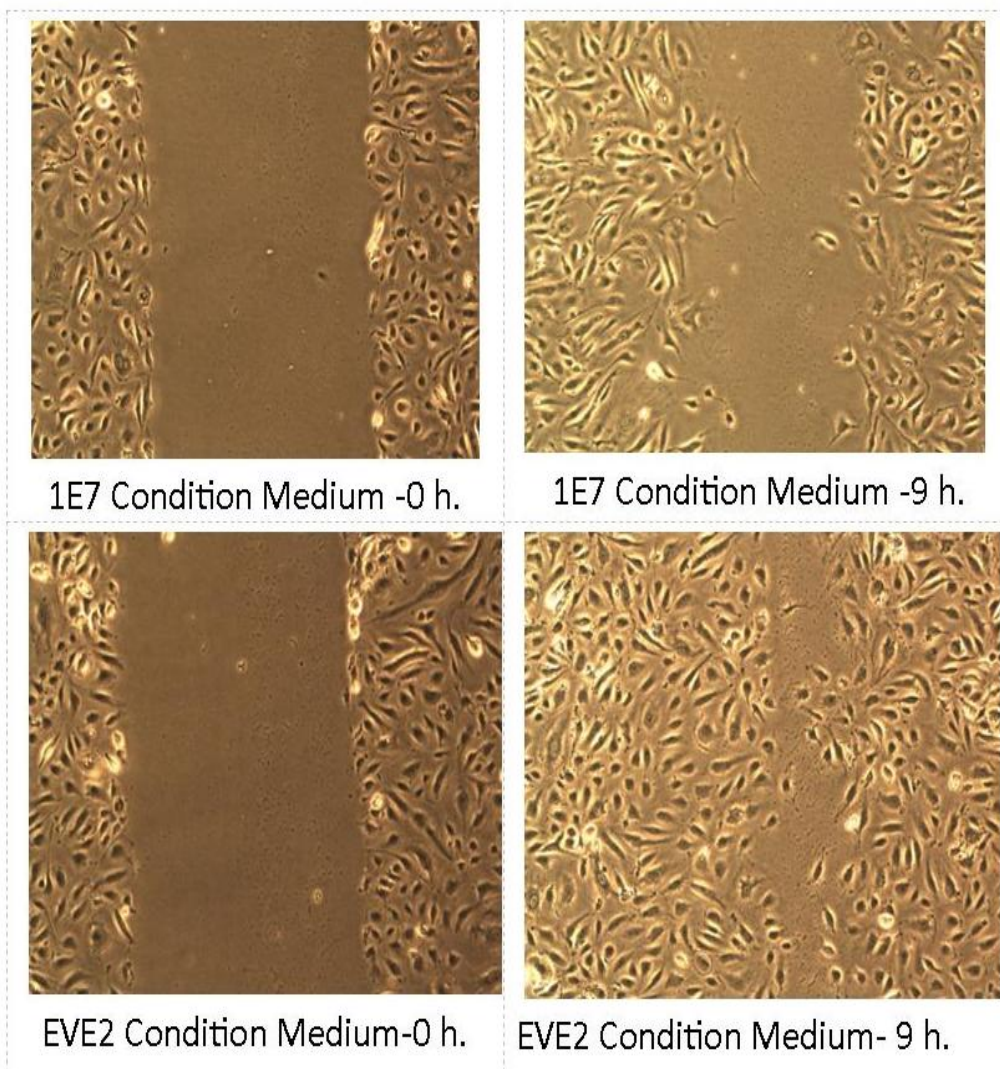


**Figure 3. 25: Conditioned medium collected from 15-LOX-1 expressing HCT 116 cells after 72h reduced HUVEC migration compared conditioned medium collected from control cells.**

Representative photographs show HUVEC motility by wound healing assay after incubation in condition medium that obtained 15-LOX-1 expressing HCT-116 (1E7) and control cells (EV) for 9 hours.

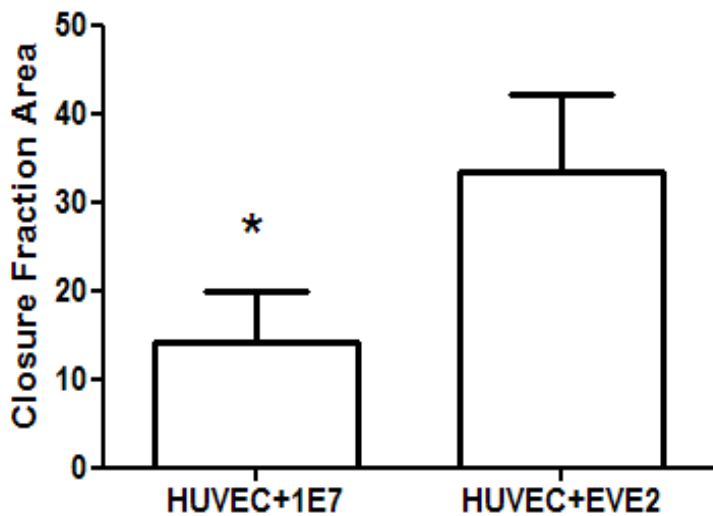


**Figure 3. 26: Conditioned medium collected from 15-LOX-1 expressing HCT 116 cells after 72h reduced HUVEC motility compared control cells.**

HUVEC+1E7: HUVEC grown in conditioned medium from 15-LOX-1 expressing HCT116 cells, HUVEC+EVE2: HUVEC grown in conditioned medium from empty vector transfected HCT-116 cells.

Finally, an endothelial tube formation assay was carried out. The endothelial tube formation assay is based on the principle of incubating subconfluent HUVEC in Matrigel with conditioned medium and allowing for the formation of capillary like structures or tubes. Conditioned medium collected from 15-LOX-1 expressing cells after 72h caused HUVEC to form tubes (Fig. 3.27) with significantly reduced total skeleton length, number of branching points, nodal structures and tubes compared to empty vector transfected HCT-116 cells (\*\*P<0.01 and \*P<0.05, Fig. 3.28).

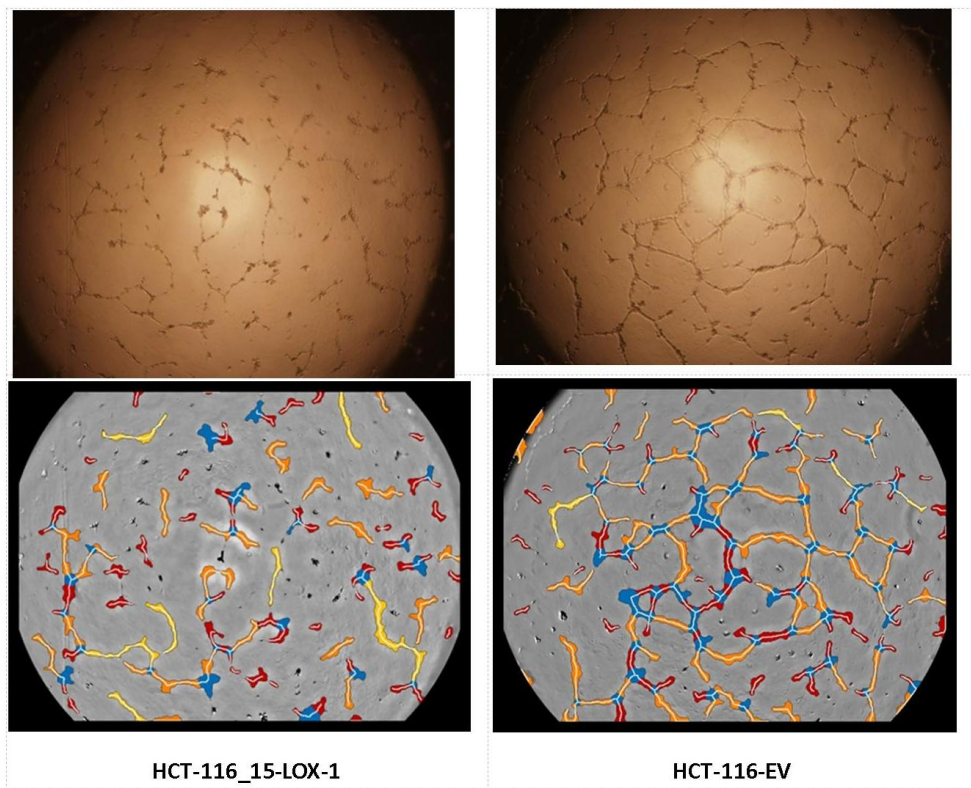


**Figure 3. 27: Representative photographs show HUVEC Tube Formation Assay (10x objective) in 15-LOX-1 expressing HCT116 and control cells.**  
HCT116\_15-LOX-1: 15-LOX-1 expressing HCT116 cells, HCT116\_EV: Empty vector transfected HCT-116 cells.

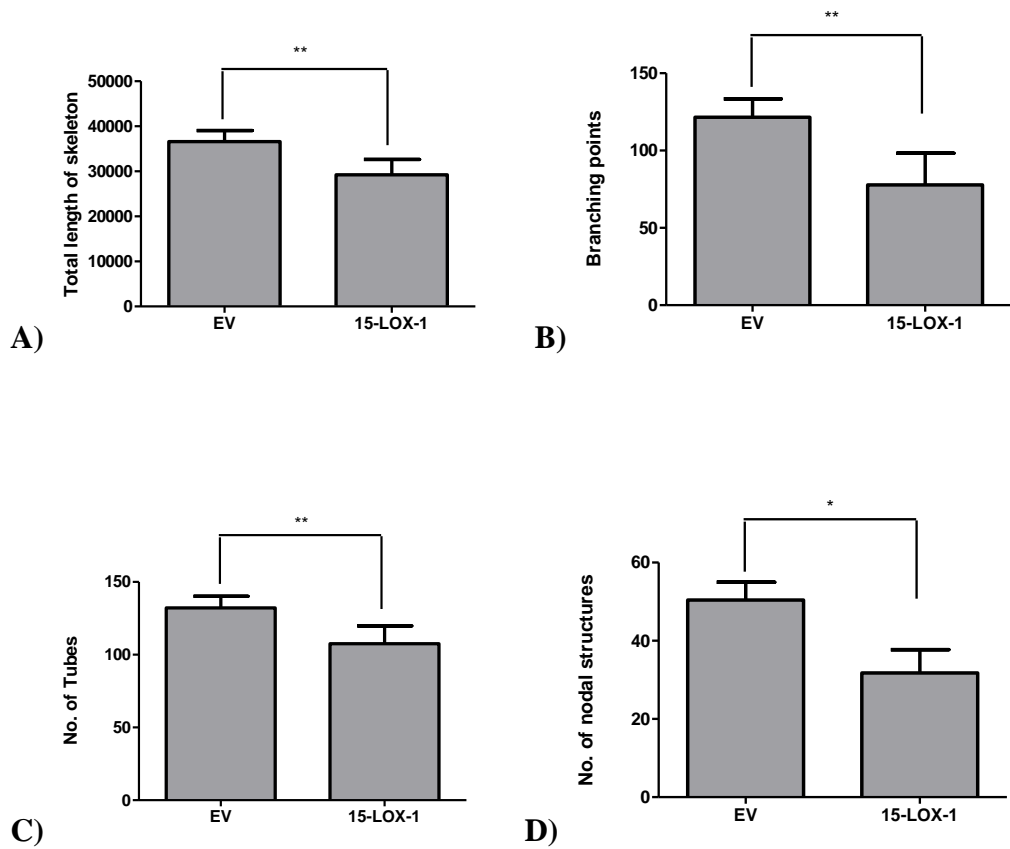


**Figure 3. 28: Conditioned medium collected from 15-LOX-1 expressing HCT 116 cells after 72h reduced HUVEC tube formation compared conditioned medium collected from control cells.**

Quantitative analysis of (A) Total Length of skeleton (B) Number of branching points (C) Number of tubes. (D) Number of nodal structures.

## **Section II: The mechanism of antitumorigenic effect of 15-LOX-1 in CRC**

The data shown above indicated that 15-LOX-1 has anti-tumorigenic properties by ameliorating several of the hallmarks of cancer such as by inducing apoptosis, decreasing cell proliferation, reducing motility and invasive potential as well as reducing angiogenesis in HCT-116 CRC cells. In order to determine the mechanistic underpinnings behind these observations, we hypothesized that these effects shown by 15-LOX-1 could be through the suppression of the inflammatory transcription factor NF-κB. NF-κB (p65 and p50 heterodimer) is normally held inactive in the cytoplasm by Inhibitor of kappa B (IκB) protein. In the presence of a stimulus, the IκB protein is degraded in the proteasome and NF-κB is free to move to the nucleus where it can bind to its consensus sequence and become transcriptionally active.

### **3.2.1 15-LOX-1 Expression Reduces Nuclear Translocation of NF-κB**

Nuclear extracts isolated from the 15-LOX-1 expressing cells and control cells were probed for translocation of the NF-κB subunit p65 using Western blot (Fig. 3.29). The results indicate that forced expression of 15-LOX-1 in HCT-116 cell lines could reduce the nuclear translocation of the NF-κB subunit p65 when compared to the EV-transfected cells. Additionally, preincubation of the 15-LOX-1 expressing cells with 1 μM of the 15-LOX-1 inhibitor PD146176, could reverse the inhibition in nuclear translocation of p65.

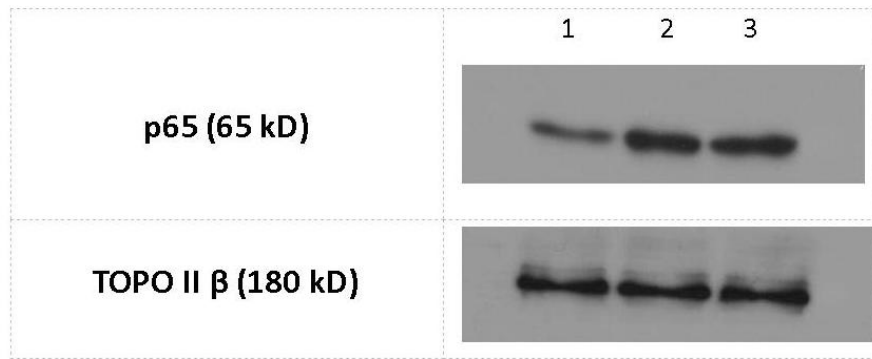


**Figure 3. 29: 15-LOX-1 expression reduces NF-κB p65 nuclear translocation.**

Reduced translocation of p65 was observed in nuclear extracts isolated from HCT-116 cells with forced expression of 15-LOX-1 (lane 1) compared to control empty vector (EV) transfected cells (lane 2). This effect was reversed when the cells were treated with 1  $\mu$ M 15-LOX-1 inhibitor PD146176 (lane 3).

NF-κB is normally held in the cytoplasm by I $\kappa$ B proteins and following a pro-inflammatory stimulus, the I $\kappa$ B proteins are phosphorylated and degraded in the proteosome. We therefore determined the protein levels of I $\kappa$ B- $\alpha$  and phosphorylated I $\kappa$ B- $\alpha$  in the cytoplasmic extracts of the 15-LOX-1 expressing HCT-116 and control HCT-116 cells by Western blot (Fig. 3.30). The data indicate a higher level of I $\kappa$ B $\alpha$  in the cytoplasm of 15-LOX-1 expressing HCT-116 cells when compared to EV-transfected cells. Additionally, the phosphorylated form of I $\kappa$ B- $\alpha$  was found to be much lower in the 15-LOX-1 expressing cells when compared to the control cells, indicating that degradation of I $\kappa$ B $\alpha$  and release of active NF-κB was inhibited when 15-LOX-1 was expressed. When the 15-LOX-1 expressing cells were treated with 1  $\mu$ M PD146176 and probed for the protein levels of I $\kappa$ B $\alpha$  and its phosphorylated form, we observed a reduction of I $\kappa$ B $\alpha$  level along with an increase in its phosphorylated form. This further confirms that the retention of the NF-κB subunits by I $\kappa$ B- $\alpha$  in the cytoplasm most likely directly resulted from the expression of 15-LOX-1.

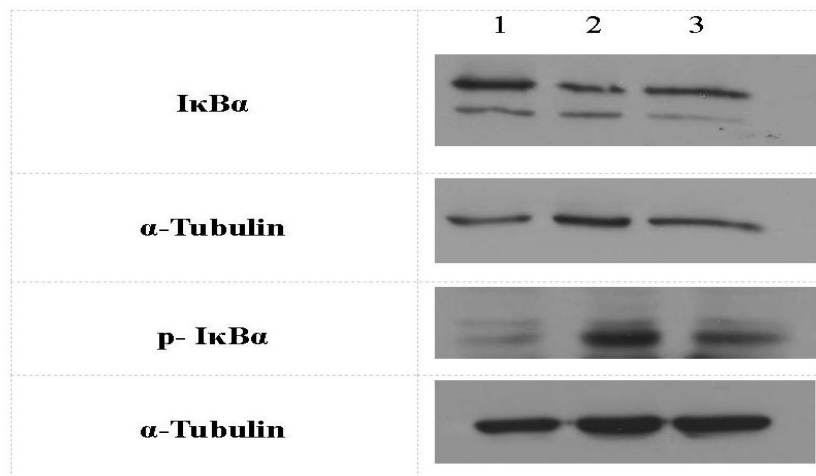


**Figure 3. 30: 15-LOX-1 expression affects p-IκB- $\alpha$  and IκB- $\alpha$  amount in cytoplasm in HCT116 cells.**

15-LOX-1 transfection in HCT116 cells resulted in increased levels of IκB- $\alpha$  (lane 1) and decreased levels of phosphorylated IκB- $\alpha$  (lane 1) in the cytoplasm when compared to control EV cells (lane 2). This effect was also reversed upon treatment with 1  $\mu$ M PD146176 (lane 3).

### 3.2.2 15-LOX-1 expression reduces the DNA-binding activity of NF-κB

To determine whether the loss of nuclear translocation of the NF-κB subunits was also associated with a decrease in the DNA-binding activity of the transcription factor, the DNA-binding activity of the p50 subunit was determined using the NF-κB (human p50) Transcription Factor Assay Kit. Nuclear extracts from 15-LOX-1 expressing HCT-116 cells were incubated in a 96-well plate containing the NF-κB consensus sequence. Once the binding reaction was complete, a colorimetric detection of the active (i.e., DNA bound) p50 was carried out with a primary antibody against p50 followed by a horseradish peroxidase conjugated secondary antibody. The data (Fig. 3.31) indicate that the amount of active DNA bound p50 protein was significantly ( $P<0.05$ ) lower in the 15-LOX-1 expressing cells when compared to the control cells. Additionally, when the cells were incubated with PD146176, the DNA bound active form of p50 increased to the same level as the control EV-transfected cells, further confirming the specificity of 15-LOX-1 in inhibiting the DNA-binding activity of NF-κB.

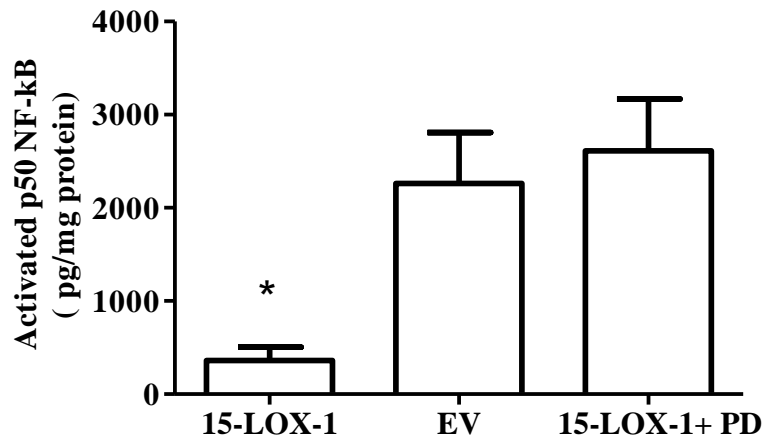


**Figure 3. 31: 15-LOX-1 expression reduces NF-κB DNA binding.**

Nuclear extracts were applied on the NF-κB (human p50) Transcription Factor Assay Kit. HCT-116 expressing 15-LOX-1 showed significantly reduced p50 DNA binding when compared to control EV cells, or when the 15-LOX-1 expressing cells were treated with 1μM PD146176.

### 3.2.3 15-LOX-1 expression reduces the transcriptional activity of NF-κB

The transcriptional activity of NF-κB in the 15-LOX-1 expressing cells was next determined. For this purpose, the 15-LOX-1 expressing and control cells were transfected with the PathDetect cis-Reporting system (Stratagene Agilent), the cells were collected and then assayed for luciferase activity. This assay works on the principle of the transcription of a luciferase reporter gene in the presence of a TATA box promoter and an NF-κB cis-enhancer element. The data (Fig. 3.32) indicate that two monoclonals of 15-LOX-1 expressing HCT-116 cells (1E7 and 1F4) could significantly reduce the transcriptional activity of NF-κB when compared to control EV transfected cells ( $P<0.01$  for 1E7 compared to control cells (EV) and  $P<0.001$  for 1F4 compared to EV). Additionally, this inhibitory effect of 15-LOX-1 on NF-κB transcriptional activity was observed even when the cells were treated with TNF-α for 6 h in order to activate NF-κB ( $P<0.01$  for 1E7 compared to EV and  $P<0.001$  for 1F4 compared to EV). Moreover, when the cells were treated with 1 μM PD146176, the transcriptional activity of NF-κB in 1E7 and 1F4 cells returned to the level

observed with the EV transfected control cells ( $P>0.05$  for both comparisons), thereby further attesting the role of 15-LOX-1 in inhibiting the transcriptional activity of NF- $\kappa$ B.

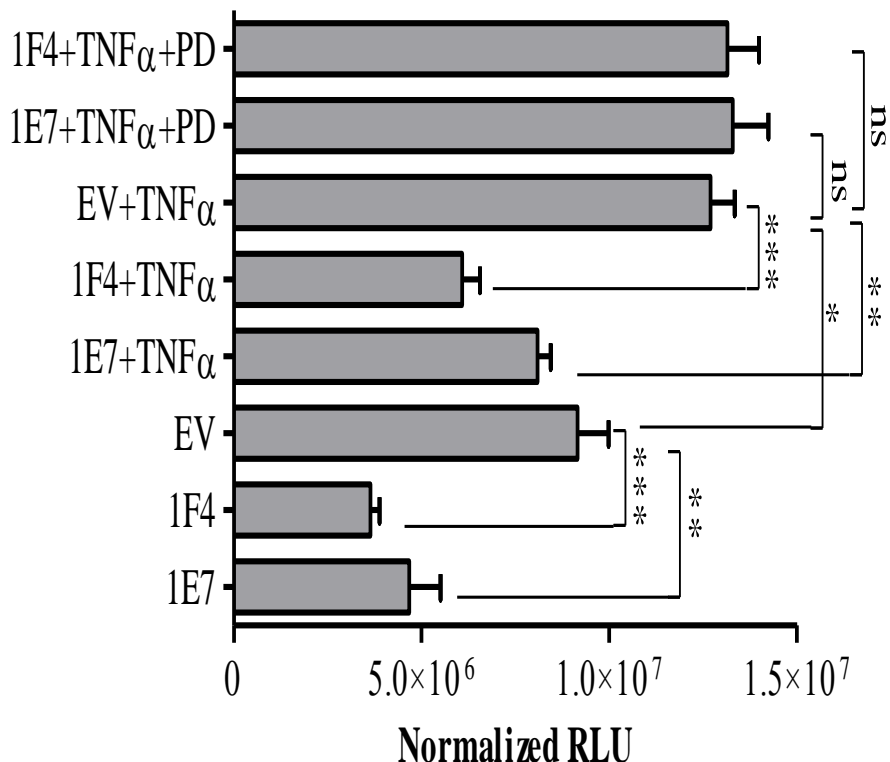


**Figure 3. 32: Luciferase assays indicate reduced NF- $\kappa$ B transcriptional activity in 15-LOX-1 expressing cells.**

Two monoclonals of HCT-116 cells (1E7 and 1F4) stably expressing 15-LOX-1 were transfected with the NF- $\kappa$ B Pathdetect cis-Reporting plasmid and the cells were collected 24 h later. Significantly reduced NF- $\kappa$ B transcriptional activity was observed in 15-LOX-1 expressing cells compared to the control cells (EV). This inhibition persisted even when the NF- $\kappa$ B pathway in the cells was activated with treatment with TNF- $\alpha$  for 6 h. Treatment of the cells with 1  $\mu$ M PD146176 could reverse this inhibition and the transcriptional activity could reach the levels similar to the control (EV) cells.  $\beta$ -Galactosidase was used for normalization. Statistical comparisons were carried out using one-way ANOVA with Tukey's multiple comparison tests.

### **3.2.4 13(S)-HODE increases PPAR $\gamma$ transcriptional activity**

The mechanism of NF- $\kappa$ B inhibition by 15-LOX-1 was next determined. PPAR $\gamma$ , an orphan nuclear receptor, is known to have antineoplastic effects in CRC, one of which is by the inhibition of NF- $\kappa$ B (Straus & Glass, 2007). First, the transcriptional activity of PPAR $\gamma$  was determined by transfecting the 15-LOX-1 expressing and control cells with the PPRE-3xTK-Luc construct, which has three copies of the PPAR $\gamma$  response element (PPRE) upstream of a TK driven luciferase reporter gene. The data (Fig. 3.33) indicate that both monoclonal 15-LOX-1 expressing HCT-116 cells (1E7 and 1F4) could increase the transcriptional activity of PPAR $\gamma$  when compared to the EV-transfected cells. This increase in activity is most likely due to the production of 13(S)-HODE in the 15-LOX-1 expressing cell lines and this endogenous 13(S)-HODE could serve as a ligand for the activation of PPAR $\gamma$  (Chabane et al, 2009). When the 1E7 cells were incubated with the PPAR $\gamma$  antagonist GW9662, the PPAR $\gamma$  transcriptional activity was reduced and reached levels similar to the EV-transfected cells treated with GW9662 ( $P>0.05$ ). Additionally, the decrease in PPAR $\gamma$  activity in the GW9662-treated EV-transfected cells was found to be statistically not significant when compared to the untreated EV cells ( $P>0.05$ ).

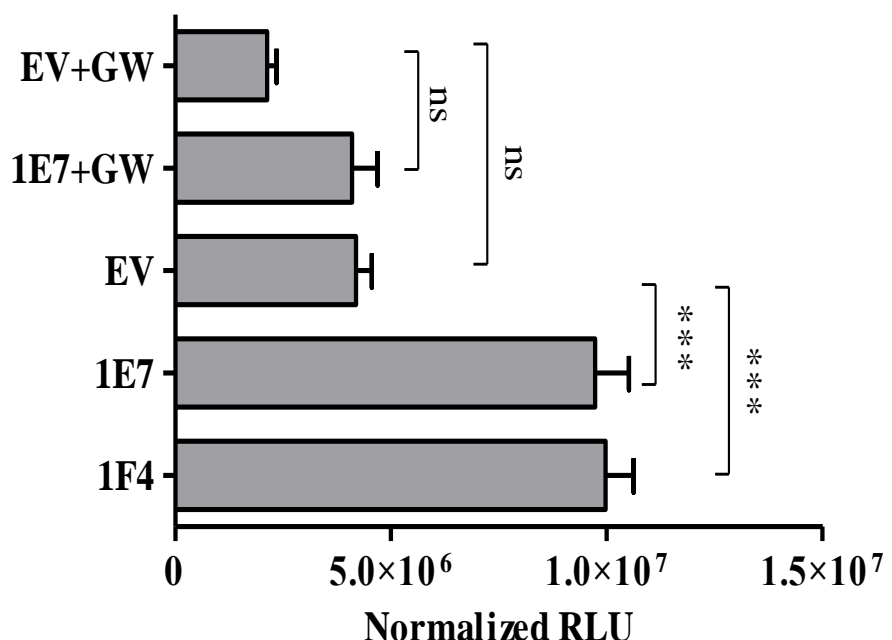


**Figure 3. 33: The 15-LOX-1 expressing cells showed higher PPAR $\gamma$  transcriptional activity compared to the control cells.**

The HCT-116 cells were transfected with a PPRE-3xTK-Luc construct. 1E7 and 1F4 cells showed significantly increased transcriptional activity of PPAR $\gamma$ , likely resulting from the increased levels of the PPAR $\gamma$  ligand 13(S)-HODE in these cells compared to the control (EV) cells. Treatment of the cells with 1  $\mu$ M of the PPAR $\gamma$  specific antagonist GW9662 (GW) could reverse the increase in luciferase activity. Statistical comparisons were carried out using one-way ANOVA with Tukey's multiple comparison tests.

Next, whether the increase in PPAR $\gamma$  transcriptional activity was due to 13(S)-HODE (the 15-LOX-1 metabolite) acting as a ligand for PPAR $\gamma$  was confirmed. For this purpose, parental HCT-116 cells were treated with 100  $\mu$ M of exogenously added 13(S)-HODE for 24 h after transfection with the PPRE-3xTK-Luc construct. The result showed a significant increase ( $P<0.05$ ) in the transcriptional activity of PPAR $\gamma$  in 13(S)-HODE treated parental HCT-116 cells (Fig. 3.34) when compared to the vehicle-treated cells.

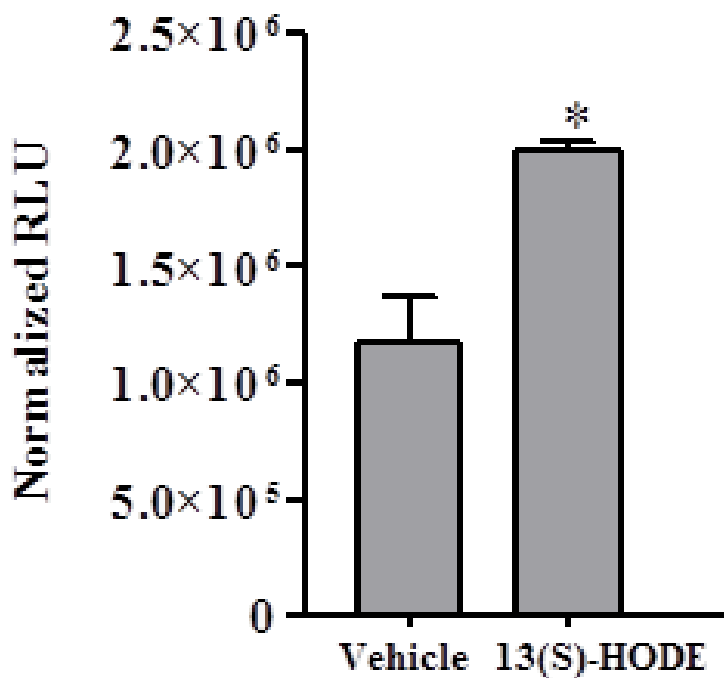


**Figure 3. 34: Exogenous 13-(S)-HODE (15-LOX-1 metabolite) showed higher PPAR $\gamma$  transcriptional activity.**

Parental HCT-116 treated with 100  $\mu$ M of exogenously added 13(S)-HODE for 24 h after transfection with the PPRE-3xTK-Luc construct showed a significant increase in the PPAR $\gamma$  transcriptional activity when compared to vehicle treated cells.  $\beta$ -Galactosidase was used for normalization. The 13(S)-HODE treatment data were analyzed for statistical significance using Mann–Whitney U-test.

### 3.2.5 PPAR $\gamma$ inhibition activates NF- $\kappa$ B nuclear translocation in 15-LOX-1 expressing cells

Previous studies have indicated that PPAR $\gamma$  activation is associated with an inhibition of NF- $\kappa$ B activity in the colon (Chen et al, 2003; Wahli, 2008). The present study indicated that cells with forced expression of 15-LOX-1 showed an inhibition of NF- $\kappa$ B nuclear translocation, DNA binding and transcriptional activity, along with a transcriptional activation of PPAR $\gamma$ . Whether the two events are related was next determined.

In order to determine whether the inhibition in nuclear translocation of p65 observed by Western blot (Fig. 3.29) in the 15-LOX-1 expressing cells (1E7) was due to PPAR $\gamma$  activation, the HCT-116 cells were incubated with the PPAR $\gamma$  specific antagonist GW9662 (1  $\mu$ M) for 24h. Immunofluorescence studies for p65 were conducted using this cells and photographed image under confocal microscope (Fig 3.35). The images were analyzed by Image J to obtain nuclear AF488/PI pixel intensity ratio in order to quantify the NF- $\kappa$ B nuclear translocation. Our data (Fig 3.36) showed that 15-LOX-1 expressing cells (1E7) significantly decrease nuclear translocation of p65 when compared to EV-transfected cells ( $P<0.05$ ). Moreover, the inhibition in nuclear translocation of NF- $\kappa$ B in 15-LOX-1 expressing cells is rescued by the incubation of the cells with 1  $\mu$ M of the 15-LOX-1-specific inhibitor PD146176. Additionally, when the cells were treated with 1  $\mu$ M of GW9662, a similar reversal of the inhibition in translocation of p65 protein is observed, indicating that attenuation of PPAR $\gamma$  activity in the 15-LOX-1 expressing cells could rescue the inhibition of NF- $\kappa$ B.

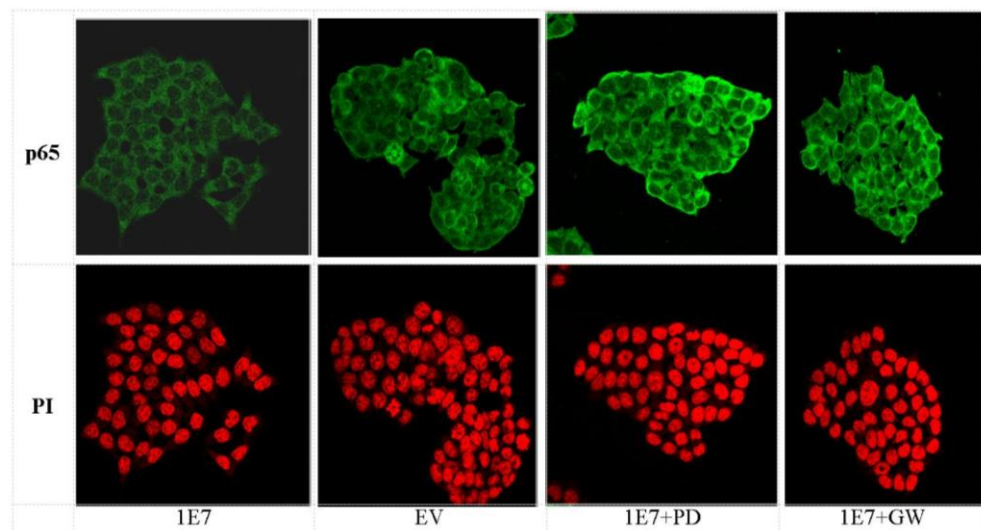


**Figure 3. 35: Representative photographs show 15-LOX-1 expressing and control HCT116 cells immunofluorescence assay result for p65.**  
Treated (GW9662 or PD146176) and untreated the cells were incubated with p65 antibody and counterstained with an Alexa Fluor 488 secondary antibody. Propidium iodide (PI) was used to visualize the cell nucleus.

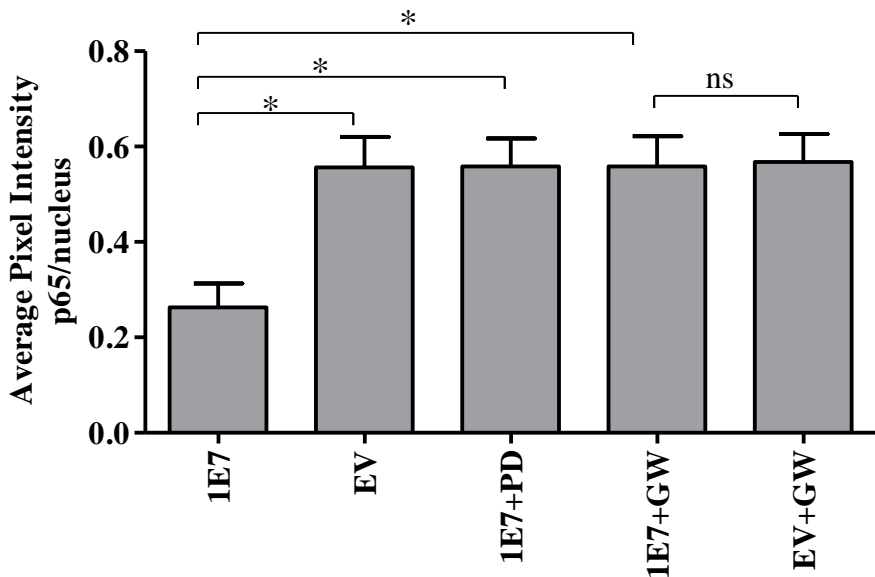


**Figure 3. 36: Inhibition of NF- $\kappa$ B in 15-LOX-1 expressing cells (1E7) could be reversed by treatment with the PPAR $\gamma$ -specific antagonist GW9662 (GW).**

The fluorescence intensity of p65 staining was quantified by AF488/PI pixel intensity ratio. A significantly reduced nuclear translocation of NF- $\kappa$ B was observed in 15-LOX-1 expressing 1E7 cells when compared to the control cells (EV). This inhibition could be reversed by the treatment of 1E7 cells with 1  $\mu$ M of either the 15-LOX-1 inhibitor PD146176 (PD) or GW9662 (GW). Statistical comparisons were carried out using Mann–Whitney U-test.

Immunofluorescence studies for p65 nuclear translocation was also carried out using a second clone of the 15-LOX-1 expressing HCT-116 cells (1F4 monoclonal) after treatment with the PPAR $\gamma$  specific antagonist GW9662 (1  $\mu$ M) for 24 h and photographed image under confocal microscope (Fig 3.37). The images were analyzed as described previously. The data (Fig 3.38) showed that the 1F4 15-LOX-1 expressing clone could also significantly decrease nuclear translocation of p65 when compared to EV-transfected cells ( $P<0.05$ ).

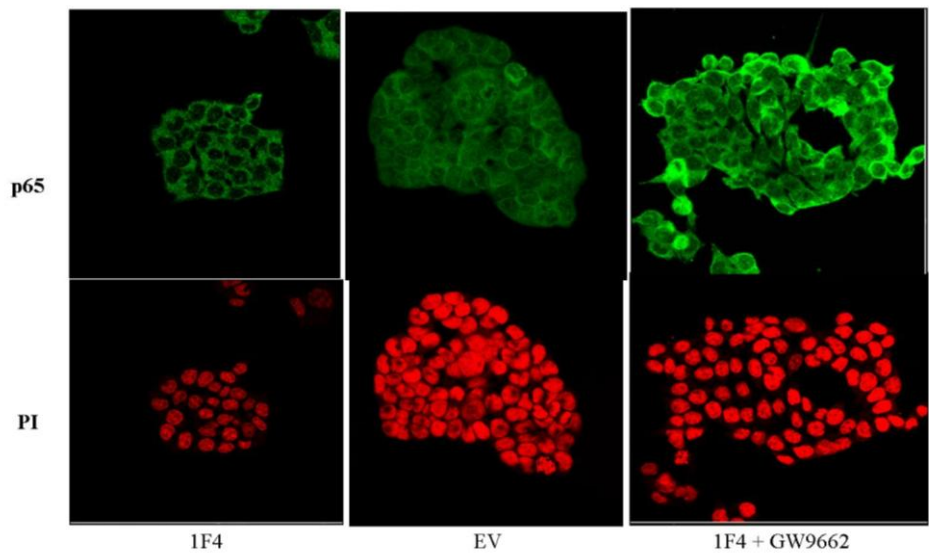


**Figure 3. 37: Representative photographs show 15-LOX-1 expressing (1F4) and control HCT116 cells immunofluorescence assay result for p65.**  
Treated (GW9662) and untreated the cells were incubated with p65 antibody and counterstained with an Alexa Fluor 488 secondary antibody. Propidium iodide (PI) was used to visualize the cell nucleus.

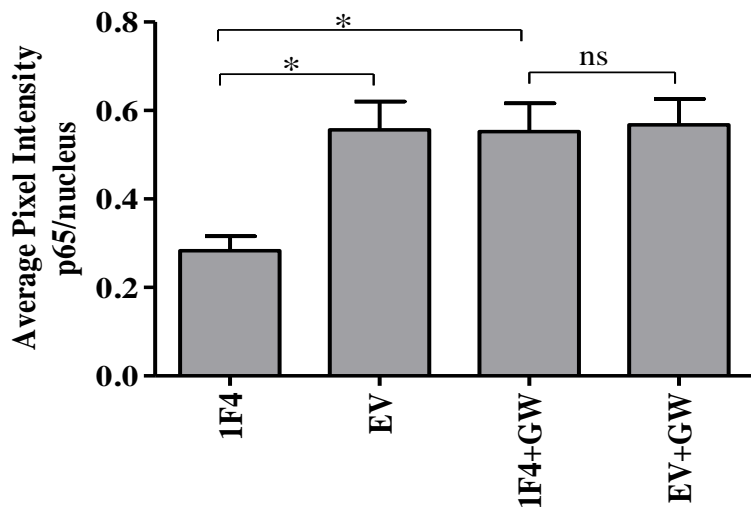


**Figure 3. 38: Inhibition of NF-κB in 15-LOX-1 expressing cells (1F4) could be reversed by treatment with the PPAR $\gamma$ -specific antagonist GW9662 (GW).**  
The fluorescence intensity of p65 staining was quantified by AF488/PI pixel intensity ratio. A significantly reduced nuclear translocation of NF-κB was observed in 15-LOX-1 expressing 1F4 cells when compared to the control cells (EV). This inhibition could be reversed by the treatment of 1F4 cells with 1  $\mu$ M of GW9662 (GW). Statistical comparisons were carried out using Mann–Whitney U-test.

Next, immunofluorescence studies for p50 using 15-LOX-1 expressing (1E7) and control HCT116 cells were carried out and the image was photographed with a confocal microscope (Fig 3.39). Image analysis was done as described above. The data (Fig 3.40) showed that 15-LOX-1 expressing cells (1E7) could significantly decrease nuclear translocation of p50 when compared to EV-transfected cells ( $P<0.05$ ). Moreover, the inhibition in nuclear translocation of NF- $\kappa$ B in 15-LOX-1 expressing cells could be rescued by the incubation of the cells with 1  $\mu$ M of the 15-LOX-1-specific inhibitor PD146176. Additionally, when the cells were treated with 1  $\mu$ M of GW9662, a similar reversal of the inhibition in translocation of p50 protein could be observed, indicating that attenuation of PPAR $\gamma$  activity in the 15-LOX-1 expressing cells could rescue the inhibition of NF- $\kappa$ B.

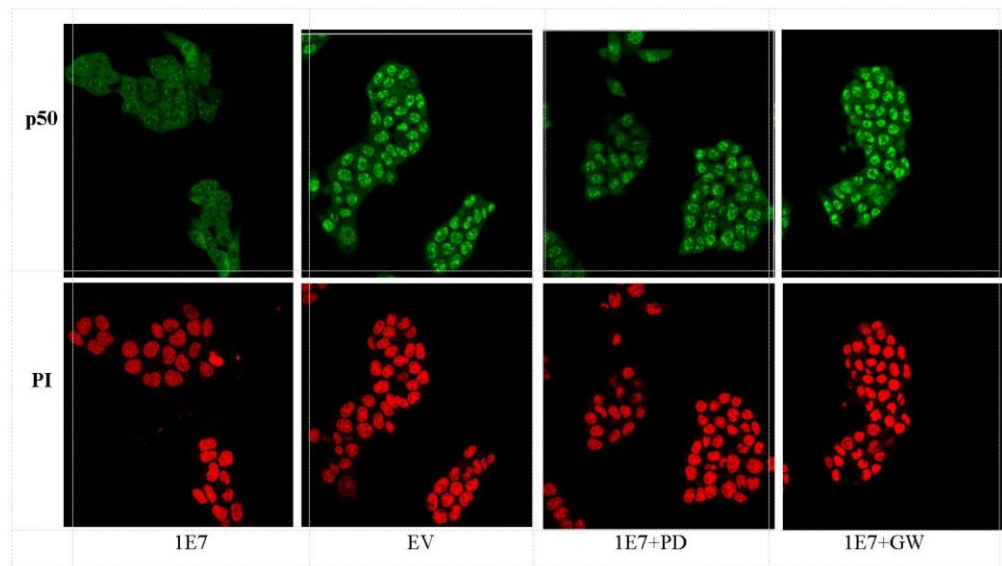


**Figure 3. 39: Representative photographs show 15-LOX-1 expressing and control HCT116 cells immunofluorescence assay result for p50.**  
Treated (GW9662 or PD146176) and untreated the cells were incubated with p50 antibody and counterstained with an Alexa Fluor 488 secondary antibody. Propidium iodide (PI) was used to visualize the cell nucleus.

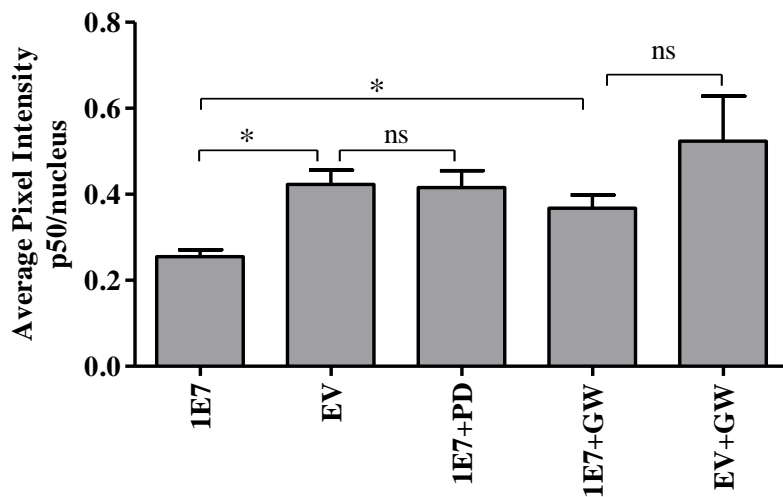


**Figure 3. 40: Inhibition of NF- $\kappa$ B in 15-LOX-1 expressing cells (1E7) could be reversed by treatment with the PPAR $\gamma$ -specific antagonist GW9662 (GW).**

The fluorescence intensity of p50 staining was quantified by AF488/PI pixel intensity ratio. A significantly reduced nuclear translocation of NF- $\kappa$ B was observed in 15-LOX-1 expressing 1E7 cells when compared to the control cells (EV). This inhibition could be reversed by the treatment of 1E7 cells with 1  $\mu$ M of either the 15-LOX-1 inhibitor PD146176 (PD) or GW9662 (GW). Statistical comparisons were carried out using Mann–Whitney U-test.

Immunofluorescence studies were also carried out for p50 nuclear translocation using the 1F4 monoclonal of 15-LOX-1 expressing cells after treatment with the PPAR $\gamma$  specific antagonist GW9662 (1  $\mu$ M) for 24 h (Fig 3.41). The data (Fig 3.42) showed that the 1F4 monoclonal also had a significantly lower nuclear translocation of p50 when compared to the EV-transfected cells ( $P<0.05$ ).

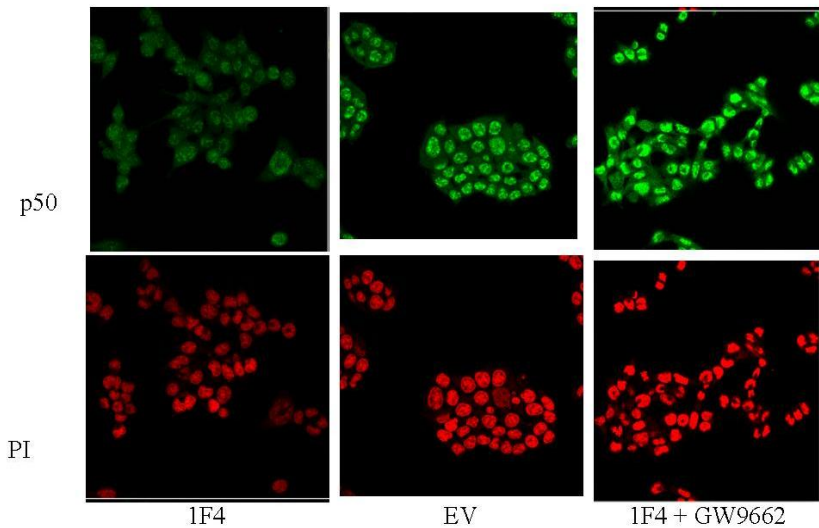


**Figure 3. 41: Representative photographs show 15-LOX-1 expressing (1F4) and control HCT116 cells immunofluorescence assay result for p50.**

Treated (GW9662) and untreated the cells were incubated with p50 antibody and counterstained with an Alexa Fluor 488 secondary antibody. Propidium iodide (PI) was used to visualize the cell nucleus.

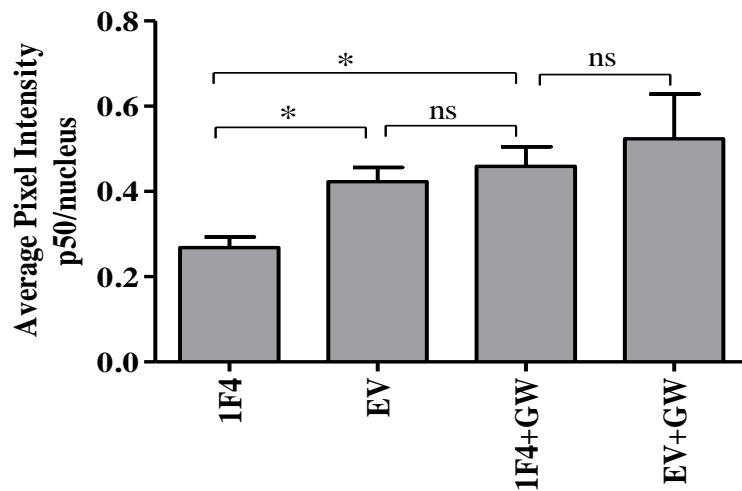


**Figure 3. 42: Inhibition of NF- $\kappa$ B in 15-LOX-1 expressing cells (1F4) could be reversed by treatment with the PPAR $\gamma$ -specific antagonist GW9662 (GW).**

The fluorescence intensity of p50 staining was quantified by AF488/PI pixel intensity ratio. A significantly reduced nuclear translocation of NF- $\kappa$ B was observed in 15-LOX-1 expressing 1F4 cells when compared to the control cells (EV). This inhibition could be reversed by the treatment of 1F4 cells with 1  $\mu$ M of GW9662 (GW). Statistical comparisons were carried out using Mann–Whitney U-test.

To understand whether nuclear translocation inhibition of p65 and p50 was due to the endogenous production of 13(S)-HODE in the 15-LOX-1 expressing cells, immunofluorescence studies for p65 and p50 protein were carried out using parental HCT-116 cells treated with 100  $\mu$ M exogenously added 13(S)-HODE and analyzed as described above. The data (Fig. 3.43 and 44) indicate that parental HCT-116 cells treated with 100  $\mu$ M exogenously added 13(S)-HODE resulted in a significant decrease ( $P<0.05$ ) in nuclear translocation of p50 when compared to cells treated with ethanol (vehicle) only.

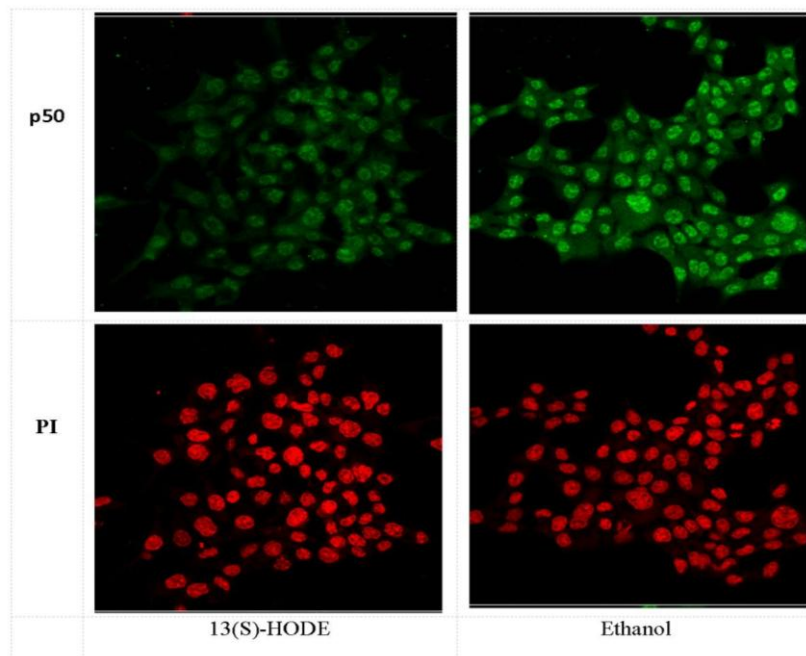


**Figure 3. 43: Representative photographs show parental HCT-116 cells immunofluorescence studies for p50.**

HCT-116 cells treated exogenously with the 15-LOX-1 product 13(S)-HODE or with the vehicle ethanol were incubated with p50 antibody and counterstained with an Alexa Fluor 488 secondary antibody. Propidium iodide (PI) was used to visualize the cell nucleus.

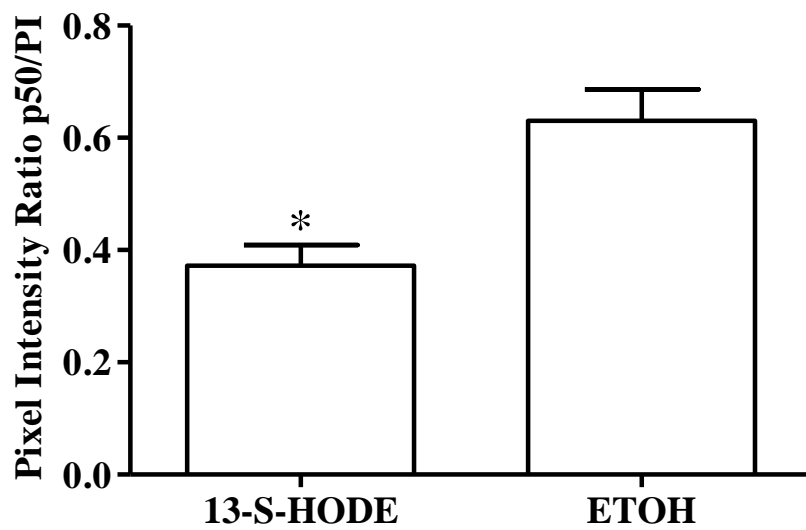


**Figure 3. 44: Nuclear translocation of NF- $\kappa$ B p50 reduced after 13(S)-HODE treatment in parental HCT-116 cells.**

Parental HCT-116 cells treated exogenously with the 15-LOX-1 product 13(S)-HODE also resulted in a significant reduction in the translocation of p50 when compared to ethanol (vehicle) treated cells. The fluorescence intensity of p50 staining was quantified by AF488/PI pixel intensity ratio. Statistical comparisons were carried out using Mann Whitney U Test.

Similarly, immunofluorescence studies carried out for p65 translocation with parental HCT-116 cells treated with 100  $\mu$ M exogenously added 13(S)-HODE also showed a significant decrease ( $P<0.05$ ) in nuclear translocation of p65 when compared to cells treated with ethanol (vehicle) only (Fig. 3.45 and 46).

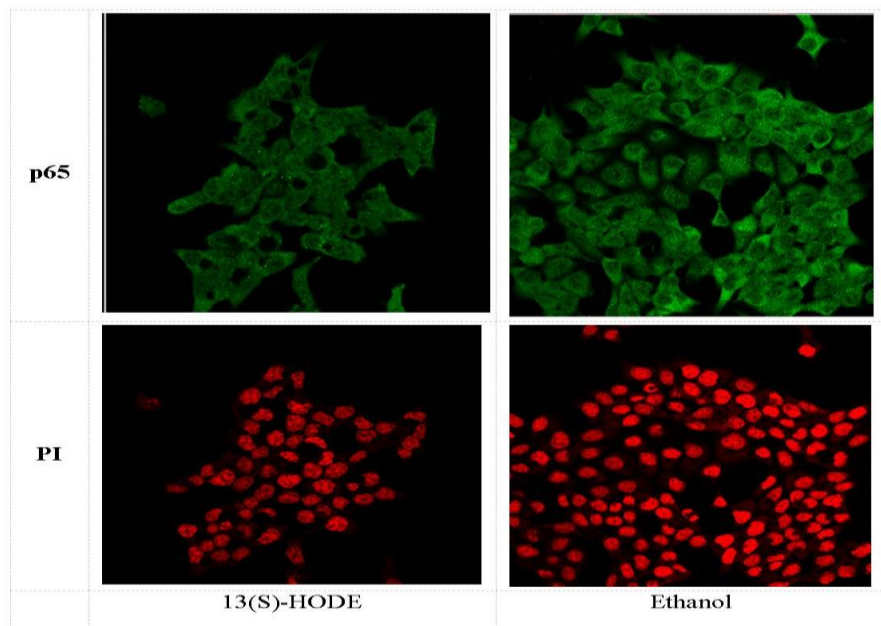


**Figure 3. 45: Representative photographs show parental HCT-116 cells immunofluorescence studies for p65.**

Treated exogenously with the 15-LOX-1 product 13(S)-HODE and treated with ethanol cells were incubated with p65 antibody and counterstained with an Alexa Fluor 488 secondary antibody. Propidium iodide (PI) was used to visualize the cell nucleus.

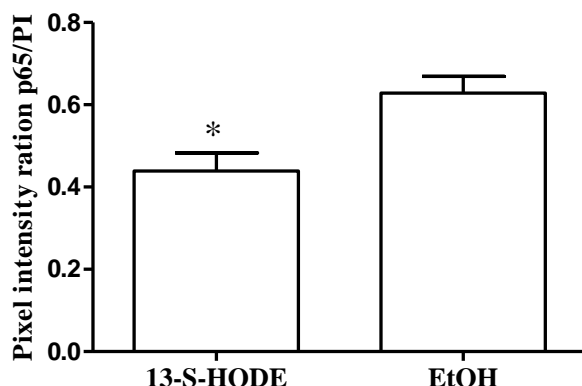


**Figure 3. 46: Nuclear translocation of NF- $\kappa$ B p65 reduced after 13(S)-HODE treatment in parental HCT-116 cells.**

Parental HCT-116 cells treated exogenously with the 15-LOX-1 product 13(S)-HODE also resulted in a significant reduction in the translocation of p65 when compared to ethanol (vehicle) treated cells. The fluorescence intensity of p65 staining was quantified by AF488/PI pixel intensity ratio. Statistical comparisons were carried out using Mann Whitney U Test.

### **3.2.6 PPAR $\gamma$ inhibition enhances the transcriptional activity of NF- $\kappa$ B in 15-LOX-1 expressing cells**

The transcriptional activity of NF- $\kappa$ B was next determined in 15-LOX-1 expressing and control cells in the presence (or not) of 1  $\mu$ M of the PPAR $\gamma$  antagonist GW9662 using the Pathdetect NF- $\kappa$ B cis- Reporting system. The data (Fig. 3.47) indicate that treatment of the 15-LOX-1 expressing 1F4 cells with GW9662 resulted in a significant ( $P<0.05$ ) increase in the NF- $\kappa$ B transcriptional activity when compared to untreated 1F4 cells. However, no such increase in transcriptional activity was observed when the EV-transfected cells were treated with GW9662 ( $P>0.05$ ). Additionally, the NF- $\kappa$ B transcriptional activity in GW9662-treated 1F4 cells reached the same level as the EV cells ( $P>0.05$ ).

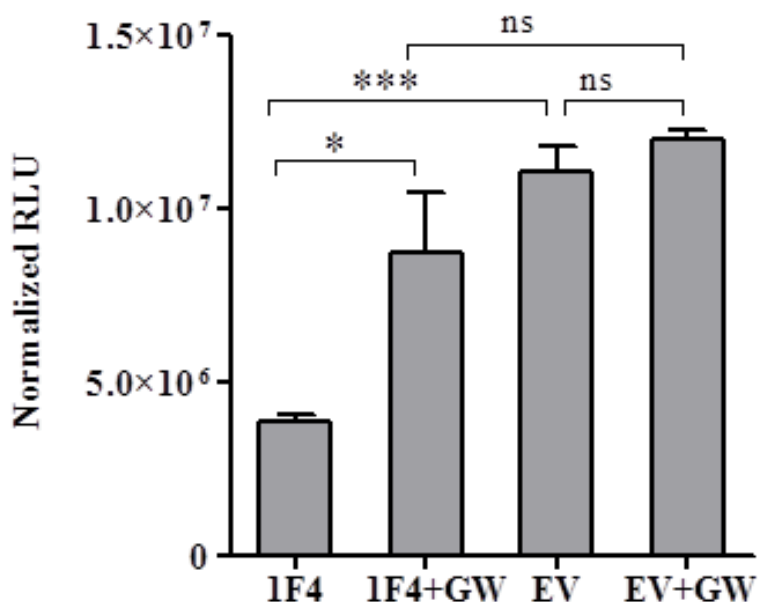


**Figure 3. 47: Luciferase assays indicating increased transcriptional activity of NF- $\kappa$ B when the 15-LOX-1 expressing HCT-116 cells (1F4) were treated with the PPAR $\gamma$ -specific antagonist GW9662 (GW).**

The cells were transfected with the NF- $\kappa$ B Pathdetect cis-Reporting plasmid for 24 h, treated with 1  $\mu$ M GW9662 for 24 h after which the cells were collected and processed for luciferase activity.  $\beta$ -Galactosidase was used for normalization. Statistical comparisons were carried out using one-way ANOVA with Tukey's multiple comparison tests.

Treatment of parental HCT-116 with 100  $\mu$ M 13(S)-HODE for 24 h after transfection with the reporter construct also resulted in a significant loss of NF- $\kappa$ B transcriptional activity ( $P<0.01$ ) when compared to cells treated with the vehicle ethanol (Fig. 3.48). Additionally, when the HCT-116 cells were treated with 1mM GW9662 for 24 h following the treatment with 13(S)-HODE, a recovery of the NF- $\kappa$ B transcriptional activity was observed.

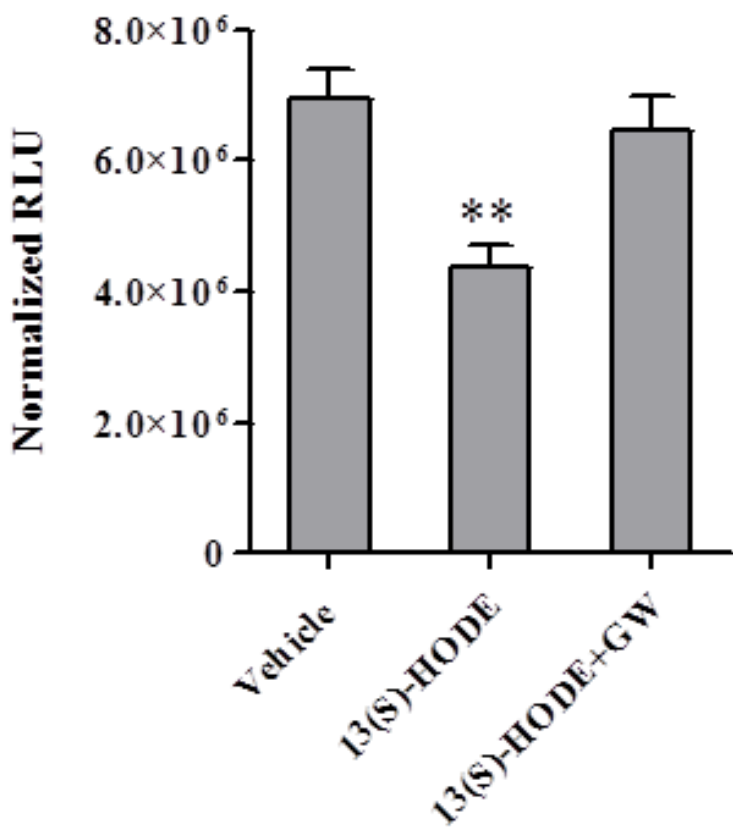


**Figure 3. 48: Luciferase assays indicating increased transcriptional activity of NF- $\kappa$ B when wild-type HCT-116 cells incubated with 100  $\mu$ M 13(S)-HODE were treated with the PPAR $\gamma$ -specific antagonist GW9662 (GW).**

The cells were transfected with the NF- $\kappa$ B Pathdetect cis-Reporting plasmid for 24 h, treated with 100  $\mu$ M 13(S)-HODE for 24 h and 1  $\mu$ M GW9662 for 24 h after which the cells were collected and processed for luciferase activity.  $\beta$ -Galactosidase was used for normalization. Statistical comparisons were analyzed for statistical significance using Mann–Whitney U-test.

### **3.2.7 Inhibition of PPAR $\gamma$ increases cellular proliferation**

In order to determine whether the inhibition of NF- $\kappa$ B via activation of PPAR $\gamma$  was reflected functionally in the cells, HCT-116 cells stably expressing 15-LOX-1 was treated with the PPAR $\gamma$  antagonist GW9662 (1  $\mu$ M). The data (Fig. 3.49) show that inhibition of PPAR $\gamma$  in the 15-LOX-1 expressing cells could increase the proliferation of the cells significantly ( $P<0.001$ ) to a level similar to the control EV-transfected cells. Treatment of the EV cells with GW9662 (EV\_GW) did not change their proliferation, most likely because PPAR $\gamma$  is not activated in these cells ( $P>0.05$ ). On the other hand, treatment of the EV cells with 32  $\mu$ M of SN-50 (EV\_SN-50), specific peptide inhibitor of NF- $\kappa$ B, resulted in a dramatic reduction of proliferation. As NF- $\kappa$ B activation provides mitogenic signals, inhibition of NF- $\kappa$ B is likely to cause a growth arrest, as is also seen when the cells express 15-LOX-1. The growth inhibition with SN-50, however, appears to be more pronounced than that with 15-LOX-1 expression.

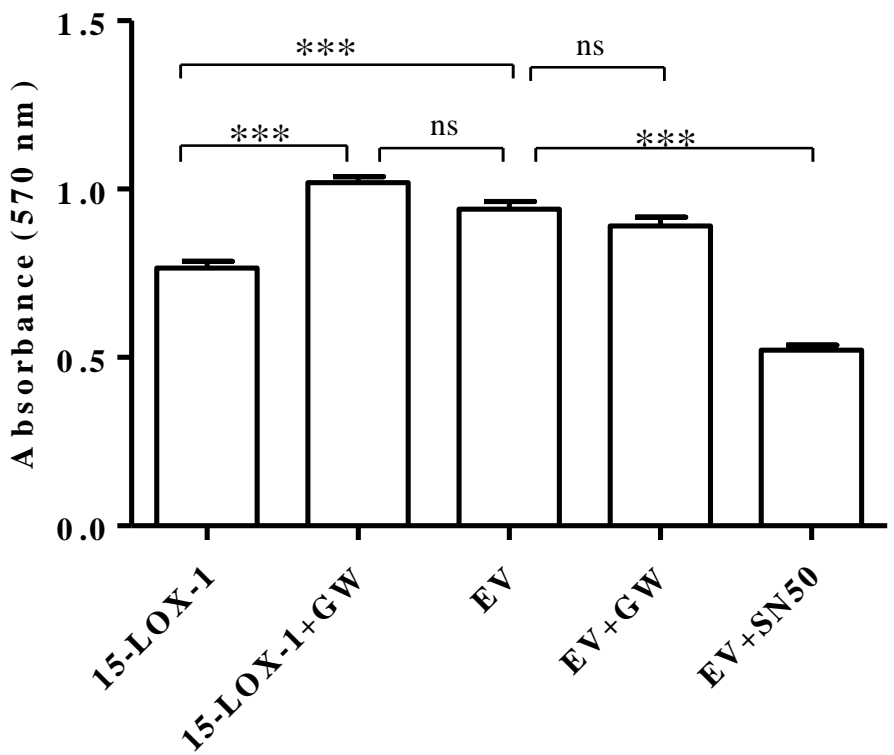


**Figure 3. 49: The proliferation of 15-LOX-1 expressing cells increases when PPAR $\gamma$  is inhibited.**

MTT assay indicates that 15-LOX-1 expressing 1E7 cells, but not the empty vector-transfected control cells, treated with 1  $\mu$ M GW9662 results in a significant increase in the proliferation. Treatment of control cells with 32  $\mu$ M SN-50, a specific peptide inhibitor for NF- $\kappa$ B resulted in a decrease in proliferation. This decrease, however, was more pronounced than the inhibition in proliferation observed with the expression of 15-LOX-1 alone. The data for eight replicates is shown here and statistical comparisons were carried out using one-way ANOVA with Tukey's multiple comparison test.

## **CHAPTER 4**

### **DISCUSSION**

The eicosanoid pathway, in which arachidonic acid is metabolized by lipoxygenases and cyclooxygenases to bioactive inflammatory lipids such as prostaglandins and leukotrienes, play a crucial role in tumor development, growth, and progression. Six human lipoxygenases (LOXs) isoforms have been identified to date (Hennig et al, 2007). Of these, 5-LOX, 8-LOX, and 12-LOX are well known for their protumorigenic effects while 15-LOX-2 has anti-tumorigenic effects in cancer (Furstenberger et al, 2006; Shureiqi & Lippman, 2001). However, the role of 15-LOX-1 in cancer is controversial. Studies in prostate cancer supported that 15-LOX-1 has protumorigenic effects based on following observations:

1. Kelavkar et. al. showed that 15-LOX-1 could be induced by an oncogenic mutant form of p53 in prostate cancer cells (Kelavkar & Badr, 1999).
2. Overexpression of 15-LOX-1 in PC-3 human prostate cancer cells increased tumorigenesis in mouse xenograft models (Kelavkar et al, 2001).
3. 15-LOX-1 upregulated the MAP kinase pathway and disrupted the balance of Bcl family members across the mitochondrial membrane through its main metabolite 13(S)-HODE in prostate cancer (Kelavkar et al, 2002).
4. 15-LOX-1 contributes to prostate cancer bone metastasis by increasing insulin like growth factor- receptor (IGFR-1) expression (Kelavkar & Cohen, 2004).
5. Conditional expression of human 15-LOX-1 in mouse prostate induces prostatic intraepithelial neoplasia in the FLiMP mouse model (Kelavkar et al, 2006).

Initial studies carried out in the colon also corroborated the finding of the prostate cancer model studies and indicated the protumorigenic effects of 15-LOX-1 in CRC. Hsi et al. (2001) demonstrated that 13(S)-HODE down-regulated PPAR- $\gamma$  expression by increasing its phosphorylation via an MAPK-signaling-dependent pathway in the HCT-116 colon cancer cell line (Hsi et al, 2001). Yoshinaga et al. (2004) showed that forced expression of 15-LOX-1 in colon cancer cell lines and resultant increase in the 13(S)-HODE metabolite activated the MEK/ERK signal transduction pathway and inhibited expression of the p21 tumor suppressor protein (Yoshinaga et al, 2004).

However, subsequently, many studies have indicated that transcription of 15-LOX-1 is repressed in colon cancer cells. Some of these mechanisms are as follows:

1. Liu et al. showed that DNA hyper-methylation is associated with silenced 15-LOX-1 transcription and that demethylation is required for 15-LOX-1 transactivation (Liu et al, 2004).
2. Overexpression of transcriptional regulatory protein GATA-6 contributes to silencing of 15-LOX-1 in colorectal cancer cells (Shureiqi et al, 2007).
3. It was found that 15-LOX-1 transcription can be silenced by DNA methyltransferase (DNMT)-1 independently of DNA methylation in colorectal cancer cells (Zuo et al, 2008b).
4. Chromatin modification in the 15-LOX-1 promoter is associated with 15-LOX-1 transcriptional activation (Zuo et al, 2008a).
5. Zuo et al (2009) identified a region in the 15-LOX-1 promoter that is targeted by the repressive nucleosome remodeling and histone deacetylase (NuRD) complex to mediate 15-LOX-1 transcription suppression in CRC cells (Zuo et al, 2009).

Additionally, a number of in vitro and in vivo studies have appeared in the literature that supports the anti-tumorigenic role of 15-LOX-1 in CRC and other cancers. Some of these studies are as follows:

1. Nixon et al. (2004) showed that 15-LOX-1 expression was downregulated in colorectal cancer epithelia compared with normal colonic epithelia (Nixon et al, 2004).
2. Higher ratios of 15-LOX-1 expression in tumor tissue to 15-LOX-1 expression in normal tissue were associated with better prognosis in patients with stage IV colorectal cancer (Heslin et al, 2005).
3. 15-LOX-1 re-expression via nonsteroidal anti-inflammatory drugs, histone deacetylase inhibitors (HDACIs) or transfection with plasmid or adenoviral vectors inhibited tumorigenesis in cancer cells (Zuo et al, 2008a).
4. The induction of terminal differentiation in transformed Caco-2 colonic cells was associated with 15-LOX-1 expression and 13-S-HODE production (Kamitani et al, 1998).
5. Selective molecular targeting of 15-LOX-1 expression was shown to be sufficient to inhibit tumorigenesis in mice (Wu et al, 2008).
6. Targeted transgenic 15-LOX-1 expression in the intestine suppresses azoxymethane-induced colonic tumorigenesis (Zuo et al, 2012).

While several other studies have further attested the ability of 15-LOX-1 to inhibit tumorigenesis (Hennig et al, 2007; Hsi et al, 2004; Nixon et al, 2004; Philips et al, 2008; Shureiqi et al, 2003) the knowledge on the role of 15-LOX-1 on metastasis and angiogenesis is fragmentary in CRC cells. Moreover, the mechanisms behind how the re-expression of 15-LOX-1 leads to antitumorigenic effects in CRC have not been well studied yet.

HCT-116 cells normally do not express any 15-LOX-1. In this study, we developed human colorectal epithelial cell lines (1E7, 1F8 and 1F4 monoclonal) that stably express an ectopically added 15-LOX-1 vector or empty vector (EVE2) using HCT116 cells. The expression of 15-LOX-1 in these clones was confirmed by PCR and Western blots. The protein product was also determined to be functionally active by establishing that cells expressing 15-LOX-1 had significantly higher levels of the enzymatic product 13(S)-HODE from the oxygenation of linoleic acid.

#### **4.1 Functional effects of 15-LOX-1 expression in CRC HCT-116 Cells**

##### **4.1.1 Effect on proliferation and apoptosis**

Immortality, with continuous proliferation is one of the major hallmarks of cancer (Hanahan & Weinberg, 2000). Therefore, the effect of the expression of 15-LOX-1 on cellular proliferation was first examined. Our data showed that the proliferation of two clones of HCT-116 cells stably expressing 15-LOX-1 (1E7 and 1F8) was significantly slower when compared to the empty vector transfected cells. As both of the monoclonal HCT-116 behaved similarly in their expression of 15-LOX-1 and the rate of proliferation, we carried out all further experiments with the 1E7 clone of HCT-116. A similar reduction in proliferation 72–96 h following transient transfection in HCT-116 cells of 15-LOX-1, using adenoviral delivery, has been reported (Wu et al, 2008). Hennig et al, (2007) reported that 15-LOX-1 expression could decrease cellular proliferation in MiaPaCa2 and S2-O13 pancreatic cancer cell lines ectopically expressing 15-LOX-1 (Hennig et al, 2007). Additionally, Tavakoli-Yaraki (2012) recently reported that treatment of human breast cancer cell lines with a histone deacetylase inhibitor Trichostatin A could reduce proliferation by upregulating 15-LOX-1 (Tavakoli-Yaraki et al, 2012).

Another hallmark of cancer is the avoidance of apoptosis (Hanahan & Weinberg, 2011). Previous studies have suggested that the re-expression of 15-LOX-1 in gastric, colonic, esophageal and pancreatic cancers causes the induction of apoptosis (Hennig et al, 2007; Heslin et al, 2005; Shureiqi et al, 2000; Shureiqi et al, 2001; Wu et al, 2003). Expression of 15-LOX-1 in the HCT-116 cells in this study also increased apoptosis as seen from the increased number of apoptotic cells by acridine orange staining (Fig 3.7), caspase-3 activity (Fig 3.8) and annexin V staining (Fig 3.10). Moreover, a reduction in the protein levels of the anti-apoptotic proteins XIAP and Bcl-XL was observed in the HCT116 cell lines. These data corroborate with the findings of Wu et al. (2008) who reported that 15-LOX-1 expression decreases the expression of the anti-apoptotic proteins XIAP and Bcl-XL and increases caspase-3 activity in HT-29 and HCT-116 cell lines (Wu et al, 2008). XIAP mostly inhibits the function of caspases involved the extrinsic and intrinsic pathways of apoptosis. Therefore, downregulation of XIAP expression gets rid of the inhibitory effect on caspase-3 which activates the apoptotic pathway in the presence of 15-LOX-1 in HCT-116 cell lines.

#### **4.1.2 Effect on cellular motility and metastasis**

Cancer metastasis is a complex process and is frequently the reason for cancer mortality. It is a multi-step, multi-factor process involving cancer cells, host cells, extracellular matrix and many metastasis-associated proteins (Qian et al, 2005). To confirm the association between 15-LOX-1 expression and metastasis, we also analyzed HCT116 cell lines with a known ability of metastasis. Functional studies showed that 15-LOX-1 expression in HCT-116 cells could reduce anchorage-independent growth by forming fewer colonies on soft agar compared to empty pcDNA3.1 expressing cells and untransfected cells. This result is opposite to the findings of the Kelavkar group who showed that 15-LOX-1 overexpressing PC3 cells showed an increased ability to grow in agar compared control PC3 cells in prostate cancer (Kelavkar et al, 2001). It is likely that the differences in these results arise from the different organs that were studied, i.e. colon versus prostate. Tumor cell

invasion involves detachment of tumor cells from the underlying basement membrane, local proteolysis, and migration of tumor cells (Joyce & Pollard, 2009; Kawasaki et al, 2008).

The present study showed that stable expression of 15-LOX-1 in HCT-116 significantly reduced the ability of the cells to adhere to fibronectin, a component of the ECM. A similar reduction in the binding of cancer cells to components of the ECM has been attributed to the metastasis suppressive properties of gefitinib, galectin-9, and 15-hydroxyprostaglandin dehydrogenase on CRC (Li et al, 2008; Nobumoto et al, 2008; Toda et al, 2006). HCT-116 cells expressing 15-LOX-1 also displayed slower motility, as shown by their inability to heal a scratch wound, whereas parental HCT-116 and empty vector transfected cells could almost completely heal the wound within 72 h. The ability of HCT-116 cells to migrate through a Transwell insert membranes with 8  $\mu$ m pores and invade through Matrigel, a reconstituted basement membrane was next examined. These systems are in vitro analyses of the invasive potential of malignant as well as normal cells. The data indicate that 15-LOX-1 expression reduced the ability of HCT-116 cells to migrate through the Transwell insert membranes. Additionally, when a layer of the Matrigel matrix was added to the insert membranes, the cells' ability to digest the Matrigel matrix occluding the membrane and migrating through the pores was significantly inhibited when they expressed 15-LOX-1. Taken together our data provide, for the first time, compelling evidence supporting an inhibitory role for 15-LOX-1 on the metastatic potential of CRC cell lines.

How 15-LOX-1 modulates the migratory behavior of colon cancer cells was next determined. MTA-1, a component of the nucleosome remodeling and histone deacetylase repression complex, is involved in the transcriptional repression of many different genes including 15-LOX-1, estrogen receptor, and BRCA1 (Mazumdar et al, 2001; Molli et al, 2008; Zuo et al, 2009). MTA-1 is regulated by the epidermal growth factor receptor family and is found to be overexpressed in epithelial cancers including breast and colorectal carcinoma (Giannini & Cavallini, 2005; Nicolson et al, 2003; Zuo et al, 2009), and forced

overexpression of the protein is associated with increased invasiveness and anchorage-independent growth (Mahoney et al, 2002; Mazumdar et al, 2001). A decreased expression of MTA-1 protein was observed when 15-LOX-1 was expressed stably in HCT-116 cell lines. Furthermore, when the HCT-116 cells expressing 15-LOX-1 were incubated with 1  $\mu$ M PD146176, the expression of MTA-1 was restored to the same level as the control cells. Therefore, it may be proposed that the decrease in the invasive phenotype observed for the 15-LOX-1 overexpressing cells could be due to the reduced expression of MTA-1. Zuo et al. (2009) have shown a negative correlation between 15-LOX-1 and MTA-1 expression in paired normal and cancerous colorectal mucosa (Zuo et al, 2009). Based on that study and the current thesis, we speculate the possible presence of a negative feedback loop between 15-LOX-1 and MTA-1 expression, an idea that warrants further studies. Forced expression of 15-LOX-1 causes a loss of MTA-1 expression and results in a decrease in cellular motility and invasion. Overexpression of MTA-1, commonly observed in malignant epithelial cells, causes a repression of 15-LOX-1 expression and increases the migratory capacity of the cells.

#### **4.1.3 Effect on neoangiogenesis**

The potential antitumorigenic effect of 15-LOX-1 could also be related to angiogenesis, which is the process of new blood vessel formation (Chia et al, 2010; Harats et al, 2005). However, the effect of 15-LOX-1 on angiogenesis in CRC is not known (Bhattacharya et al, 2009). Therefore, we wanted to clarify the effects of 15-LOX-1 on the angiogenesis. Binding of the angiogenic factor VEGF-A to specific receptors in endothelial cell is first step in angiogenesis (Reinmuth et al, 2003). Therefore, we analyzed the secretion of the angiogenic factor VEGF-A from HCT-116 cells ectopically expressing 15-LOX-1 as well as the control cells. The results indicated that VEGF-A secretion was significantly decreased in 15-LOX-1 expressing cells compared to empty vector transfected HCT116 cells. Viita et al. (2008) observed that adenoviral expression of 15-LOX-1 in rabbit abdominal aortic smooth muscle cell could reduce the production of the transduced human VEGFA<sub>165</sub>

protein (Viita et al, 2008). Viita et. al. (2009) also showed that 15-LOX-1 efficiently reduced secreted VEGF-A<sub>165</sub> by in rabbit eye cells (Viita et al, 2009). Therefore, our results show that 15-LOX-1 can reduce secretion of VEGF-A<sub>165</sub> not only in non-epithelial cells, but also in epithelial malignant CRC cells.

After the binding of angiogenic factors such as VEGF-A to specific receptors in endothelial cells, these cells can then proliferate, migrate and form new capillary tubes (Reinmuth et al, 2003). Therefore, an MTT assay was carried out to measure HUVEC proliferation in the presence of conditioned medium from HCT-116 expressing 15-LOX-1 and the control cells. The data (Fig 3.24) indicated that HUVECs grown in conditioned medium from 15-LOX-1 expressing cells proliferated significantly less compared to the control cells. Next, we performed wound-healing assay to determine the ability of migration of the HUVECs when grown in conditioned medium. It was observed that the 72h conditioned medium obtained from 15-LOX-1 expressing HCT 116 cells caused less HUVEC migration compared to control cells. Finally, an endothelial tube formation assay was carried out. It was observed that 15-LOX-1 expressing cells showed significantly reduced total skeleton length, number of branching points, nodal structures and tubes compared to empty vector transfected HCT-116 cells. Recently, Yan et al (2012) showed that the effect of 15-LOX-1 overexpression is an anti-angiogenic factor in hypoxia-induced in retinal microvascular endothelial cells (Yan et al, 2012). Taken together our data provides, for the first time, evidence supporting an inhibitory role for 15-LOX-1 on the angiogenic potential of CRC cell lines.

#### **4.2 The mechanism of antitumorigenic effect of 15-LOX-1 in CRC via inhibition of NF-κB**

15-LOX-1 has been convincingly shown to have tumor suppressive properties in the colon in the recent years and various mechanisms have been proposed for these properties (Bhattacharya et al, 2009). Shureiqi et al (2007) showed that

overexpression of the transcription factor GATA-6 contributes to process of silencing 15-LOX-1 in human colon cancer cells (Shureiqi et al, 2007). COX-2 inhibitors (NSAIDs) were shown to stimulate 15-LOX-1 expression via downregulation of GATA-6 (Shureiqi et al, 2002). Deguchi et al. (2005) suggested that activation of protein kinase G up-regulates expression of 15-lipoxygenase-1 in human colon cancer cells (Deguchi et al, 2005). Other research groups found that the methyltransferase inhibitor 5-aza-2-deoxycytidine induces apoptosis via induction of 15-lipoxygenase-1 in colorectal cancer cells (Hsi et al, 2005). In addition, Liu et al. (2004) reported that IL-4 and IL-13 play important roles in transactivating 15-LOX-1 (Liu et al, 2004). Kim et al (2005) showed that overexpression of 15-LOX-1 induces growth arrest through phosphorylation of p53 in human colorectal cancer cells (Kim et al, 2005). 15-LOX-1-derived oxidative metabolites of linoleic and arachidonic acid are natural ligands of peroxisome proliferator activated receptors (PPARs), which regulate cell proliferation and apoptosis (Shureiqi et al, 2003; Zuo et al, 2006). Several isoforms of PPARs are expressed in a tissue and context specific manner. PPAR $\gamma$  is associated with adipocyte differentiation and is said to have anti-inflammatory properties as well (Cipolletta et al, 2012). PPAR $\beta/\delta$ , on the other hand, have procarcinogenic properties and may be overexpressed in CRC cells (Zuo et al, 2006). Although Shao et al. (1998) initially reported that 15-LOX-1-derived oxidative metabolites of linoleic acid could inhibit PPAR $\gamma$  activity via MAP kinase phosphorylation (Shao et al, 1998), Zuo et al, later reported that 15-LOX-1 could activate PPAR $\gamma$  in CRC cells through the inhibition of PPAR $\beta/\delta$  (Zuo et al, 2006). However, whether 15-LOX-1 or its metabolites can affect the inflammatory transcription factor NF- $\kappa$ B or not has not been reported yet.

NF- $\kappa$ B target genes have been implicated in carcinogenesis because they affect many of the hallmarks of cancer such as proliferation, escape from apoptosis, metastasis and angiogenesis. Examples of these target genes include: TNF- $\alpha$ , IL-1 $\beta$ , and IL-6 which are involved in proliferation, the antiapoptotic proteins of XIAP, Bcl-2 and Bcl-xL which are involved in escape from apoptosis, intercellular adhesion molecule-1 (ICAM-1), vascular cell adhesion molecule-1 (VCAM-1) and MMP-9 which are involved in metastasis, and VEGF and IL-8 which are angiogenic inducers

and involved angiogenesis(Aggarwal et al, 2006). We therefore hypothesized that the functional changes observed in the HCT-116 cells may have resulted from the inhibition of NF- $\kappa$ B.

The activation of NF- $\kappa$ B as a transcription factor is dependent on several factors such as phosphorylation status of I $\kappa$ B, nuclear translocation of the NF- $\kappa$ B subunits and DNA binding (Mayo & Baldwin, 2000). In cancer cells, NF- $\kappa$ B can be constitutively active, resulting in the activation of inflammatory and anti-apoptotic pathways. The proinflammatory and pro-carcinogenic lipoxygenases such as 5-LOX and 12-LOX have been shown to activate NF- $\kappa$ B (Bonizzi et al, 1999; Kandouz et al, 2003). However, the effect of the 15-LOX-1 pathway on NF- $\kappa$ B activity is not known. A recent report by Shureiqi et al. indicated that 15-LOX-1 expression in LoVo CRC cells resulted in a decrease of the expression of the NF- $\kappa$ B target gene IL-1 $\beta$ , TNF- $\alpha$  and iNOS, (Shureiqi et al, 2010; Zuo et al, 2012). In T cells, 13-HODE, but not 15-HETE, could effectively reduce DNA binding and transcriptional activity of NF- $\kappa$ B (Yang et al, 2002). Additionally, Kandouz et al. (2003) reported that 13(S)-HODE treatment of PC-3 cells could effectively inhibit NF- $\kappa$ B DNA binding (Kandouz et al, 2003). In this study, it has been examined effect of ectopic expression of 15-LOX-1 on NF- $\kappa$ B activity in HCT116 cells. We have shown here for the first time that the expression of 15-LOX-1 inhibited the nuclear translocation of NF- $\kappa$ B by inhibiting the phosphorylation and degradation of I $\kappa$ B $\alpha$ . A similar loss in nuclear translocation of NF- $\kappa$ B was observed when the cells were treated with exogenous 13(S)-HODE. Additionally, this loss of nuclear translocation was accompanied by an inhibition of the DNA binding ability of p50 and p65. These results are consistent with very recent findings showing that 15-LOX-1 transgenic expression reduced nuclear translocation of NF- $\kappa$ B and DNA binding ability of p50 and p65 in colonic epithelial cells (Zuo et al, 2012). Moreover, luciferase assays indicated that 15-LOX-1 expression could inhibit the transcriptional activity of NF- $\kappa$ B even when the cells were activated with TNF- $\alpha$ . All these effects were rescued when the cells were preincubated with the 15-LOX-1 inhibitor PD146176, indicating the specificity of the inhibitory effect of 15-LOX-1.

The mechanism by which 15-LOX-1 caused the inhibition of NF- $\kappa$ B was next examined. One of the characteristics of oxidized lipids such as 13(S)-HODE (the metabolic product of the oxygenation of linoleic acid by 15-LOX-1) is their ability to act as ligands for nuclear receptors such as PPAR $\gamma$  (Itoh et al, 2008). PPAR $\gamma$  has characteristics of a colon cancer tumor suppressor provided the APC gene is not mutated (Sarraf et al, 1999). Using luciferase reporter gene assays, it was shown in the present thesis that 13(S)-HODE produced endogenously, or added exogenously could increase the transcriptional activity of PPAR $\gamma$  in HCT-116 cells, which has a wild-type APC gene. These results are consistent with findings showing that the 15-LOX-1 products activate PPAR $\gamma$  in human chondrocytes using a PPRE reporter plasmid (Chabane et al, 2009). Additionally, Hsi et al (2011) showed that 15-LOX-1 metabolites can modulate PPAR $\gamma$  and activate PPAR $\gamma$  in glioblastoma cells (Hsi et al, 2011).

Having confirmed that the 15-LOX-1 expressing cells had an activated PPAR $\gamma$ , it was next examined whether the inhibition of NF- $\kappa$ B observed in these cells was via the activation of PPAR $\gamma$ . Inhibition of PPAR $\gamma$  with the antagonist GW9662 resulted in a rescue of the phosphorylation of I $\kappa$ B $\alpha$ , as well as recovery of the loss of nuclear translocation and transcriptional activity of NF- $\kappa$ B in 15-LOX-1 expressing cells. Several cell-specific mechanisms have been proposed for the inhibition of NF- $\kappa$ B by PPAR $\gamma$ , including suppression of I $\kappa$ B kinase activity in pancreatic acinar AR42J cells, inhibition of nuclear translocation and DNA binding of p65 in rat pancreatic beta cells, as well as transrepression of NF- $\kappa$ B transcriptional activity by SUMOylated PPAR $\gamma$  (Kim et al, 2007; Pascual et al, 2005; Wan et al, 2008). A recent study has indicated that in rat glomerular mesangial cells, unliganded PPAR $\gamma$  was found to physically associate with p65 and was necessary for the transcriptional activity of NF- $\kappa$ B. In the presence of 15-PGJ2, a natural agonist of PPAR $\gamma$ , this physical association was disrupted, leading to a loss of NF- $\kappa$ B activity (Wen et al, 2010). PPAR $\gamma$  inhibits NF- $\kappa$ B activity in non-small-cell lung cancer cells (Bren-Mattison et al, 2008). Other study shows that pollen-derived PPE1 inhibits NF- $\kappa$ B activation via a PPAR- $\gamma$  dependent mechanism (Gilles et al, 2009). Gao et al. (2011) have recently reported that activation of PPAR $\gamma$  by troglitazone is effective

for HMGB1 inhibition via suppressing NF-κB transcriptional activity in endothelial cells (Gao et al, 2011). Therefore, in this it was hypothesized that transcriptional activation of PPAR $\gamma$  via ectopic expression 15-LOX-1 could inhibit NF-κB activity in HCT-116 cell lines.

Previous studies have showed that 15-LOX-1 expression resulted in phosphorylation of ERK1/2 and PPAR $\gamma$ , thereby assigning a protumorigenic role to 15-LOX-1 (Hsi et al, 2001; Yoshinaga et al, 2004). It was also claimed that the phosphorylated PPAR $\gamma$  was transcriptionally less active but no PPAR $\gamma$  transcriptional activity assays were reported in that study (Hsi et al, 2001). On the other hand, studies carried out in our lab have shown that 15-LOX-1 expression leads to the phosphorylation of ERK1/2 which could in turn phosphorylate PPAR $\gamma$ , although the overall levels of total ERK1/2 were low. However, we have observed that 15-LOX-1 expressing HCT-116 cells show a higher transcriptional activity of PPAR $\gamma$  when compared to EV-transfected cells (Cimen et al, 2011). Additionally, it has been shown that PPAR $\gamma$ , phosphorylated via ERK1/2, can physically associate with p65 and inhibit its transcriptional activity (Chen et al, 2003).

15-LOX-1 expression in HCT-116 cell increases transcriptional activation of PPAR $\gamma$  and it also activates the MAPK pathway leading to the phosphorylation of PPAR $\gamma$ . This phosphorylated form of PPAR $\gamma$  may associate with p65 and inhibit NF-κB activity (Cimen et al, 2011). This study has therefore addressed the controversy regarding the alleged pro-tumorigenic nature of 15-LOX-1 with regard to MAPK activation and PPAR $\gamma$  phosphorylation in CRC.

Finally, it was also established that the inhibition of NF-κB via the activation of PPAR $\gamma$  was functionally reflected in the proliferation of the cells. Inhibition of PPAR $\gamma$  with GW9662 in the 15-LOX-1 expressing cells, but not control cells, resulted in a significant increase in the proliferation to levels similar to the control cells. Additionally, treatment of the control cells with SN-50, a specific peptide inhibitor of NF-κB, resulted in a significant decrease in proliferation (EV-SN-50). This decrease, however, was more pronounced than the decrease in proliferation

observed when the cells were forced to express 15-LOX-1. This may be because SN-50 is a direct inhibitor of NF-κB, which acts by antagonizing the translocation of p65 to the nucleus. 15-LOX-1, on the other hand, is an indirect inhibitor of NF-κB, acting via PPAR $\gamma$ .

## **CHAPTER 5**

### **CONCLUSIONS**

On the basis of the major findings of this study, the following conclusions can be drawn:

- i) 15-LOX-1 expression was stably achieved in HCT-116 colorectal cancer cell lines transfected with 15-LOX-1 mammalian expression vector. RT-PCR and Western blot analysis were justified this expression and the presence of statistically significant amount of the enzymatic reaction product 13(S)-HODE showed that 15-LOX-1 protein is active.
- ii) The expression of 15-LOX-1 significantly reduced cell proliferation as shown by an MTT assay. The presence of the 15-LOX-1 specific inhibitor recovered this reduced proliferation.
- iii) Reduction of cell proliferation resulted in an increase of apoptosis. 15-LOX-1 expressing HCT-116 cells were shown to undergo significantly higher amount apoptosis as compared to control cells using acridine orange staining and annexin V/PI staining assays. Furthermore, the expression of 15-LOX-1 was shown to induce apoptosis through downregulation of the antiapoptotic protein XIAP and Bcl-xL and activation of caspase-3.
- iv) The expression of 15-LOX-1 decreased the metastatic potential of HCT-116 cells. This decrease in HCT-116 cells was shown by marked reduction in their motility, loss of their capacity for anchorage-independent growth and decreased adhesion to the extracellular matrix, loss of their invasive and migratory capacity. Furthermore, the expression of 15-LOX-1 decreased expression of MTA-1. This is an indication of possible inverse relation between the regulation of 15-LOX-1 expression and the metastatic potential of CRC cells.

- v) The expression of 15-LOX-1 resulted in a loss of the angiogenic potential of HCT-116 cells as shown by the following experiments:
- 15-LOX-1 expression caused a significant decrease in the secretion of VEGF-A in HCT-116 cells.
  - Conditioned medium collected from 15-LOX-1 expressing HCT 116 cells after 72h caused significantly less HUVEC proliferation and migration compared to HUVECs grown with conditioned medium from control cells.
  - In an in vitro endothelial tube formation assay, HUVECs grown in conditioned medium from 15-LOX-1 expressing HCT-116 cells resulted in endothelial cell tubes with significantly reduced total skeleton length, number of branching points, nodal structures and no. of tubes compared to HUVECs grown in conditioned medium from empty vector transfected HCT-116 cells.
- vi) To understand the mechanistic underpinnings of the functional changes that accompany 15-LOX-1 expression, it was hypothesized that expression of 15-LOX-1 results in an inhibition of the inflammatory transcription factor NF-κB via the activation of the nuclear orphan receptor PPAR $\gamma$ .
- Endogenously produced 13(S)-HODE from ectopic expression of 15-LOX-1 in HCT-116 cells as well as exogenously added 13(S)-HODE could act as a ligand for PPAR $\gamma$  and increase its transcriptional activity.
  - 15-LOX-1 expression resulted in an increase in the cytoplasmic levels of the NF-κB inhibitor I $\kappa$ B- $\alpha$  and a decrease in its phosphorylation and degradation in HCT-116 cells. This implied that the NF-κB subunits could be retained in an inactive form in the cytoplasm.

- A decreased nuclear translocation of p65 and p50 was also observed in the presence of 15-LOX-1 expression, which could be reversed with the 15-LOX-1-specific inhibitor PD146176 and the PPAR $\gamma$  antagonist GW9662.
- 15-LOX-1 expression resulted in decreased binding of NF- $\kappa$ B subunits p50 and p65 to their consensus DNA-binding sequences and decreased NF- $\kappa$ B transcriptional activity, both of which could be reversed by GW9662. Cells expressing 15-LOX-1 show increased phosphorylation of PPAR $\gamma$  through increased phosphorylation of ERK1/2 (Cimen et al, 2011).
- Functionally, the inhibition of PPAR $\gamma$  in the 15-LOX-1 expressing cells, but not the control cells, resulted in a significant increase in cellular proliferation.

These findings, along with data available in the published literature provide evidence that 15-LOX-1 is a major player in several functional and biochemical changes that occur during the progression of colorectal carcinogenesis. These properties of 15-LOX-1 further emphasize the importance of this protein as a possible therapeutic option in colorectal carcinogenesis.

## REFERENCES

- Adams JM, Cory S (2007) The Bcl-2 apoptotic switch in cancer development and therapy. *Oncogene* **26:** 1324-1337
- Aggarwal BB, Shishodia S, Sandur SK, Pandey MK, Sethi G (2006) Inflammation and cancer: How hot is the link? *Biochemical Pharmacology* **72:** 1605-1621
- Bhattacharya S, Mathew G, Jayne DG, Pelengaris S, Khan M (2009) 15-Lipoxygenase-1 in Colorectal Cancer: A Review. *Tumor Biology* **30:** 185-199
- Bonizzi G, Piette J, Schoonbroodt S, Greimers R, Havard L, Merville MP, Bours V (1999) Reactive oxygen intermediate-dependent NF-kappa B activation by interleukin-1 beta requires 5-lipoxygenase or NADPH oxidase activity. *Molecular and Cellular Biology* **19:** 1950-1960
- Bren-Mattison Y, Meyer AM, Van Putten V, Li H, Kuhn K, Stearman R, Weiser-Evans M, Winn RA, Heasley LE, Nemenoff RA (2008) Antitumorigenic effects of peroxisome proliferator-activated receptor-gamma in. *Mol Pharmacol* **73:** 709-717
- Brockman JA, Gupta RA, DuBois RN (1998) Activation of PPAR gamma leads to inhibition of anchorage-independent growth of human colorectal cancer cells. *Gastroenterology* **115:** 1049-1055
- Bronstein JC, Bull AW (1993) The correlation between 13-hydroxyoctadecadienoate dehydrogenase (13-HODE dehydrogenase) and intestinal-cell differentiation. *Prostaglandins* **46:** 387-395
- Bull AW, Steffensen KR, Leers J, Rafter JJ (2003) Activation of PPAR gamma in colon tumor cell lines by oxidized metabolites of linoleic acid, endogenous ligands for PPAR gamma. *Carcinogenesis* **24:** 1717-1722
- Buroker NE, Barboza J, Huang JY (2009) The I kappa B alpha gene is a peroxisome proliferator-activated receptor cardiac target gene. *Febs Journal* **276:** 3247-3255
- Cathcart MC, Lysaght J, Pidgeon GP (2011) Eicosanoid signalling pathways in the development and progression of colorectal cancer: novel approaches for prevention/intervention. *Cancer and Metastasis Reviews* **30:** 363-385
- Chabane N, Zayed N, Benderdour M, Martel-Pelletier J, Pelletier JP, Duval N, Fahmi H (2009) Human articular chondrocytes express 15-lipoxygenase-1 and-2: potential role in osteoarthritis. *Arthritis Research & Therapy* **11(2):R44**
- Chen F, Wang MC, O'Connor JP, He M, Tripathi T, Harrison LE (2003) Phosphorylation of PPAR gamma via active ERK1/2 leads to its physical association with p65 and inhibition of NF-kappa beta. *Journal of Cellular Biochemistry* **90:** 732-

- Chia JS, Du JL, Hsu WB, Sun A, Chiang CP, Wang WB (2010) Inhibition of metastasis, angiogenesis, and tumor growth by Chinese herbal cocktail Tien-Hsien Liquid. *Bmc Cancer* 10:175
- Cimen I, Astarci E, Banerjee S (2011) 15-Lipoxygenase-1 Exerts Its Tumor Suppressive Role by Inhibiting Nuclear Factor-Kappa B Via Activation of PPAR Gamma. *Journal of Cellular Biochemistry* **112**: 2490-2501
- Cipolletta D, Feuerer M, Li A, Kamei N, Lee J, Shoelson SE, Benoist C, Mathis D (2012) PPAR-gamma is a major driver of the accumulation and phenotype of adipose tissue T-reg cells. *Nature* **486**: 549-U151
- Coussens LM, Werb Z (2002) Inflammation and cancer. *Nature* **420**: 860-867
- Dai S, Abu-Amer W, Karuppaiah K, Abu-Amer Y (2011) Evidence that the kinase-truncated c-Src regulates NF-kappaB signaling by. *J Cell Biochem* **112**: 2463-2470
- Dasgupta S, Srinidhi S, Vishwanatha JK (2012) Oncogenic activation in prostate cancer progression and metastasis: Molecular. *J Carcinog* **11**: 4
- Deguchi A, Xing SW, Shureiqi I, Yang PY, Newman RA, Lippman SM, Feinmark SJ, Oehlen B, Weinstein IB (2005) Activation of protein kinase G up-regulates expression of 15-lipoxygenase-1 in human colon cancer cells. *Cancer Research* **65**: 8442-8447
- Dorai T, Aggarwal BB (2004) Role of chemopreventive agents in cancer therapy. *Cancer Letters* **215**: 129-140
- Ferrara N (2004) Vascular endothelial growth factor: Basic science and clinical progress. *Endocrine Reviews* **25**: 581-611
- Forman BM, Tontonoz P, Chen J, Brun RP, Spiegelman BM, Evans RM (1995) 15-deoxy-delta(12,14)-prostaglandin j(2) is a ligand for the adipocyte determination factor ppar-gamma. *Cell* **83**: 803-812
- Furstenberger G, Krieg P, Muller-Decker K, Habenicht AJR (2006) What are cyclooxygenases and lipoxygenases doing in the driver's seat of carcinogenesis? *International Journal of Cancer* **119**: 2247-2254
- Gao M, Hu Z, Zheng Y, Zeng Y, Shen X, Zhong D, He F (2011) Peroxisome proliferator-activated receptor gamma agonist troglitazone inhibits. *Shock* **36**: 228-234
- Giannini R, Cavallini A (2005) Expression analysis of a subset of coregulators and three nuclear receptors in human colorectal carcinoma. *Anticancer Research* **25**: 4287-4292

Gilles S, Mariani V, Bryce M, Mueller MJ, Ring J, Jakob T, Pastore S, Behrendt H, Traidl-Hoffmann C (2009) Pollen-derived E1-phytoprostanes signal via PPAR-gamma and NF-kappaB-dependent. *J Immunol* **182**: 6653-6658

Gillmor SA, Villasenor A, Fletterick R, Sigal E, Browner MF (1997) The structure of mammalian 15-lipoxygenase reveals similarity to the lipases and the determinants of substrate specificity. *Nature Structural Biology* **4**: 1003-1009

Glasgow WC, Everhart AL (1997) The role of linoleic acid metabolism in the proliferative response of cells overexpressing the erbB-2/HER2 oncogene. *Eicosanoids and Other Bioactive Lipids in Cancer, Inflammation, and Radiation Injury* **3** *407*: 393-397

Grivennikov SI, Karin M (2010) Dangerous liaisons: STAT3 and NF-kappa B collaboration and crosstalk in cancer. *Cytokine & Growth Factor Reviews* **21**: 11-19

Gulliksson M, Brunnstrom A, Johannesson M, Backman L, Nilsson G, Harvima I, Dahlen B, Kumlin M, Claesson HE (2007) Expression of 15-lipoxygenase type-1 in human mast cells. *Biochimica Et Biophysica Acta-Molecular and Cell Biology of Lipids* **1771**: 1156-1165

Hanahan D, Weinberg RA (2000) The hallmarks of cancer. *Cell* **100**: 57-70

Hanahan D, Weinberg RA (2011) Hallmarks of Cancer: The Next Generation. *Cell* **144**: 646-674

Harats D, Ben-Shushan D, Cohen H, Gonon A, Barshack I, Goldberg I, Greenberger S, Hodish I, Harari A, Varda-Bloom N, Levanon K, Grossman E, Chaitidis P, Kuhn H, Shaish A (2005) Inhibition of carcinogenesis in transgenic mouse models over-expressing 15-lipoxygenase in the vascular wall under the control of murine preproendothelin-1 promoter. *Cancer Letters* **229**: 127-134

Hartnett L, Egan LJ (2012) Inflammation, DNA methylation and colitis-associated cancer. *Carcinogenesis* **33**: 723-731

Hayden MS, Ghosh S (2008) Shared principles in NF-kappa B signaling. *Cell* **132**: 344-362

Hennig R, Kehl T, Noor S, Ding XZ, Rao SM, Bergmann F, Furstenberger G, Buchler MW, Friess H, Krieg P, Adrian TE (2007) 15-lipoxygenase-1 production is lost in pancreatic cancer and overexpression of the gene inhibits tumor cell growth. *Neoplasia* **9**: 917-926

Heslin MJ, Hawkins A, Boedefeld W, Arnoletti JP, Frolov A, Soong R, Urist MM, Bland KI (2005) Tumor-associated down-regulation of 15-lipoxygenase-1 is reversed by celecoxib in colorectal cancer. *Annals of Surgery* **241**: 941-946

Hofer MD, Chang MC, Hirko KA, Rubin MA, Nose V (2009) Immunohistochemical

and clinicopathological correlation of the metastasis-associated gene 1 (MTA1) expression in benign and malignant pancreatic endocrine tumors. *Modern Pathology* **22**: 933-939

Hsi LC, Kundu S, Palomo J, Xu B, Ficco R, Vogelbaum MA, Cathcart MK (2011) Silencing IL-13R alpha 2 Promotes Glioblastoma Cell Death via Endogenous Signaling. *Molecular Cancer Therapeutics* **10**: 1149-1160

Hsi LC, Wilson L, Nixon J, Eling TE (2001) 15-Lipoxygenase-1 metabolites down-regulate peroxisome proliferator-activated receptor gamma via the MAPK signaling pathway. *Journal of Biological Chemistry* **276**: 34545-34552

Hsi LC, Xi XP, Lotan R, Shureiqi I, Lippman SM (2004) The histone deacetylase inhibitor suberoylanilide hydroxamic acid induces apoptosis via induction of 15-lipoxygenase-1 in colorectal cancer cells. *Cancer Research* **64**: 8778-8781

Hsi LC, Xi XP, Wu YQ, Lippman SM (2005) The methyltransferase inhibitor 5-aza-2-deoxycytidine induces apoptosis via induction of 15-lipoxygenase-1 in colorectal cancer cells. *Molecular Cancer Therapeutics* **4**: 1740-1746

Il Lee S, Zuo XS, Shureiqi I (2011) 15-Lipoxygenase-1 as a tumor suppressor gene in colon cancer: is the verdict in? *Cancer and Metastasis Reviews* **30**: 481-491

Itoh T, Fairall L, Amin K, Inaba Y, Szanto A, Balint BL, Nagy L, Yamamoto K, Schwabe JWR (2008) Structural basis for the activation of PPAR gamma by oxidized fatty acids. *Nature Structural & Molecular Biology* **15**: 924-931

Jemal A, Bray F, Center MM, Ferlay J, Ward E, Forman D (2011) Global Cancer Statistics. *Ca-a Cancer Journal for Clinicians* **61**: 69-90

Joyce JA, Pollard JW (2009) Microenvironmental regulation of metastasis. *Nature Reviews Cancer* **9**: 239-252

Kai L, Wang J, Ivanovic M, Chung YT, Laskin WB, Schulze-Hoepfner F, Mirochnik Y, Satcher RL, Levenson AS (2011) Targeting Prostate Cancer Angiogenesis Through Metastasis-Associated Protein 1 (MTA1). *Prostate* **71**: 268-280

Kamitani H, Geller M, Eling T (1998) Expression of 15-lipoxygenase by human colorectal carcinoma Caco-2 cells during apoptosis and cell differentiation. *Journal of Biological Chemistry* **273**: 21569-21577

Kandouz M, Nie DT, Pidgeon GP, Krishnamoorthy S, Maddipati KR, Honn KV (2003) Platelet-type 12-lipoxygenase activates NF-kappa B in prostate cancer cells. *Prostaglandins & Other Lipid Mediators* **71**: 189-204

Karin M (2006a) NF-kappa B and cancer: Mechanisms and targets. *Molecular Carcinogenesis* **45**: 355-361

Karin M (2006b) Nuclear factor-kappa B in cancer development and progression.

*Nature* **441**: 431-436

Kawasaki G, Yanamoto S, Yoshitomi I, Yamada S, Mizuno A (2008) Overexpression of metastasis-associated MTA1 in oral squamous cell carcinomas: correlation with metastasis and invasion. *International Journal of Oral and Maxillofacial Surgery* **37**: 1039-1046

Kelavkar U, Glasgow W, Eling TE (2002) The effect of 15-lipoxygenase-1 expression on cancer cells. *Curr Urol Rep* **3**: 207-214

Kelavkar U, Wang SS, Montero A, Murtagh J, Shah K, Badr K (1998) Human 15-lipoxygenase gene promoter: analysis and identification of DNA binding sites for IL-13-induced regulatory factors in monocytes. *Molecular Biology Reports* **25**: 173-182

Kelavkar UP, Badr KF (1999) Effects of mutant p53 expression on human 15-lipoxygenase-promoter activity and murine 12/15-lipoxygenase gene expression: Evidence that 15-lipoxygenase is a mutator gene. *Proceedings of the National Academy of Sciences of the United States of America* **96**: 4378-4383

Kelavkar UP, Cohen C (2004) 15-lipoxygenase-1 expression upregulates and activates insulin-like growth factor-1 receptor in prostate cancer cells. *Neoplasia* **6**: 41-52

Kelavkar UP, Nixon JB, Cohen C, Dillehay D, Eling TE, Badr KF (2001) Overexpression of 15-lipoxygenase-1 in PC-3 human prostate cancer cells increases tumorigenesis. *Carcinogenesis* **22**: 1765-1773

Kelavkar UP, Parwani AV, Shappell SB, Martin WD (2006) Conditional expression of human 15-lipoxygenase-1 in mouse prostate induces prostatic intraepithelial neoplasia: The FLiMP mouse model. *Neoplasia* **8**: 510-522

Kelloff GJ, Schilsky RL, Alberts DS, Day RW, Guyton KZ, Pearce HL, Peck JC, Phillips R, Sigman CC (2004) Colorectal adenomas: A prototype for the use of surrogate end points in the development of cancer prevention drugs. *Clinical Cancer Research* **10**: 3908-3918

Kim EK, Kwon KB, Koo BS, Han MJ, Song MY, Song EK, Han MK, Park JW, Ryu DG, Park BH (2007) Activation of peroxisome proliferator-activated receptor-gamma protects pancreatic beta-cells from cytokine-induced cytotoxicity via NF kappa B pathway. *International Journal of Biochemistry & Cell Biology* **39**: 1260-1275

Kim JS, Baek SJ, Bottone FG, Sali T, Eling TE (2005) Overexpression of 15-lipoxygenase-1 induces growth arrest through phosphorylation of p53 in human colorectal cancer cells. *Molecular Cancer Research* **3**: 511-517

Krishnamoorthy S, Honn KV (2011) Eicosanoids and other lipid mediators and the tumor hypoxic microenvironment. *Cancer and Metastasis Reviews* **30**: 613-618

Kuhn H, Thiele BJ (1999) The diversity of the lipoxygenase family - Many sequence data but little information on biological significance. *Febs Letters* **449**: 7-11

Kuhn H, Walther M, Kuban RJ (2002) Mammalian arachidonate 15-lipoxygenases - Structure, function, and biological implications. *Prostaglandins & Other Lipid Mediators* **68-9**: 263-290

Lee KS, Kim SR, Park SJ, Park HS, Min KH, Jin SM, Lee MK, Kim UH, Lee YC (2006) Peroxisome proliferator activated receptor-gamma modulates reactive oxygen. *J Allergy Clin Immunol* **118**: 120-127

Li MN, Xie J, Cheng L, Chang BM, Wang Y, Lan XQ, Zhang D, Yin YQ, Cheng NL (2008) Suppression of Invasive Properties of Colorectal Carcinoma SW480 Cells by 15-Hydroxyprostaglandin Dehydrogenase Gene. *Cancer Investigation* **26**: 905-912

Liu C, Xu DW, Sjoberg J, Forsell P, Bjorkholm M, Claesson HE (2004) Transcriptional regulation of 15-lipoxygenase expression by promoter methylation. *Experimental Cell Research* **297**: 61-67

Lowe SW, Lin AW (2000) Apoptosis in cancer. *Carcinogenesis* **21**: 485-495

Mackenzie F, Ruhrberg C (2012) Diverse roles for VEGF-A in the nervous system. *Development* **139**: 1371-1380

Mahoney MG, Simpson A, Jost M, Noe M, Kari C, Pepe D, Choi YW, Uitto J, Rodeck U (2002) Metastasis-associated protein (MTA)1 enhances migration, invasion, and anchorage-independent survival of immortalized human keratinocytes. *Oncogene* **21**: 2161-2170

Mal M, Koh PK, Cheah PY, Chan ECY (2011) Ultra-pressure liquid chromatography/tandem mass spectrometry targeted profiling of arachidonic acid and eicosanoids in human colorectal cancer. *Rapid Communications in Mass Spectrometry* **25**: 755-764

Marzook H, Li DQ, Nair VS, Mudvari P, Reddy SDN, Pakala SB, Santhoshkumar TR, Pillai MR, Kumar R (2012) Metastasis-associated Protein 1 Drives Tumor Cell Migration and Invasion through Transcriptional Repression of RING Finger Protein 144A. *Journal of Biological Chemistry* **287**: 5615-5626

Mayo MW, Baldwin AS (2000) The transcription factor NF-kappa B: control of oncogenesis and cancer therapy resistance. *Biochimica Et Biophysica Acta-Reviews on Cancer* **1470**: M55-M62

Mazumdar A, Wang RA, Mishra SK, Adam L, Bagheri-Yarmand R, Mandal M, Vadlamudi RK, Kumar R (2001) Transcriptional repression of oestrogen receptor by metastasis-associated protein 1 corepressor. *Nature Cell Biology* **3**: 30-37

Melstrom LG, Bentrem DJ, Salabat MR, Kennedy TJ, Ding XZ, Strouch M, Rao

SM, Witt RC, Ternent CA, Talamonti MS, Bell RH, Adrian TA (2008) Overexpression of 5-Lipoxygenase in Colon Polyps and Cancer and the Effect of 5-LOX Inhibitors In vitro and in a Murine Model. *Clinical Cancer Research* **14:** 6525-6530

Michalik L, Desvergne B, Wahli W (2004) Peroxisome-proliferator-activated receptors and cancers: Complex stories. *Nature Reviews Cancer* **4:** 61-70

Miura K, Fujibuchi W, Ishida K, Naitoh T, Ogawa H, Ando T, Yazaki N, Watanabe K, Haneda S, Shibata C, Sasaki I (2011) Inhibitor of apoptosis protein family as diagnostic markers and therapeutic targets of colorectal cancer. *Surgery Today* **41:** 175-182

Molli PR, Singh RR, Lee SW, Kumar R (2008) MTA1-mediated transcriptional repression of BRCA1 tumor suppressor gene. *Oncogene* **27:** 1971-1980

Nicolson GL, Nawa A, Toh Y, Taniguchi S, Nishimori K, Moustafa A (2003) Tumor metastasis-associated human MTA1 gene and its MTA1 protein product: Role in epithelial cancer cell invasion, proliferation and nuclear regulation. *Clinical & Experimental Metastasis* **20:** 19-24

Nixon JB, Kamitani H, Baek SJ, Eling TE (2003) Evaluation of eicosanoids and NSAIDs as PPAR gamma ligands in colorectal carcinoma cells. *Prostaglandins Leukotrienes and Essential Fatty Acids* **68:** 323-330

Nixon JB, Kim KS, Lamb PW, Bottone FG, Eling TE (2004) 15-lipoxygenase-1 has anti-tumorigenic effects in colorectal cancer. *Prostaglandins Leukotrienes and Essential Fatty Acids* **70:** 7-15

Nobumoto A, Nagahara K, Oomizu S, Katoh S, Nishi N, Takeshita K, Niki T, Tominaga A, Yamauchi A, Hirashima M (2008) Galectin-9 suppresses tumor metastasis by blocking adhesion to endothelium and extracellular matrices. *Glycobiology* **18:** 735-744

Pascual G, Fong AL, Ogawa S, Gamliel A, Li AC, Perissi V, Rose DW, Willson TM, Rosenfeld MG, Glass CK (2005) A SUMOylation-dependent pathway mediates transrepression of inflammatory response genes by PPAR-gamma. *Nature* **437:** 759-763

Philips BJ, Dhir R, Hutzley J, Sen M, Kelavkar UP (2008) Polyunsaturated fatty acid metabolizing 15-Lipoxygenase-1 (15-LO-1) expression in normal and tumorigenic human bladder tissues. *Applied Immunohistochemistry & Molecular Morphology* **16:** 159-164

Pidgeon GP, Lysaght J, Krishnamoorthy S, Reynolds JV, O'Byrne K, Nie D, Honn KV (2007) Lipoxygenase metabolism: roles in tumor progression and survival. *Cancer and Metastasis Reviews* **26:** 503-524

Prat A, Casado E, Cortes J (2007) New approaches in angiogenic targeting for colorectal cancer. *World Journal of Gastroenterology* **13**: 5857-5866

Qian H, Yu J, Li Y, Wang H, Song C, Zhang X, Liang X, Fu M, Lin C (2007) RNA interference of metastasis-associated gene 1 inhibits metastasis of B16F10. *Biol Cell* **99**: 573-581

Qian HL, Lu N, Xue LY, Liang X, Zhang XY, Fu M, Xie YQ, Zhan QM, Liu ZH, Lin C (2005) Reduced MTA1 expression by RNAi inhibits in vitro invasion and migration of esophageal squamous cell carcinoma cell line. *Clinical & Experimental Metastasis* **22**: 653-662

Reinmuth N, Parikh AA, Ahmad SA, Liu WB, Stoeltzing O, Fan F, Takeda A, Akagi M, Ellis LM (2003) Biology of angiogenesis in tumors of the gastrointestinal tract. *Microscopy Research and Technique* **60**: 199-207

Rumi MA, Ishihara S, Kazumori H, Kadokawa Y, Kinoshita Y (2004) Can PPAR gamma ligands be used in cancer therapy? *Curr Med Chem Anticancer Agents* **4**: 465-477

Sankaran D, Pakala SB, Nair VS, Sirigiri DNR, Cyanam D, Ha NH, Li DQ, Santhoshkumar TR, Pillai MR, Kumar R (2012) Mechanism of MTA1 Protein Overexpression-linked Invasion MTA1 regulation of hyaluronan-mediated motility receptor (HMMR) expression and function. *Journal of Biological Chemistry* **287**: 5483-5491

Sarraf P, Mueller E, Jones D, King FJ, DeAngelo DJ, Partridge JB, Holden SA, Chen LB, Singer S, Fletcher C, Spiegelman BM (1998) Differentiation and reversal of malignant changes in colon cancer through PPAR gamma. *Nature Medicine* **4**: 1046-1052

Sarraf P, Mueller E, Smith WM, Wright HM, Kum JB, Aaltonen LA, de la Chapelle A, Spiegelman BM, Eng C (1999) Loss-of-function mutations in PPAR gamma associated with human colon cancer. *Molecular Cell* **3**: 799-804

Sasaki T, Fujii K, Yoshida K, Shimura H, Sasahira T, Ohmori H, Kuniyasu H (2006) Peritoneal metastasis inhibition by linoleic acid with activation of PPAR gamma in human gastrointestinal cancer cells. *Virchows Archiv* **448**: 422-427

Sendobry SM, Cornicelli JA, Welch K, Bocan T, Tait B, Trivedi BK, Colbry N, Dyer RD, Feinmark SJ, Daugherty A (1997) Attenuation of diet-induced atherosclerosis in rabbits with a highly selective 15-lipoxygenase inhibitor lacking significant antioxidant properties. *British Journal of Pharmacology* **120**: 1199-1206

Shao D, Rangwala SM, Bailey ST, Krakow SL, Reginato MJ, Lazar MA (1998) Interdomain communication regulating ligand binding by PPAR-gamma. *Nature* **396**: 377-380

Shappell SB, Olson SJ, Hannah SE, Manning S, Roberts RL, Masumori N, Jisaka M, Boeglin WE, Vader V, Dave DS, Shook MF, Thomas TZ, Funk CD, Brash AR, Matusik RJ (2003) Elevated expression of 12/15-lipoxygenase and cyclooxygenase-2 in a transgenic mouse model of prostate carcinoma. *Cancer Research* **63**: 2256-2267

Shibuya M, Claesson-Welsh L (2006) Signal transduction by VEGF receptors in regulation of angiogenesis and lymphangiogenesis. *Experimental Cell Research* **312**: 549-560

Shureiqi I, Chen DN, Day RS, Zuo XS, Hochman FL, Ross WA, Cole RA, Moy O, Morris JS, Xiao LC, Newman RA, Yang PY, Lippman SM (2010) Profiling Lipoxygenase Metabolism in Specific Steps of Colorectal Tumorigenesis. *Cancer Prevention Research* **3**: 829-838

Shureiqi I, Chen DN, Lotan R, Yang PY, Newman RA, Fischer SM, Lippman SM (2000) 15-Lipoxygenase-1 mediates nonsteroidal anti-inflammatory drug-induced apoptosis independently of cyclooxygenase-2 in colon cancer cells. *Cancer Research* **60**: 6846-6850

Shureiqi I, Jiang W, Fischer SM, Xu XC, Chen DN, Lee JJ, Lotan R, Lippman SM (2002) GATA-6 transcriptional regulation of 15-lipoxygenase-1 during NSAID-induced apoptosis in colorectal cancer cells. *Cancer Research* **62**: 1178-1183

Shureiqi I, Jiang W, Zuo XS, Wu YQ, Stimmel JB, Leesnitzer LM, Morris JS, Fan HZ, Fischer SM, Lippman SM (2003) The 15-lipoxygenase-1 product 13-S-hydroxyoctadecadienoic acid down-regulates PPAR-delta to induce apoptosis in colorectal cancer cells. *Proceedings of the National Academy of Sciences of the United States of America* **100**: 9968-9973

Shureiqi I, Lippman SA (2001) Lipoxygenase modulation to reverse carcinogenesis. *Cancer Research* **61**: 6307-6312

Shureiqi I, Xu XC, Chen DN, Lotan R, Morris JS, Fischer SM, Lippman SM (2001) Nonsteroidal anti-inflammatory drugs induce apoptosis in esophageal cancer cells by restoring 15-lipoxygenase-1 expression. *Cancer Research* **61**: 4879-4884

Shureiqi I, Zuo XS, Broaddus R, Wu Y, Guan BX, Morris JS, Lippman SM (2007) The transcription factor GATA-6 is overexpressed in vivo and contributes to silencing 15-LOX-1 in vitro in human colon cancer. *Faseb Journal* **21**: 743-753

Sordillo LM, Weaver JA, Cao YZ, Corl C, Sylte MJ, Mullarky IK (2005) Enhanced 15-HPETE production during oxidant stress induces apoptosis of endothelial cells. *Prostaglandins & Other Lipid Mediators* **76**: 19-34

Straus DS, Glass CK (2007) Anti-inflammatory actions of PPAR ligands: new insights on cellular and molecular mechanisms. *Trends in Immunology* **28**: 551-558

Tavakoli-Yaraki M, Karami-Tehrani F, Salimi V, Sirati-Sabet M (2012) Induction of

apoptosis by Trichostatin A in human breast cancer cell lines. *Tumour Biol*

Terzic J, Grivennikov S, Karin E, Karin M (2010) Inflammation and Colon Cancer. *Gastroenterology* **138**: 2101-U2119

Toda D, Ota T, Tsukuda K, Watanabe K, Fujiyama T, Murakami M, Naito M, Shimizu N (2006) Gefitinib decreases the synthesis of matrix metalloproteinase and the adhesion to extracellular matrix proteins of colon cancer cells. *Anticancer Research* **26**: 129-134

Vickers A (2000) Recent advances - Complementary medicine. *British Medical Journal* **321**: 683-686

Viita H, Kinnunen K, Eriksson E, Lahtenvuo J, Babu M, Kalesnykas G, Heikura T, Laidinen S, Takalo T, Yla-Herttuala S (2009) Intravitreal Adenoviral 15-Lipoxygenase-1 Gene Transfer Prevents Vascular Endothelial Growth Factor A-Induced Neovascularization in Rabbit Eyes. *Human Gene Therapy* **20**: 1679-1686

Viita H, Markkanen J, Eriksson E, Nurminen M, Kinnunen K, Babu M, Heikura T, Turpeinen S, Laidinen S, Takalo T, Yla-Herttuala S (2008) 15-lipoxygenase-1 prevents vascular endothelial growth factor A- and placental growth factor-induced angiogenic effects in rabbit skeletal muscles via reduction in growth factor mRNA levels, NO bioactivity, and downregulation of VEGF receptor 2 expression. *Circulation Research* **102**: 177-184

Vogelstein B, Kinzler KW (2004) Cancer genes and the pathways they control. *Nature Medicine* **10**: 789-799

Wahli W (2008) A gut feeling of the PXR, PPAR and NF-kappa B connection. *Journal of Internal Medicine* **263**: 613-619

Walther M, Anton M, Wiedmann M, Fletterick R, Kuhn H (2002) The N-terminal domain of the reticulocyte-type 15-lipoxygenase is not essential for enzymatic activity but contains determinants for membrane binding. *Journal of Biological Chemistry* **277**: 27360-27366

Wan HY, Yuan YZ, Qian AH, Sun Y, Qiao MM (2008) Pioglitazone, a PPAR gamma ligand, suppresses NFKB activation through inhibition of 1 kappa B kinase activation in cerulein-treated AR42J cells. *Biomedicine & Pharmacotherapy* **62**: 466-472

Wang DZ, DuBois RN (2010) Therapeutic Potential of Peroxisome Proliferator-Activated Receptors in Chronic Inflammation and Colorectal Cancer. *Gastroenterology Clinics of North America* **39**: 697-707

Wang SL, Liu ZJ, Wang LS, Zhang XR (2009) NF-kappa B Signaling Pathway, Inflammation and Colorectal Cancer. *Cellular & Molecular Immunology* **6**: 327-334

Wasilewicz MP, Kolodziej B, Bojulko T, Kaczmarczyk M, Sulzyc-Bielicka V, Bielicki D, Ciepiela K (2010) Overexpression of 5-lipoxygenase in sporadic colonic adenomas and a possible new aspect of colon carcinogenesis. *International Journal of Colorectal Disease* **25**: 1079-1085

Wen XY, Li YJ, Liu YH (2010) Opposite Action of Peroxisome Proliferator-activated Receptor-gamma in Regulating Renal Inflammation FUNCTIONAL SWITCH BY ITS LIGAND. *Journal of Biological Chemistry* **285**: 29981-29988

Wu J, Xia HHX, Tu SP, Fan DM, Lin MCM, Kung HF, Lam SK, Wong BCY (2003) 15-Lipoxygenase-1 mediates cyclooxygenase-2 inhibitor-induced apoptosis in gastric cancer. *Carcinogenesis* **24**: 243-247

Wu Y, Fang B, Yang XQ, Wang L, Chen D, Krasnykh V, Carter BZ, Morris JS, Shureiqi I (2008) Therapeutic molecular targeting of 15-lipoxygenase-1 in colon cancer. *Molecular Therapy* **16**: 886-892

Yan Y, He T, Shen Y, Chen X, Diao B, Li Z, Liu Q, Xing YQ (2012) Adenoviral 15-lipoxygenase-1 gene transfer inhibits hypoxia-induced proliferation. *Int J Ophthalmol* **5**: 562-569

Yang WL, Frucht H (2001) Activation of the PPAR pathway induces apoptosis and COX-2 inhibition in HT-29 human colon cancer cells. *Carcinogenesis* **22**: 1379-1383

Yang XY, Wang LH, Mihalic K, Xiao WH, Chen TS, Li P, Wahl LM, Farrar WL (2002) Interleukin (IL-4) indirectly suppresses IL-2 production by human T lymphocytes via peroxisome proliferator-activated receptor gamma activated by macrophage-derived 12/15-lipoxygenase ligands. *Journal of Biological Chemistry* **277**: 3973-3978

Yoshinaga M, Buchanan FG, DuBois RN (2004) 15-LOX-1 inhibits p21 (Cip/WAF1) expression by enhancing MEK-ERK1/2 signaling in colon carcinoma cells. *Prostaglandins & Other Lipid Mediators* **73**: 111-122

Yuri M, Sasahira T, Nakai K, Ishimaru S, Ohmori H, Kuniyasu H (2007) Reversal of expression of 15-lipoxygenase-1 to cyclooxygenase-2 is associated with development of colonic cancer. *Histopathology* **51**: 520-527

Zhang C, Hao L, Wang L, Xiao Y, Ge H, Zhu Z, Luo Y, Zhang Y (2010) Elevated IGFIR expression regulating VEGF and VEGF-C predicts lymph node metastasis in human colorectal cancer. In *BMC Cancer* Vol. 10, p 184. England

Zuo X, Morris JS, Broaddus R, Shureiqi I (2009) 15-LOX-1 transcription suppression through the NuRD complex in colon cancer cells. *Oncogene* **28**: 1496-1505

Zuo X, Shureiqi I (2012) Eicosanoid profiling in colon cancer: Emergence of a

pattern. In *Prostaglandins Other Lipid Mediat.* 2012 Elsevier Inc

Zuo X, Wu Y, Morris JS, Stimmel JB, Leesnitzer LM, Fischer SM, Lippman SM, Shureiqi I (2006) Oxidative metabolism of linoleic acid modulates PPAR-beta/delta suppression of PPAR-gamma activity. *Oncogene* **25:** 1225-1241

Zuo XS, Morris JS, Shureiqi I (2008a) Chromatin Modification Requirements for 15-Lipoxygenase-1 Transcriptional Reactivation in Colon Cancer Cells. *Journal of Biological Chemistry* **283:** 31341-31347

Zuo XS, Peng ZL, Wu YQ, Moussalli MJ, Yang XL, Wang Y, Parker-Thornburg J, Morris JS, Broaddus RR, Fischer SM, Shureiqi I (2012) Effects of Gut-Targeted 15-LOX-1 Transgene Expression on Colonic Tumorigenesis in Mice. *Journal of the National Cancer Institute* **104:** 709-716

Zuo XS, Shen L, Issa JP, Moy O, Morris JS, Lippman SM, Shureiqi I (2008b) 15-Lipoxygenase-1 transcriptional silencing by DNA methyltransferase-1 independently of DNA methylation. *Faseb Journal* **22:** 1981-1992

## APPENDICES

### APPENDIX A

#### VECTOR MAPS

##### A.1 pcDNA3.1/Zeo (+) Control Vector

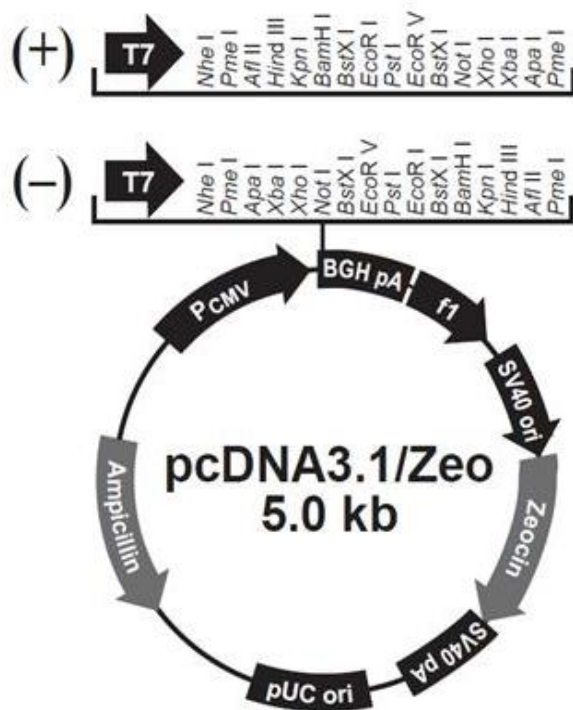


**Figure 5. 1: pcDNA3.1/Zeo (+) 5015 nucleotides Plasmid Map**

CMV promoter: bases 209-863; T7 promoter priming site: bases 863-882; Multiple cloning site: bases 895-1010; BGH reverse priming site: bases 1022-1039; BGH polyadenylation signal: bases 1021-1235; f1 origin: bases 1298-1711; SV40 promoter and origin: bases 1776-2101; EM7 promoter: bases 2117-2183; Zeocin™ resistance gene: bases 2184-2558; SV40 polyadenylation: bases 2688-2817; pUC origin: bases 3201-3874 (C); bla promoter: bases 4880-4978 (C); Ampicillin (bla) resistance gene: bases 4019-4879 (C)

### A.2 pSV- $\beta$ -Galactosidase Control Vector (Promega, USA)

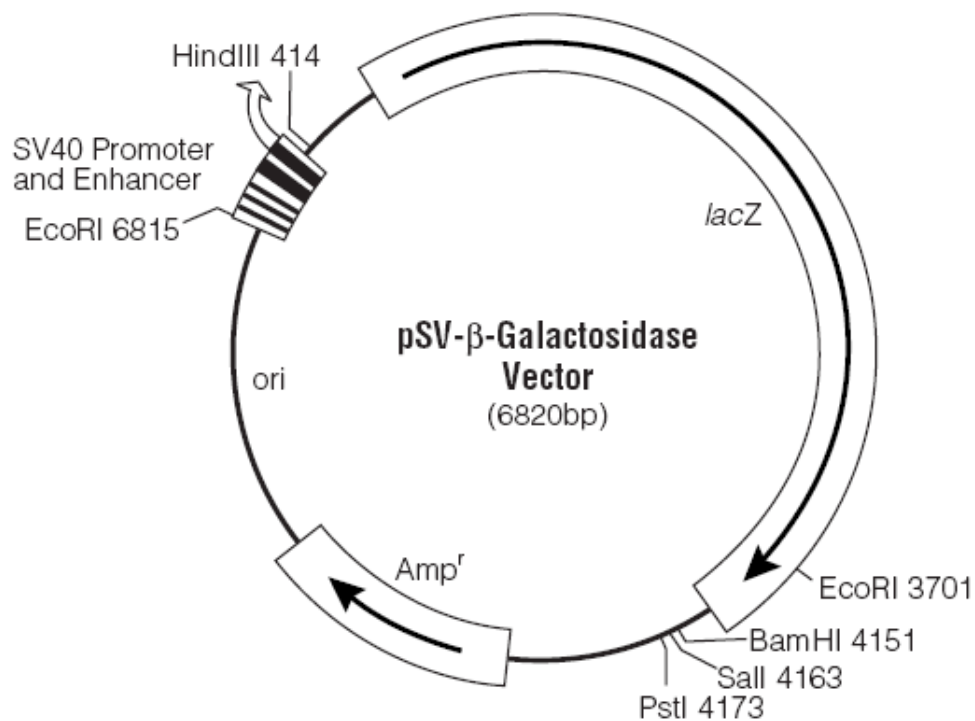


**Figure 5. 2: pSV- $\beta$ -Galactosidase Plasmid Map**

## APPENDIX B

### SCREENING OF 15-LOX-1 EXPRESSING MONOCLOONE CELLS WITH RT-PCR ANALYSIS

**B1: Screening of 15-LOX-1 expressing 1E7 monoclonal cells with RT-PCR analysis after stable transfection of HCT-116 cell lines.**

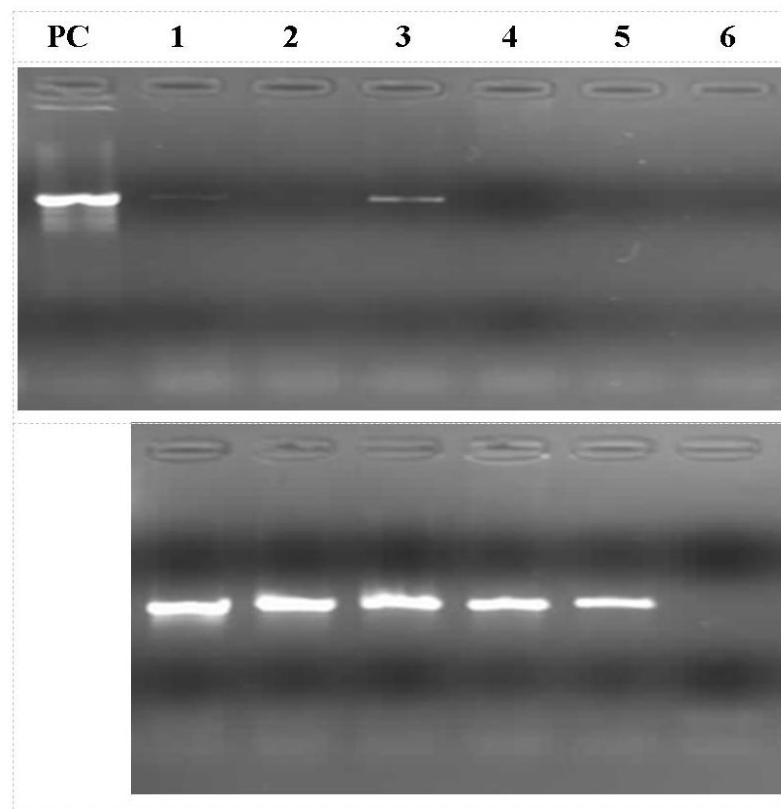


**Figure 5. 3: Screening of 15-LOX-1 expressing 1E7 monoclonal cells with RT-PCR analysis after stable transfection of HCT-116 cell lines.**  
PC: 15-LOX-1 vector (positive control); Lane 1: 1E2; Lane 2: 1E3; lane 3:1E7; Lane 4: empty vector (pcDNA3.1) transfected cells (EVE2); lane 5: parental HCT-116 cells; lane 6: negative control.

**B2: Screening of 15-LOX-1 expressing 1F4 monoclonal cells with RT-PCR analysis after stable transfection of HCT-116 cell lines.**

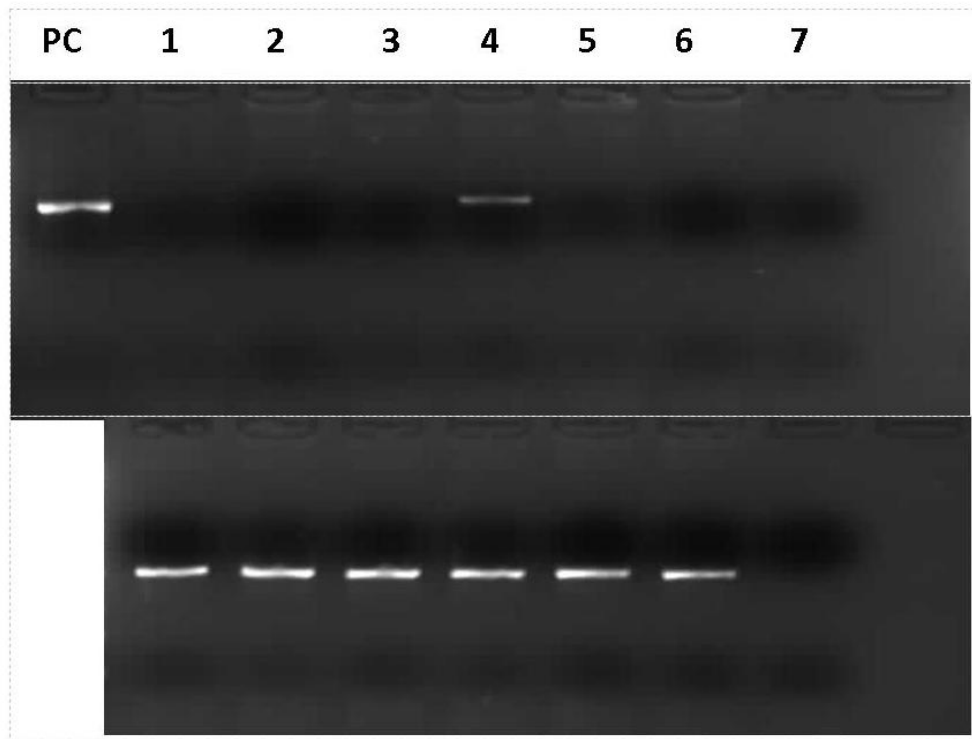


**Figure 5. 4: Screening of 15-LOX-1 expressing 1F4 monoclonal cells with RT-PCR analysis after stable transfection of HCT-116 cell lines.**  
PC: 15-LOX-1 vector (positive control); Lane 1: 1F1; Lane 2: 1F2; lane 3:1F3; Lane 4: 1F4; Lane 5: empty vector (pcDNA3.1) transfected cells (EVE2); lane 6: parental HCT-116 cells; lane 7: negative control.

## APPENDIX C

### STANDART CURVES

#### C.1 Protein concentration standard curve

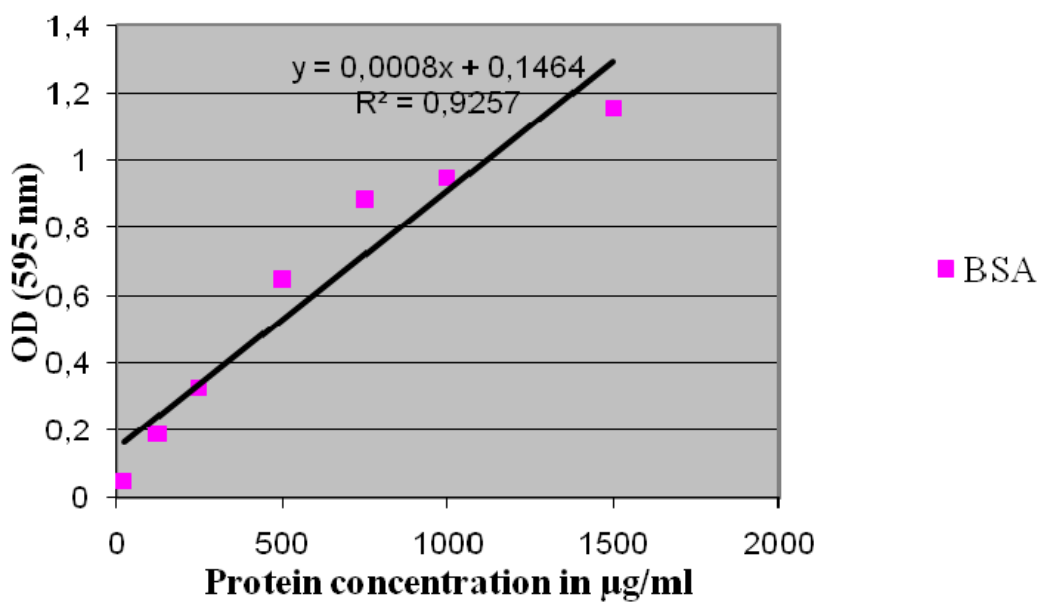
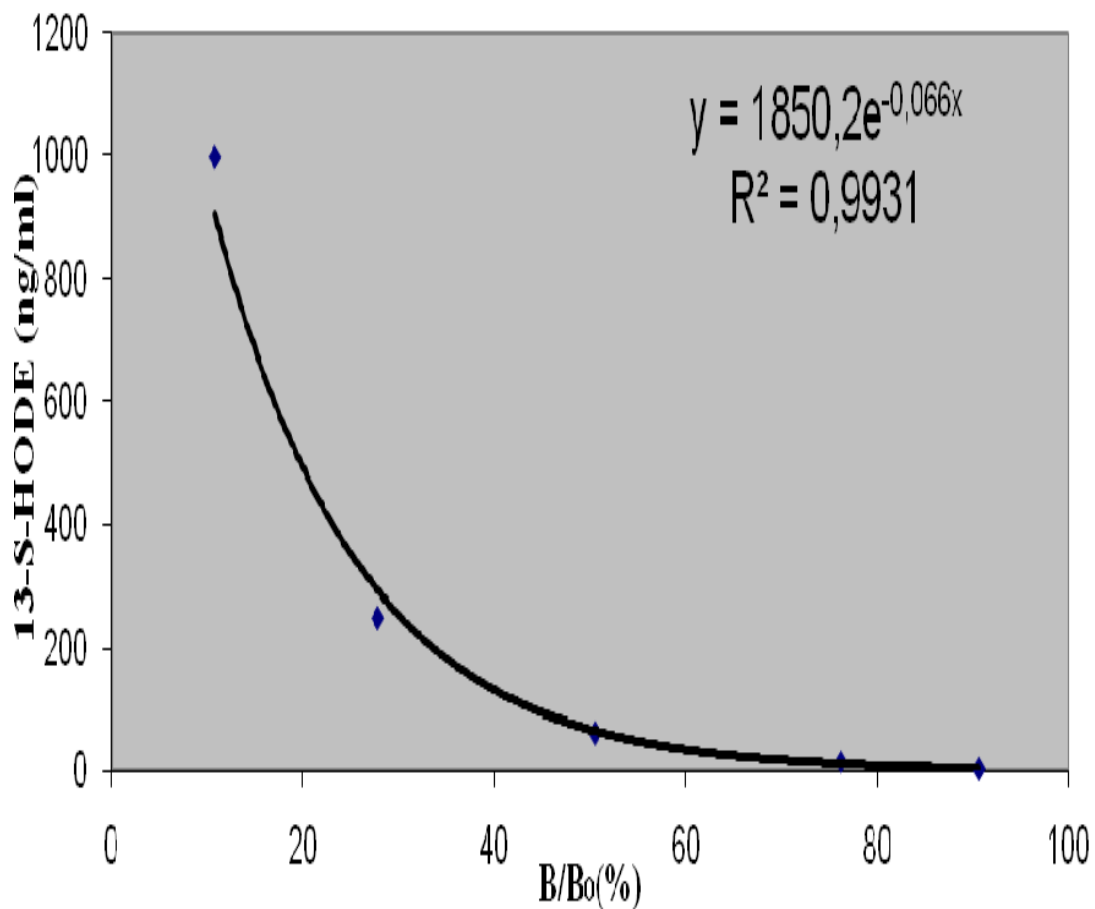


Figure 5. 5: Protein concentration standard curve

### C.2 13-HODE enzyme activity standard curve



**Figure 5. 6: 13-HODE enzyme activity standard curve**

### C.3 Activated NFKB standard curve

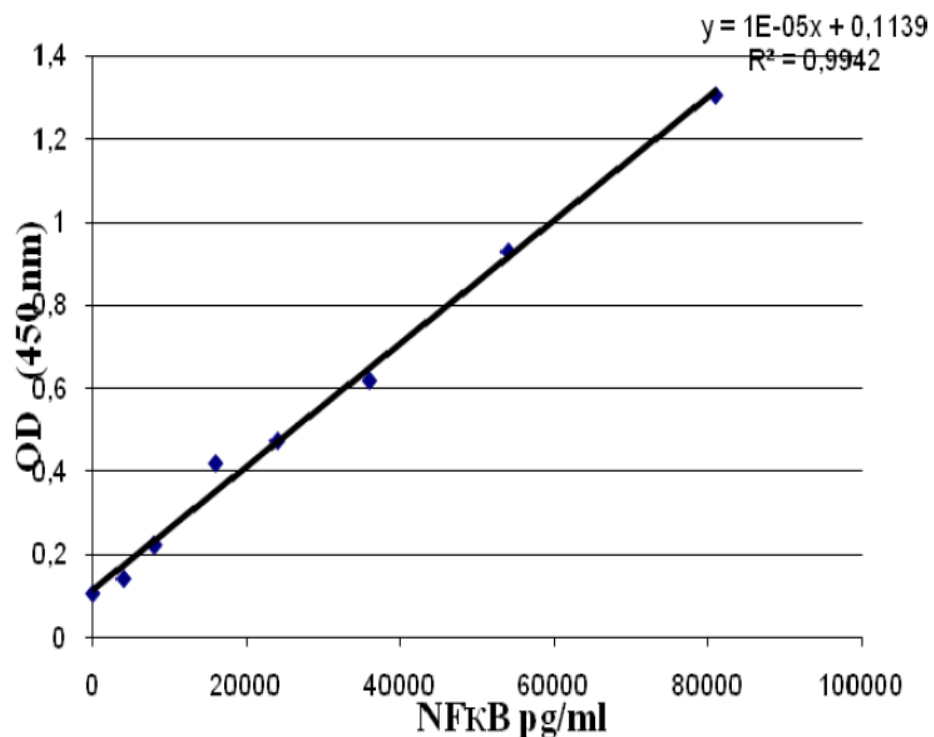


**Figure 5. 7: Activated NFKB standard curve**

**C.4: VEGF-A protein concentration standard curve**

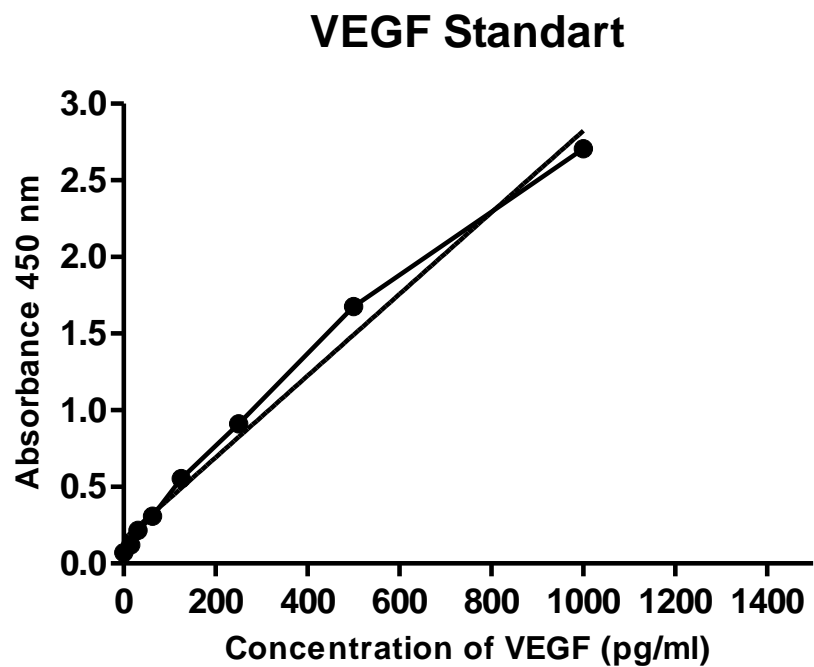


**Figure 5. 8: VEGF-A protein concentration standard curve**

## **CURRICULUM VITAE**

### **Personal Information**

Surname, Name: Çimen İsmail  
Date of birth: 17.09.1978  
Nationality : Turkish  
Gender: Male  
Marital status: Single  
Phone : +90 0542 428 12 36  
E-Mail : ismailcimen78@gmail.com

### **EDUCATION**

1. Eskişehir Osmangazi University, Eskişehir, Turkey, MSc. in Department of Medical Genetics, September, 2007.  
Thesis title : “Determination of genetic markers by FISH analysis on cells that obtained from bladder washing and voided urine in patients with transitional cell carcinoma of the bladder” Supervisor: Assistant Prof. Dr. Oğuz ÇİLİNİR.
2. Hacettepe University, Ankara, Turkey BSc. in Department of Biology, August, 2003. Undergraduate Project: Investigation of Cytotoxic, Mutagenic and Antimutagenic Effects of Meron by Salmonella Mutagenicity Assay. Supervisor: Prof.Dr.Nuran DİRİL.

### **RESEARCH EXPERIENCE**

- 1. Project Assistantship (2007-2009) from TÜBİTAK (The Scientific and Technological Research Council of Turkey).** Project Title: The mechanism of anti tumorigenic effects of 15-LOX-1 in colon cancer. Funding by TÜBİTAK (106S193), (2006-2009) Turkey. Project leader: Associate Professor Dr Sreeparna Banerjee, Middle East Technical University, Department of Biological Sciences, Ankara, Turkey.
- 2. Project Assistantship (2010-2012) from TÜBİTAK (The Scientific and Technological Research Council of Turkey).** Project Title: The effect of differentiation on ICAM-1 and VCAM-1 regulation in colon cancer cells. Funding by TÜBİTAK (110S165), (2010-2013) Turkey. Project leader: Associate Professor Dr Sreeparna Banerjee, Middle East Technical University, Department of Biological Sciences, Ankara, Turkey.

## **PUBLICATIONS**

1. Tunçay Çağatay S, Cimen I, Savaş B, Banerjee S. MTA-1 expression is associated with metastasis and epithelial to mesenchymal transition in colorectal cancer cells. *Tumor Biology* 2013, DOI: 10.1007/s13277-013-0662-x
2. Astarci E, Sade A, Cimen I, Savaş B, and Banerjee S (2012) The NF-κB target genes ICAM-1 and VCAM-1 are differentially regulated during spontaneous differentiation of Caco-2 cells. *FEBS J* 279(16), 2966-2986.
3. Cimen I, Astarci, E and Banerjee S (2011) 15-Lipoxygenase-1 exerts its tumor suppressive role by inhibiting nuclear factor-kappa B via activation of PPAR gamma. *J Cell Biochem*, 112(9), 2490-2501.
4. Sade A, Tunçay S, Cimen I, Severcan F, Banerjee S (2012) Celecoxib reduces fluidity and decreases metastatic potential of colon cancer cell lines irrespective of COX-2 expression. *Biosci Rep* 32(1), 35-44.
5. Cimen I, Tuncay S and Banerjee S (2009) 15-Lipoxygenase-1 expression suppresses the invasive properties of the colorectal carcinoma cell lines HCT-116 and HT-29. *Cancer Sci* 100, 2283-2291.

## **MEETING and SEMINARS**

1. Cimen I. 15-lipoxygenase-1 has tumor suppressive properties in colorectal carcinogenesis. Molecular Biotechnology Center (MBC), University of Turin, 12 Oct. 2012 (invited talk).
2. Cimen I, Astarci E and Banerjee S. 15-LOX-1 is antitumorigenic by inhibiting NF-κB via PPAR $\gamma$  in colorectal cancer cells. 36th FEBS CONGRESS Biochemistry for Tomorrow's Medicine Torino, Italy, June 25-30 2011.
3. Cimen I, Tuncay S, Astarci E and Banerjee S. (2011). 15-lipoxygenase-1 has tumor suppressive properties in colorectal carcinogenesis. International Conference on Frontiers In Carcinogenesis and Cancer Prevention: Scientific Advances and Public Health Initiatives Bangalore, India. Feb 16-18, 2011 (invited talk).
4. Sade, A, Tunçay S, Cimen I., Severcan, F and Banerjee S. (2010). Biophysical and functional characterization of celecoxib in colorectal cancer cell lines. 4th International Meeting on Medicinal and Pharmaceutical Chemistry & 6th International Symposium on Pharmaceutical Chemistry, 30 September – 2 October, 2010 Ankara, Turkey.
5. Cimen, I., S. Tuncay, S. Banerjee. (2009). 15-Lipoxygenase-1 (15-LO-1) in the proliferation, adhesion, migration, and invasion of colorectal carcinoma cell lines, The European Human Genetics Conference May 23-26, 2009-ACV, Vienna, Austria.

6. Cimen I., Tunçay, S, Ustuner, D., and Banerjee, S (2009). An in vitro study of the tumor suppressive properties of 15-lipoxygenase-1 in colorectal cancer, International Symposium on Health Informatics and Bioinformatics (HIBIT) April 16-17, 2009 Ankara, Turkey (Oral presentation).
7. Cilingir O., Cimen I., Durak B., Can C., Bademci G. and S. Artan (2007). FISH-detected genetic markers on bladder washings from patients with bladder cancer. 6th European Cytogenetics Conference 7-10 July 2007. Istanbul, Turkey.
8. Durak B., Bademci G., Aldemir Ö., Şener B., Cimen I. and Artan S. (2007). Skewed X inactivation in a case have partial trisomy 10q with mild phenotype caused by an unbalance X;10 translocation, 6th European Cytogenetics Conference 7-10 July 2007, Istanbul Turkey.
9. Çilingir O, Müslümanoğlu M.H, Özdemir M, Korkmaz C, Kaşifoğlu T, Çimen İ, Uzun D, Basmacı T, Kutlay Ö, Artan S (2006). Ailesel Akdeniz Ateşi Tanısı Konmuş Hastalarda Mutasyon Anaizleri. VII Ulusal Prenatal Tanı ve Tıbbi Genetik Kongresi, 17-20 May, 2006. Kayseri, Turkey.

#### **BURSARIES AND AWARDS:**

1. TÜBİTAK (Scientific and Technological Research Council of Turkey) bursary 01/09/2007-present, Middle East Technical University, Department of Biological Sciences, Ankara, Turkey. Project leader: Associate Professor Dr. Sreeparna Banerjee.
2. The European Society of Human Genetics (ESHG), European Human Genetics Conference, Conference Fellowship, Vienna, Austria May 23-26, 2009.
3. 36th FEBS CONGRESS Biochemistry for Tomorrow's Medicine, Conference Fellowship Torino, Italy, June 25-30 2011.

**Languages:** Turkish (native), English (Very good)

**Hobbies:** Music; playing classical guitar